EFFECT OF CONJUGATE HEAT TRANSFER ON FLOW OF NANOFLUID IN AN ENCLOSURE WITH HEAT CONDUCTING VERTICAL WALL AND UNIFORM HEAT FLUX

by

Ishrat Zahan
Student No. 0412093009P
Registration No. 0412093009, Session: April-2012

MASTER OF PHILOSOPHY
IN
MATHEMATICS

Department of Mathematics
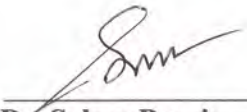Bangladesh University of Engineering and Technology (BUET)
Dhaka-1000
September - 2017

The thesis entitled "**EFFECT OF CONJUGATE HEAT TRANSFER ON FLOW OF NANOFLUID IN AN ENCLOSURE WITH HEAT CONDUCTING VERTICAL WALL AND UNIFORM HEAT FLUX**", submitted by Ishrat Zahan, Roll no: 0412093009P, Registration No.0412093009, Session April-2012 has been accepted as satisfactory in partial fulfillment of the requirement for the degree of Master of Philosophy in Mathematics on 27 September 2017.

Board of Examiners

1.
   _____

   Dr. Md. Abdul Alim   Chairman
   Professor   (Supervisor)
   Department of Mathematics, BUET, Dhaka.

2.
   _____

   Head   Member
   Department of Mathematics, BUET, Dhaka.   (Ex-Officio)

3.
   _____

   Dr. Md. Manirul Alam Sarker   Member
   Professor
   Department of Mathematics, BUET, Dhaka.

4
   _____

   Dr. Salma Parvin   Member
   Professor
   Department of Mathematics, BUET, Dhaka.

5.
   _____

   Dr. Md. Mustafa Kamal Chowdhury   Member
   Ex-Professor (BUET)   (External)
   110 Lake Garden (C1)
   Lake Circus Road, Kolabagan, Dhaka.

Certificate of Research

This is to certify that the work presented in this thesis is carried out by the author under the supervision of Dr. Md. Abdul Alim, Professor, Department of Mathematics, Bangladesh University of Engineering & Technology, Dhaka.

Dr. Md. Abdul Alim

Ishrat 27/09/2017

Ishrat Zahan

Candidate's Declaration

It is hereby declared that this thesis or any part of it has not been submitted elsewhere for the award of any degree or diploma.

Ishrat 27/09/17

Ishrat Zahan

This work is dedicated

to

my Parents and Daughter

Acknowledgement

I would like to affirm the continual mercy, help and blessing showered by the Almighty without which it would have been impossible to accomplish the arduous job I was assigned to. I owe a deep depth to my supervisor, Dr. Md. Abdul Alim, Professor, Department of Mathematics, Bangladesh University of Engineering and Technology who restlessly supported me through the M. Phil process. I would like to thank him for his invaluable contribution. His knowledge about the M. Phil process is beyond par. His contribution to this thesis, however, does not only encompass his role as an academic supervisor, but include his ongoing friendship, care and support on a personal level without which this journey may have never been completed.

My special thanks to Dr. Salma Parvin, Professor, Department of Mathematics, Bangladesh University of Engineering and Technology, whose support was imperative in the beginning stages of the M. Phil process. Her stimulating and enthusiastic encouragement and guidance in regards to fluid dynamics in general and my M. Phil topic in particular have challenged and greatly contributed to my thinking on dissertation.

I owe my gratitude to all my colleagues in Department of Mathematics, BUET who have assisted me by providing relevant books, necessary information and valuable suggestions.
My deep love and appreciation goes to my family members for creating a delightful atmosphere as well as relieving me from family duties in order to complete the courses, research studies and final production of the thesis work. These past several years have not been an easy ride for me, both academically and personally. I truly thank my family members for keeping faith in my quirkiness and intellect as well as sticking by my side, even when I was irritable and depressed.

Abstract

An elaborate numerical study of developing a model regarding conjugate effect of fluid flow and heat transfer in a heat conducting vertical walled cavity filled with copper-water nanofluid has been presented in this thesis. This model is mainly adopted for a cooling of electronic device and to control the fluid flow and heat transfer mechanism in an enclosure. The numerical results have been provided in graphical form showing effect of various relevant non-dimensional parameters. The relevant governing equations have been solved by using finite element method of Galerkin weighted residual approach. The analysis uses a two dimensional rectangular enclosure under conjugate convective conductive heat transfer conditions. The enclosure exposed to a constant and uniform heat flux at the left vertical thick wall generating a natural convection flow. The thicknesses of the remaining parts of the walls are assumed to be zero. The right wall is kept at a low constant temperature, while the horizontal walls are assumed to be adiabatic. A moveable divider is attached at the bottom wall of the cavity. The governing equations are derived for the conceptual model in the Cartesian coordinate system.

Firstly, conjugate heat transfer in a rectangular enclosure filled with nanofluid is numerically investigated. Study have been carried out for the solid volume fraction $0 \leq \phi \leq 0.05$. The effects of Rayleigh number, the value of convective heat transfer coefficient, location of the divider position, the solid fluid thermal conductivity ratio and thickness of solid wall on the hydrodynamic and thermal characteristic of flow have been analyzed. Results are presented in the form of streamlines, isotherms and average Nusselt number. An increase in the average Nusselt number was found with the solid concentration for the whole range of Rayleigh number. In addition, the obtained results show a considerable effect on the heat transfer enhancement. In particular it is interesting to mention that divider can be located inside the partition to control heat transfer especially in electronic device.

Secondly, the numerical solution will also be carried out for the problem of MHD conjugate natural convection flow in a rectangular enclosure filled with electrically conducting fluid. The effect of Hartmann number on the pertinent parameters on the flow and temperature fields and heat transfer performance of the enclosure will also be examined. It is expected that the heat transfer rate will increase with an increase of Rayleigh number, divider position and solid fluid thermal conductivity ratio, but it should

decrease with an increase of the Hartmann number. It is also expected that an increase of the solid volume fraction will enhance the heat transfer performance.

Contents

Nomenclature

C_p Specific heat capacity (J/K)

B_0 magnetic field stregth (Wb/m^2)

g   gravitational acceleration (m/s^2)

Gr Grashof number ($\beta g H^4 q'' / k v^2$)

H   height of cavity (m)

h_∞ convective heat transfer coefficient (W/ m^{2}K)

Ha Hartmann number

L   width of cavity (m)

l_1 distance between the left wall and the divider (m)

K thermal conductivity (W/mK)

K_r conductivity ratio $\left(K_r = \frac{\kappa_w}{k_f} \right)$

Nu Nusselt number

Nu_l local Nusselt number

Nu_{av} average Nusselt number

p   pressure (N/ m^2)

P   dimensionless pressure

Pr Prandtl number, $\frac{v_f}{\alpha_f}$

q'' or q heat generation per area,(W/ m^2)

Ra Rayleigh number ($\beta g H^4 q'' / k v \alpha$)

T   temperature (K)

T_∞ ambient air flow

u,v   components of velocity (m/s)

U,V   dimensionless velocity components

x,y   Cartesian coordinates (m)

w width of the thick wall (m)

w_1 dimensionless width of the thick wall

X,Y   dimensionless Cartesian coordinates

Greek symbols

α thermal diffusivity (m^{2}s^{-1})

β coefficient of thermal expansion (K^{-1})

ϕ solid volume fraction

ΔT Ref. temperature difference $\left(q'' L/K_f \right)$

θ dimensionless fluid temperature

μ dynamic viscosity of the fluid (m^{2}s^{-1})

v kinematic viscosity of the fluid (m^{2}s^{-1})

ρ density of the fluid (kgm^{-3})

σ fluid electrical conductivity (Ω^{-1}.m^{-1})

ψ stream function

Subscripts
av   average
c   cold wall
f   pure fluid
nf   nanofluid
p   nanoparticles
s   solid
w   wall

Abbreviation
B E   boundary element
B V   boundary volume
CBC   convective boundary conditions
CFD   computational fluid dynamics
F D   finite difference
F E   finite element
F EM   finite element method
F V   finite volume
MHD   Magnetohydrodynamic

List of Tables

List of Figures

Chapter 1: Introduction

1.1 Introduction

Conjugate heat transfer occurs when the solution of the conductive heat transfer in the solid domain becomes as significant as the solution of the convective heat transfer in the fluid domain, to the solution of the overall heat transfer problem. It is well established that when convective heat transfer is strongly dependent on thermal boundary conditions, consideration of convective heat transfer problems as conjugate problems is necessary to obtain physically more strict results. Many research efforts have been given to the conjugate problem of forced convection heat transfer problems for both experimental and theoretical but few works have been devoted to the conjugate problem of natural convection. Heat transfer in solids and fluids is combined in the majority of applications. This is because fluid flow around solids or between solid walls, and because solid are usually immersed in a fluid. An accurate description of heat transfer modes, materials properties, flow regimes and geometrical configurations enables the analysis of temperature fields and heat transfer. Such a description is also the starting point for a numerical simulation that can be used to predict conjugate heat transfer effects or to test different configuration in order, for example, to improve thermal performances of a given application.

1.1.1 Heat Transfer by Solids and Fluids

Heat transfer in a solid

In most cases, heat transfer in solids, if only due to conduction, is described by Fourier's law defining the conductive heat flux, q proportional to the temperature gradient.

$$q = -\kappa \Delta T.$$

For a time dependent problem the temperature field in an immobile solid verifies the following form of the heat transfer equation:

$$\rho C_P \frac{\partial T}{\partial t} = \nabla.(\kappa \Delta T) + Q$$

Heat Transfer in a fluid

Due to the fluid motion, three contributions to the heat equation are included:

1. The transport of fluid implies energy transport too, which appears in the heat equation as the convective contribution. Depending on the thermal properties on

the fluid and on the flow regime, either the convective or the conductive heat transfer can dominate.

2. The viscous effect of the fluid flow produces fluid heating. This term is often neglected, nevertheless, its contribution is noticeable for fast flow in viscous fluids.

3. As soon as a fluid density is temperature dependent, a pressure work term contributes to the heat equation. This accounts for the well known effect, for example, compressing air produces heat.

1.1.2 Conjugate Heat Transfer Applications

Effective heat transfer

Efficiently combining heat transfer in fluids and solids is the key to designing effective coolers, heaters, or heat exchangers. The fluid usually plays a role of energy carrier on large distances. Natural convection is the most common way to achieve high heat transfer rate. In some applications, the performances are further improved by combining convection with phase change, for example liquid water to vapor phase change. Even so, solids are also needed, in particular to separate fluids in heat exchanger so that fluids exchange energy without being mixed. Solids are usually made of metal with high thermal conductivity. They dissipate heat by increasing the exchange area between the solid part and the surrounding fluid.

Energy Savings

Heat transfer in fluids and solids can also be combined to minimize heat losses in various devices. Because most gases have small thermal conductivities, they can be used as thermal insulators, provided they are not in motion. It is important to limit the heat close to the solid temperature, and far from the interface, the fluid temperature is close to the ambient fluid temperature. The distance where the fluid temperature varies from the solid temperature to the bulk temperature is called the thermal boundary layer.

1.1.3 Nanofluids

The fluids with nano-sized solid particles suspended in them are called ―nanofluids". In other words, nanofluid is a fluid containing nanometer-sized particles, called nanoparticles. It is well known that 1 Nano-meter = 10^{-9}m. Also, a nanoparticle is defined as the smallest unit that can still behave as a whole entity in terms of properties and transport. Suspensions of nanoparticles (i.e., particles with diameters < 100 nm) in liquids,

termed nanofluids, show remarkable thermal and optical property changes from the base liquid at low particle loadings. Nanofluids have been studied by Choi (1995) for at least 15 years and have shown promise to enhance a wide range of liquid properties. The primary limitation of convectional fluids such as water, ethylene glycol or propylene glycol is their low thermal conductivity. Use of metallic nanoparticles with high thermal conductivity will increase the effective thermal conductivity of these types of fluid remarkably. It has been shown that mixing nanoparticles in a liquid (nanofluid) has a dramatic effect on the liquid thermophysical properties such as thermal conductivity.

1.1.4 Heat Transfer in Cavities

Heat transfer in cavities is a topic of contemporary importance, because cavities filled with fluid are main components in a long list of engineering and geophysical systems. The flow and heat transfer induced in a cavity differs fundamentally from the external convective boundary layer. The flow and heat transfer in a cavity is the result of the complex interaction between finite size fluid system and thermal communication with the confining walls. It differs from the external convective boundary layer that is caused by the interaction between a single wall and a very large fluid reservoir. The complexity of this internal interaction is responsible for the diversity of flows that can exist inside the cavity.

The phenomenon of natural convection in cavities is the movement of the fluid by the buoyancy forces which occurs due to temperature differences affecting the density. By heating, the density change in the boundary layer causes the fluid to rise, that is hotter fluid is replaced by cooler fluid that again be heated and rise. The fluid flow and heat transfer in a rectangular cavity where the flow is induced by conjugate heat transfer of solid and fluid resulting from the boundary conditions and heat flux with the buoyancy force due to uniform temperature of the cavity wall studied extensively by researchers to understand the interaction between buoyancy and shearing forces in such flow situation. Therefore it is also important to understand the effect of conjugate heat transfer on fluid flow and heat transfer characteristics of natural convection in a rectangular cavity.

1.1.5 Thermal Conductivity

Thermal conductivity is the intensive property of fluid that indicates its ability to conduct heat. It is evaluated primarily in terms of Fourier's law for heat conduction. Thermal conduction is the spontaneous transfer of thermal energy through fluid, from a region of

high temperature to a region of lower temperature. Thermal conductivity of fluids is temperature dependent. The reciprocal of thermal conductivity is called thermal resistivity.

The fluids that have been traditionally used for heat transfer applications have a rather low thermal conductivity, taking into account the rising demands of modern technology. Thus, there is a need to develop new types of fluids that will be more effective in terms of heat exchange performance. In order to achieve this, it has been recently proposed to disperse small amounts of nanometer-sized solids in the fluid. The resulting ―nanofluid‖ is a multiphase material that is macroscopically uniform. If it is focused on maximizing the heat transfer coefficient, it is clear that the thermal conductivity of the fluid is the dominant parameter.

1.1.6 Heat Flux

Heat flux is defined as the amount of heat transferred per unit area per unit time from or to a surface. In a basic sense it is a derived quantity since it involves two quantities, the amount of heat transfer per unit time and the area from/to which this heat transfer takes place. In practice, the heat flux is measured by the change in temperature brought about by its effect on a sensor of known area. The temperature field set up may either perpendicular to the direction of heat flux or parallel to the direction of heat flux.

It is possible to quantify heat transfer process in terms of appropriate rate equations. These equations may be used to compute the amount of energy being transferred per unit time. Heat flux may occur in three ways, conduction heat flux, convection heat flux and radiation heat flux.

For conduction the rate equation is expressed as, $q'' = -\kappa \dfrac{dT}{dx}$

The heat flux q'' (W/m^2) is the heat transfer rate in the x direction per unit area perpendicular to the direction of transfer, and it is proportional to the temperature gradient $\dfrac{dT}{dx}$, in this direction. The proportionally constant κ is a transport property known as the thermal conductivity (W/mK) and is a characteristic of the wall material. The minus sign is a consequence of the fact that heat is transfer in the direction of decreasing temperature.

The heat transfer by convection is describe by $q = h\,A(T_w - T_\infty)$

Where,

q =Heat transfer rate (W)

h=Convective heat transfer coefficient (W/m^2K)

$T_{w=}$Wall temperature (K)

T_∞ =Free stream fluid temperature (K)

1.1.7 Magnetohydrodynamics

The branch of science, which deals with the flow of electrically conducting fluids in electric and magnetic fields, is known as Magnetohydrodynamics (MHD). The motion of the conducting fluid across the magnetic field generates electric currents which change the magnetic field and the action of the magnetic field on these currents give rise to mechanical forces, which modify the fluid flow direction. Probably the largest advance towards an understanding of such phenomena comes from the fields of astrophysics and geophysics, where it is still very important. MHD principles in the design of heat exchanger, pumps and flow meters, space vehicle propulsion, control and re-entry in creating novel power generating systems and developing confinement schemes for controlled fusion are employed by engineers. Further potential applications for MHD include electromagnets with fluid conductors, various energy conversion or storage devices, and magnetically controlled lubrication by conducting fluids etc. Charged particles in an electric circuit are accelerated by an electric field but give up some of their kinetic energy each time they collide with an ion. The increase in the kinetic or vibrational energy of the ions manifests itself as heat and a rise in the temperature of the conductor. Hence energy is transferred from the electrical power supply to the conductor and any materials with which it is in thermal contact.

1.2 Literature Review

1.2.1 Effect of Conjugate Heat Transfer

The heat transfer enhancement is one of the most important technical aims for engineering system due to its wide applications. The natural convection heat transfer in the enclosures has been studied extensively, because it is presented in various engineering systems. However the effect of the solid walls bounded to the fluid bed has received much attention in recent year due to its application in the cooling systems of electronics components, the

buildings and thermal insulation system, the nuclear reactor systems, the food storage industry and the build –in-storage solar collectors. In convection heat transfer analysis, it is common practice to consider the temperature or the heat flux at the fluid-wall-interface as known a priori. The result thus obtained is good only for heat transfer in flows bounded by wall having extremely small thermal resistance, i.e. very high thermal conductivity or very small thickness. However in actual practices, the wall thermal resistance is finite and the thermal condition at the fluid wall interfaces are different from their counterparts imposed at the outer surface of the solid walls. Such type of problems, where heat conduction in the solid is coupled with convection heat transfer in the fluid is often referred to as conjugate problem. Conjugate natural convection in a rectangular enclosure surrounded by walls was firstly examined experimentally and numerically by Kim and Viskanta (1984, 1985). Their result shows that, wall conduction effects reduce the average temperature difference across the cavity, partially stabilized the flow and decrease the heat transfer rate. Kaminski and Prakash (1986) performed a numerical study on conjugate convection in a square cavity with a thick conduction wall on one of its vertical sides. They investigated three separate models: (i) two dimensional conduction in the thick wall (ii) one dimensional horizontal wall conduction (iii) a uniform solid –fluid interface temperature. The three models predict nearly the same values for the overall heat transfer. The influence of wall conduction on natural convection in an inclined square cavity was researched by Archarya and Tsang (1987). The heat removal strategies in many engineering applications such as cooling of electronic components rely on natural convection heat transfer due to its simplicity, minimum cost, low noise, smaller size and reliability. Ostrach (1988) indicates that natural convection in enclosures has attracted considerable interest amongst researchers in the past few decades. Heat producing electronic components of the mounted on a printed circuit board above a conducting plate. The heat produced is then transferred both by conduction through the plate to its two ends and by natural convection in the surrounding fluid to the heat sink. As a result, the heat removing rate from the electronic components will depend on the coupling of the wall conduction and the fluid convection. This coupling will directly influence the temperature distribution among the components and the design of heat removing mechanisms that was investigated by Du and Bilgen (1992). Mbaye et al. (1993) study the natural convection conduction problem for a rectangular porous cavity to investigate the effect of Rayleigh number and conductivity ratio on thermal and flow field. However, in many practical situations, especially those concerned with design of thermal insulation, conduction in the walls can have an important effect on natural convection flow in the enclosure. The primary limitation of convectional fluids such as water, ethylene, glycol or propylene glycol is their low thermal conductivity. Use of metallic nanoparticles with thermal conductivity will increase the effective thermal conductivity of those types of fluid remarkably. Thus, a requirement to a new class of fluid for improving both thermal

conductivity and suspension stability leads to the development of nanofluids first introduced by Choi (1995). Kimura et al. (1997) presented a review study to show different application of conjugate convection problem for porous medium. However, the effect of the Rayleigh number, dimensionless conductivity ratio, dimensionless wall width and inclination angle on the natural convection in an inclined enclosure bounded by a solid wall were investigated by Ben Yedder and Bilgen (1997). Finite element analysis of conjugate natural convection in a square enclosure with a conducting vertical wall was studied by Misra and Sarkar (1997). Liaqat and Baytas (2001) analyzed conjugate natural convection in a square enclosure containing volumetric sources. Shao-Feng Dong and Yin- Tang (2004) investigated conjugate natural convection and conduction in a complicated enclosure. Das and Reddy (2006) conducted conjugate natural convection heat transfer in an inclined square cavity containing a conducting block. Improvement of heat transfer using nanoscale particles suspended in a base fluid has been studied extensively in recent year by Jou and Tzeng (2006). Abdullatitif Ben Nakhi and Ali (2007) experimentally studied conjugate natural convection in a sqare enclosure with inclined thin fin of arbitrary length. Nawaf and Saeid (2007) made a numerical study to investigate the effect of conduction in one of the vertical walls in conduction natural convection problem in a porous square enclosure. They observed that either increasing the Rayleigh number and the thermal conductivity ratio or decreasing the thickness of solid bounded wall average Nusselt number can be increased. In the special cases of low Rayleigh number and high conductivity walls, the values of the average Nussel numbers are increasing with the increase of wall thickness. Mobedi (2008) studied conjugate natural convection in a square cavity with finite thickness horizontal walls. Ho et al. (2008) conducted these work using nanoparticle to improve the heat transfer rate. One of the systematic numerical investigations of this peoblem was conducted by Nouanegue et al. (2009), who considered heat transfer by natural convection, conduction and radiation in an inclined square enclosure bounded with a solid wall. Varol et al. (2009) investigated conjugate heat transfer in porous triangular enclosures with thick bottom wall. However the effect of nanoparticles on heat thansfer enhancement in natural convection was conducted by Aminossadati and Ghasemi (2009) , who considered natural convection cooling of a localized heat source at the bottom of a nanofluid filled enclosure. They found that the location of the heat sources provide to significantly affect the heat source maximum temperature. This problem may be encountered in a number of electronics devices equipped with nanofluids. Studies related with convective flows in different enclosure including wall of zero thickness can be found in the investigation of Lei et al. (2008), Bednarz et al.(2009), Pesso and Iiva (2009) , Jeng et al.(2009), Ching and Wu (2010), Vorol et al. (2010) and Sankar and Younghae (2010). Improvement of heat transfer using nanoscale particles suspended in a base fluid has been studied extensively in recent year by Eiyad Abu-Nada et al. (2010). Rahman and Alim (2010) investigated MHD mixed

convection flow in a vertical lid-driven square enclosure including a heat conducting horizontal circular cylinder with Joule heating. Zhang et al. (2011) studied conjugate convection in an enclosure with time periodic sidewall temperature and inclination. Recently, Aminossadati and Ghasemi (2012) investigated conjugate convection in an inclined nanofluid filled enclosure. Belazizia et al. (2012) conducted a numerical study of conjugate natural convection in a square enclosure with top active vertical wall. They obtained for a giver wall thickness d = 0.2, either increases the Rayleigh number and the thermal conductivity ratio can increase the average Nusselt number, the interface temperature and the flow velocity. Saleh and Hashmi (2014) investigated conjugate heat transfer in Rayleigh Bénard convection in a square enclosure. They found that the strength of the circulation of each cell can be controlled by the thickness of the bottom wall, the thermal conductivity ratio and the Rayleigh number**.**

1.2.2 Heat Transfer in Cavity with MHD Effect

The classical problem of natural convection in an enclosure has many engineering applications. In some practical cases such as the crystal growth in fluid, the metal casting, the fusion reactors and the geothermal energy extractions, the natural convection is under the influence of a magnetic field. Sparrow and Cess (1961) studied effect of magnetic field on free convection heat transfer. Sing and Cowling (1963) also studied thermal conduction in magnetohydrodynamics. Magnetohydrodynamic free convection was investigated by Riley(1964). Kuiken (1970) presented a numerical investigation of magnetohydrodynamic free convection in strong flow field. Oreper and Szekely (1983) studied the effect of an externally imposed magnetic field on buoyancy driven flow in a rectangular cavity. They found that the presence of a magnetic field could suppress natural convection current and that the strength of the magnetic field was one of the important factors in determining the quality of the crystal. Ozoe and Maruo (1987) investigated magnetic and gravitational natural convection of melted silicon on two dimensional numerical computations for the rate of heat transfer. Ozoe and Okada (1989) conducted the effect of the direction of the external magnetic field on the three dimensional natural convection in a cubic enclosure. Garandet (1992) studied natural convection heat transfer in a rectangular enclosure with a transverse magnetic field. Venkatachalappa and Subbaraya (1993) investigated natural convection in a rectangular enclosure in the presence of a magnetic field with uniform heat flux from the side walls. Alchaar et al. (1995) studied natural convection heat transfer in a rectangular enclosure with a transverse magnetic field. Rudraiah et al. (1995a) investigated the effect of surface tension on buoyancy driven flow of an electrically conducting fluid in

a rectangular cavity in the presence of a vertical transverse magnetic field to see how that force damped hydrodynamics movements. Rudruiah et al. (1995b) also studied the effect of a magnetic field on free convection in a rectangular enclosure. All these investigations show there has been an increasing interest to understand the flow behavior and the heat transfer mechanism of enclosure that are filled with electrically conducting fluids and are in the influence of a magnetic field. The common finding of these studies is that the fluid within the enclosure, which is under the magnetic effects, experiences a Lorentz force. This force in turn, affects the buoyancy flow field and the heat transfer rate. Nanofluids which enhanced thermal characteristics have widely been examined to improve the heat transfer performance of many engineering applications. Sarris et al. (2005) presented a numerical study of unsteady two dimensional natural convection of an electrically conducting fluid in a laterally and volumetrically heated square cavity under the influence of a magnetic field. Ece and Byuk (2006) examined the steady and laminar natural convection flow in the presence of a magnetic field in an inclined rectangular enclosure heated and cooled on adjacent walls. They found that the magnetic field suppressed the convective flow and the heat transfer rate. They also showed that the orientation and the aspect ratio of the enclosure and the strength and direction of the magnetic field had significant effects on the flow and temperature fields. Dulikravich and Colaca (2006) also found that the convection heat transfer can be controlled by the magnetic field. A numerical investigation on the double-diffusion convective flow in a rectangular enclosure by Teamah (2008) also concluded that the heat and mass transfer mechanism and the flow characteristics inside the enclosure strongly depend on the strength of the magnetic field and the heat generation. Sivasankaran and Ho (2008) numerically studied the effect of temperature dependent properties on the natural convection of water in a cavity under the influence of a magnetic field. They showed that the heat transfer rate is influenced by the direction of the external magnetic field and decrease with an increase of the magnetic field. Mamun et al. (2008) investigated MHD –conjugate heat transfer analysis for a vertical plate in presence of viscuss dissipation and heat generation. Kanveci and Oztuna (2009) numerically simulated the natural convection flow in a laterally heated partitioned enclosure and concluded that the magnetic field and its direction affect the heat transfer performance of the enclosure. Sathiyamoorthy and Chamkha (2010) used different thermal boundary conditions to examine the steady laminar two dimensional natural convection in the presence of inclined magnetic field in a square enclosure filled with a liquid gallium. They found that the heat transfer decrease with an increase of the magnetic field and the

vertically and horizontally applied magnetic fields affect the heat transfer differently. Most of the studies on the natural convection in enclosure with the magnetic field effects have considered the electrically conducting fluid with a low thermal conductivity. This, in turn, limits the enhancement of heat transfer in the enclosure particularly in the presence of magnetic field. Mansour et al. (2010) numerically investigated the unsteady magneto-hydrodynamic free convection in an inclined square cavity filled with a fluid-saturated porous medium and with internal heat generation. Finite element analysis on the conjugate effect of joule heating and magnetohydrodynamics on double –diffusion mixed convection in a horizontal channel with an open cavity was performed by Rahman et al. (2011), Ghasemi et al. (2011) studied magnetic field effect on natural convection in a nanofluid filled square enclosure. Nemati et al. (2012) studied magnetic field effects on natural convection flow of nanofluid in a rectangular cavity using the Lattice Boltzmann model. Effect of joule heating on natural convection in non-linearly heated square enclosure from right vertical wall was investigated by Oztop and Salem (2012). They found that flow becomes weaker near the right corner of the cavity due to non-isothermal boundary condition. They also showed that both Hartmann number and joule parameter have significant effects on heat transfer and fluid flow. As discussed earlier, the magnetic field results in the decrease of convective circulating flows within the enclosure filled with electrically conducting fluid, this, in turn, results the reduction of heat transfer. The addition of nanoparticles to the fluid can improve its thermal performance and enhance the heat transfer mechanism in the enclosure. In some engineering problems such as the magnetic field sensors, the magnetic storage media and the cooling system of electronics devices enhance heat transfer in desirable whereas the magnetic field weakens the convection flow field. Up until now, no significant studies include MHD effect on conjugate heat transfer flow on the natural convection in nanofluid filled enclosure. Hence the presence study numerically examines the effect of conjugate heat transfer on flow of nanofluid under the influence of horizontally applied magnetic field.

1.3 Motivation

In the light of above discussions, it is seen that there has been a good number of works in the field of fluid flow and convection heat transfer system in cavities. A very few works have been performed applying the effect of conjugate heat transfer on flow of nanofluid having finite conducting thick wall and uniform heat flux. To the best knowledge of the

author's no studies that investigate the magnetic field effect of conjugate heat transfer flow on the natural convection of nanofluid filled enclosure with heat conducting vertical wall have been reported in the literature. The mentioned effects have not been studied yet. The study of convection phenomena in cavities is important for numerous engineering applications. To apply a system as an effective heat transfer devices such as in designing nuclear reactors system, solar collectors, electrical, microelectronic equipments containers and in many other design problems convective heat transfer is predominant. In addition, coupled of laminar conductive convective heat transfer by free convection in a rectangular enclosure has many important engineering and geophysical applications such as nuclear energy, heating and cooling of buildings, solar collectors, building, refrigerators, heat exchangers, electronic cooling, chemical processing equipment, crystal growth in liquids and micro electromechanical systems. Therefore the analysis of the fluid flow and heat transfer in cavities for different boundary conditions and shapes are necessary to ensure efficient performance of heat transfer equipments. The heat flux can present the heat created by the electronic devices. In the present study, a divider is mounted to the bottom horizontal wall. It is interesting to mention that the divider can be located inside the cavity to control heat transfer especially in electronic device. The aim of the present study is to investigate the effect of the location of heat source and also the effect of nanofluid on the natural convection flow and temperature fields in the rectangular enclosure. Indeed this geometry is mainly adopted for cooling of electronic device. For that reason, necessary numerical studies are still required to monitor the variation of fluid flow and heat transfer due to the physical changes with economic and environmental considerations due to using nanofluid in assisted convection mode, which forms the basis of the motivation behind selecting the present work.

1.4 Overview of the Present Work

The present study is a numerical investigation on the conjugate heat transfer in a thick walled cavity filled with copper-water nanofluid. In the present investigation firstly, the analysis use a two dimensional rectangular enclosure under conjugate convection-conduction heat transfer conditions and considers a range of Rayleigh numbers. The enclosure was subjected to a constant conduction-convection uniform heat flux at the left wall generating a natural convection flow. The thicknesses of the other boundaries of the wall are assumed to be zero. The right wall is kept at a low constant temperature while the

horizontal walls are assumed to be adiabatic. A heat conducting moveable divider is mounted on the bottom horizontal wall. The study has been carried out for the Rayleigh number in the range of $10^5 \leq Ra \leq 10^7$ and for the solid volume fraction $0 \leq \phi \leq 0.05$. In the present investigation later a magnetic field is applied in the horizontal direction normal to the side walls of the cavity. The studies are reveal that the heat transfers in such arrangements are different from those studied in the above literature and it will therefore prove useful from the designer's point of view in choosing the best physical condition that suits him.

1.5 Objectives of the Present Study

The overall goal of this study is to numerically simulate fluid flow and heat transfer in a two-dimensional rectangular enclosure filled with Copper-water nanofluid under conjugate convective-conductive heat transfer conditions. The investigation is to be carried out at different non-dimensional governing parameters. Results are to be presented in terms of streamlines, isotherms as well as average Nusselt number for different values of governing parameters.

The specific aims of the present research work are as follows:

➢ To develop 2D mathematical model for conjugate conductive-convective heat transfer conditions.

➢ To solve the mathematical model using FEM (Finite Element Method).

➢ To investigate the effect of Rayleigh Number, solid volume fraction of nanofluids, the location of the divider, solid fluid thermal conductivity ratio, the solid wall thickness and also the value of the ambient convective heat transfer coefficient on the flow and thermal field in the cavity.

➢ To explore the effects of Hartmann number on Rayleigh Number, solid volume fraction of nanofluids, the location of the divider, the solid fluid thermal conductivity ratio, the thickness of the solid wall and also the value of the ambient convective heat transfer coefficient on the flow and thermal field throughout the cavity.

> ➢ To present the numerical results graphically for different values of the parameters entering into the present study.

> ➢ To validate the present results with relevant published numerical results.

1.6 Scope of the Thesis

A brief description of the present numerical investigation of the conjugate heat transfer in a thick walled cavity filled with nanofluid have been presented in this thesis through five chapters as stated below.

Chapter 1 contains introduction with the aim and objectives of the present work. This chapter also includes a literature review of the past studies on fluid flow and heat transfer in cavities which are relevant to the present work. Different aspects of the previous studies have been mentioned categorically. Present study and motivation behind it has also been incorporated in this chapter.

Chapter 2 presents a short introduction of numerical methods. Then, the Finite Element Method is discussed in this chapter in details. Model equations with their solutions using the software are described in a nutshell in this chapter. Creation of geometry, meshing, implementation of physics, boundary conditions, and other rate equations, implementation of boundary are also included here.

In Chapter 3, a detailed parametric study regarding the effect of conjugate heat transfer on finite element simulation is applied to perform the analysis on the flow of laminar free convection heat transfer and fluid flow in a rectangular cavity with heat conducting vertical wall and uniform heat flux. Effects of the parameters such as Rayleigh number(Ra), convective heat transfer coefficient(h_∞), position of divider (l_1), solid fluid thermal conductivity ratio (K_r) and solid wall thickness (w_1) on heat transfer and fluid flow inside the cavity have been presented for better understanding the heat transfer mechanisms in such cavities.

Chapter 4 describes the effect of MHD on conjugate natural convection heat transfer in a rectangular enclosure with heat conducting vertical wall and uniform heat flux with solid volume fraction $\phi = 5\%$. Numerical results in terms of streamlines, isotherms for parametric studies for the relevant parameters are also performed in this chapter for the range of Hartmann number (Ha) from 0 to 60.

Finally in chapter 5, the concluding remarks of the whole work and the recommendation for the future work have been presented systematically.

Chapter 2: Numerical Techniques

2.1 Introduction

A numerical technique is a complete and unambiguous set of procedures for the solution of a problem, together with computable error estimates. The study and implementation of such methods is the province of numerical analysis. Physical phenomena may be described mathematically by ordinary or partial differential equations, which are the subject matter of analytical and numerical investigations. The partial differential equations concerning fluid mechanics and heat transfer may be solved analytically only for a limited number of cases. With the help of computer, approximate solution may be obtained numerically where the differential equations are approximated by a system of algebraic equations using discretization technique. The solution domain is discretized into small sub-domains where the numerical solutions give results at discrete locations in space and time. The accuracy of numerical results depends on the accuracy of available experimental data and the quality of discretizations used.

Computational fluid dynamics (CFD), is a branch of fluid mechanics that uses numerical methods and algorithms to solve and analyze problems of fluid flows. Computers are used to perform the calculations required to simulate the interaction of liquids and gases with surfaces defined by boundary conditions. With high-speed supercomputers, better solutions can be achieved. Engineers use CFD codes that can make physically realistic results with high accuracy in simulations using finite grids. Contained within the broad field of computational fluid dynamics are activities that cover the range from the automation of well established engineering design methods to the use of detailed solutions of the Navier-Stokes equations as substitutes for experimental research into the nature of complex flows. CFD have been used for solving wide range of fluid dynamics problem. It is most frequently used in fields of engineering where the geometry is complicated or some important features that cannot be dealt with other methods. Details are available in Ferziger and Perić (1997) and Patankar (1980).

2.2 Advantages of Numerical Analysis

The problems of fluid flow and heat transfer may be analyzed either theoretically or experimentally. From the economical point of view, experimental investigation of such problems could not draw much attention because of their inadequate flexibility and

applications. However, often experimental investigation is necessary to validate numerical method. Separate experimental arrangement set up requires for any change in the geometry and boundary condition of the systems for their investigation. Time involvement is also a factor to make it unappealing. On the other hand, the theoretical analysis can be carried out either by analytical approach or by numerical approach. In solving the practical problems, the analytical solution methods are not of much popular. Numerical methods are extremely powerful problem-solving tools that are capable of handling large systems of equation, complicated geometries etc., which is often impossible to solve analytically. General closed form solutions can be obtained only for very ideal cases and the results obtained for a particular problem, usually with uniform boundary conditions. For two-dimensional thermodynamic problems, mathematical model involve partial differential equations that are required to be solved simultaneously with some boundary conditions. Therefore, numerical methods are the easier way to find out solutions of the problems of practical interest because it reduces higher mathematics to basic arithmetic operations.

2.3 Major Steps of a Numerical Solution

According to Ferziger and Perić (1997), the main steps from various components of numerical solution are as follows:

2.3.1 Mathematical Model

The starting point of any numerical method is to develop a mathematical model which consists of a set of partial differential equations or integra-differential equations and boundary conditions. A solution method is usually designed for a particular set of equations. A general-purpose solution method, i.e. one which is applicable to all flows, is impractical, though not impossible and with most general purpose tools, they are usually not optimum for any single application.

2.3.2 Discretization Technique

After selecting the mathematical model, one has to choose a suitable discretization method, i.e. a method of approximating the differential equations by a system of algebraic equations for the variable at some set of discrete locations in space and time. There are several approaches, the most important of which are: finite difference (FD), finite volume (FV) and finite element (FE) methods.

2.3.3 Mesh

The discrete locations at which the variables are to be calculated are defined by a mesh which covers the geometric domain on which the problem is to be solved. It divides the solution domain into a finite number of sub-domains called finite elements, control volumes, etc.

2.3.4 Accuracy

Numerical solutions of physical event are only approximate solutions. Numerical solutions usually incorporate three kinds of systematic errors.

- Modeling errors which occur due to the difference between the actual physical phenomena and the exact solution of the mathematical model.

- Discretization errors, defined as the dissimilarity between the exact solution of the equation of the model and the exact solution of that algebraic system of equations obtained by discretizing these equations

- Iteration errors, defined as the difference between the iterative and exact solutions of the algebraic systems of equations.

It is important to identify these errors, and distinguish them. Various errors may cancel each other, so that sometimes a solution obtained on a coarse mesh, pretends to agree better with the experiment than a solution on a finer mesh, which should be more accurate. Therefore, meshing has to be dealt with very carefully.

2.3.5 Solution Method

Practical applications of the finite element method lead to large systems of simultaneous linear algebraic equations. Fortunately, finite element equation systems possess some properties which allow reducing storage and computing time. The finite element equation systems are: symmetric, positive definite and sparse. Symmetry allows storing only half of the matrix including diagonal entries. Positive definite matrices are characterized by large positive entries on the main diagonal. Solution can be carried out without pivoting. A sparse matrix contains more zero entries than nonzero entries. Sparsely can be used to economize storage and computations. Solution methods for linear equation systems can be divided into two large groups: direct methods and iterative methods. Direct solution methods are usually used for problems of moderate size. For large problems iterative

methods require less computing time and hence they are preferable. The choice of solver depends on the grid type and the number of nodes involved in each algebraic equation.

2.4 Finite Element Modeling: Implementation and Solution

The solution of the Fluid flow and heat transfer model equations (presented in chapters 3 and chapter 4) provides the predictions of state variables (e.g., velocity, temperature) in space and time. The solutions of coupled partial differential equations (PDE) require the numerical method. The FEM, is used to solve the model equations of fluid flow and heat transfer. The FEM solution provides a quantitative understanding of heat transfer.

2.4.1 Numerical Solution

Discretization is the first step to solve numerically a mathematical model of physical phenomena. That is, the differential equations are transformed into a ―numerical analogue‖ which can be represented in the computer and then processed by a computer program built on some algorithm. There are many discretisation schemes such as Finite difference (FD), Finite volume (FV), Finite element (FE) methods, Boundary element (BE) method and Boundary volume (BV) method. The present numerical computation has been performed by finite element method (FEM). Detailed analysis of this method is available in Chung (2002) and Dechaumphai (1999). In the past few years the growth of powerful computers with greater computational capabilities has facilitated the formulation of sophisticated numerical methods that simulate the real physical systems by solving complex mathematical models [Moens and Vandepitte (2005), Mohamed (2010), Wang and Sun (2003)]. In the literature, there are different numerical methods which include differential methods (e.g., Finite difference method, FDM), integral methods (variation and weighted residuals, e.g., FEM), and stochastic methods (e.g. Monte Carlo method) [Sandeep et al. (2008)]. In engineering applications, the FDM and the FEM are the commonly employed numerical techniques [Puri and Anantheswaran (1993), Reddy (1993)]. The former is a less complex and computationally inexpensive method compared to the latter [Wang and Sun (2003)]. However, the latter has several advantages compared to the former – the FEM is more flexible in handling the spatial variation of material properties, irregular shape and regions, nonlinear problem, mixed boundary and initial conditions [Martins et al. (2008), Zienkiewicz and Taylor (1991)]. Therefore, FEM was chosen to solve the mathematical model of heat transfer.

2.4.2 Finite Element Method

The finite element discretization divides the problem domain of interest into a finite number of elements, and each element is connected to each other at points called nodes [Sandeep et al. (2008)]. The collection of the elements and nodes is called the Finite Element mesh (Figure 2.1). The nodes typically lie on the element boundary where adjacent elements are connected. The nodal values of the field variable and the interpolating functions for the elements define the behavior of the field variable within the elements. The nodal points depict the field variable or the unknown, defined in terms of approximating or interpolating functions within each element. A detailed discussion of the FEM and techniques can be found in many books, for example Martins et al. (2008), Puri and Anantheswaran (1993).

Investigation using numerical technique is the most economical method and can address to solve complicated physical problems easily than done by the other methods. Finite
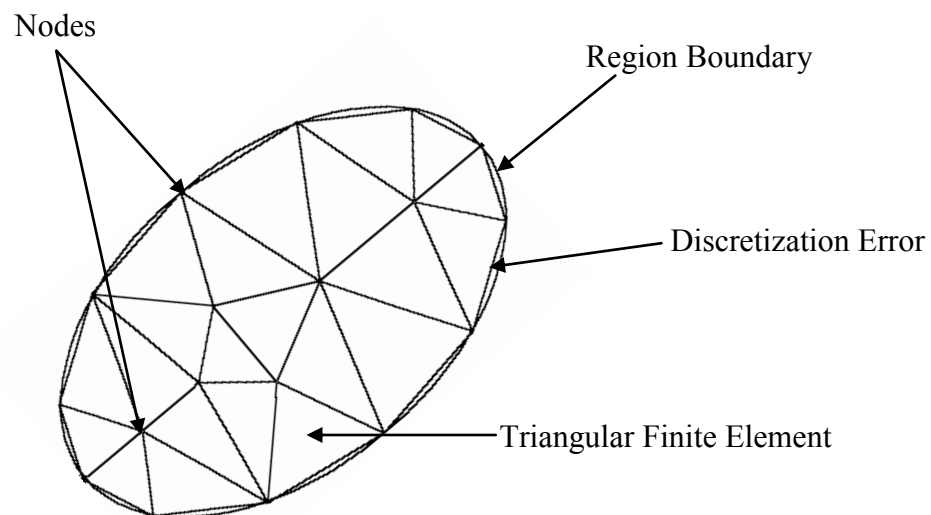
Figure 2.1**:** Two-dimensional Finite Element mesh.

element modeling appears to be the best option for the desired solution. Therefore, these are described in this chapter elaborately.

2.5 Computational Procedure

The Galerkin finite element method of Taylor and Hood (1973) and Dechaumphai (1999) is used to solve the non-dimensional governing equations along with boundary conditions for the considered problem. The equation of continuity has been used as a constraint due

to mass conservation. The finite element method is used to solve the Eqs. (3.6) - (3.9). The continuity equation is automatically fulfilled for large values of this constraint. Then the velocity components (U, V) and temperature (θ) are expanded using a basis set. The Galerkin finite element technique yields the subsequent nonlinear residual equations. Three points Gaussian quadrature is used to evaluate the integrals in these equations. Then the non-linear residual equations are solved using Newton-Raphson method to determine the coefficients of the expansions. The convergence of solutions is assumed when the relative error for each variable between consecutive iterations is recorded below the convergence criterion such that $|\psi^{n+1} - \psi^n| \leq 10^{-4}$, where n is the number of iteration and ψ is a function of U, V and θ.

Algorithm

The algorithm was originally put forward by the iterative Newton-Raphson algorithm; the discrete forms of the continuity, momentum and energy equations are solved to find out the value of the velocity and the temperature. It is essential to guess the initial values of the variables. Then the numerical solutions of the variables are obtained while the convergence criterion is fulfilled. The simple algorithm is shown by the flow chart in the next page.

Physical model

↓

Governing equations

↓

Boundary conditions

↓

Mesh generation

Initial guess values of U^*, V^*, θ^*

↓

Start

↓

Forming 6x6 matrix against an element

↓

Assemble all elements

↓

Matrix factorization

U, V, θ

↓

Convergence

No

Yes

↓

Stop
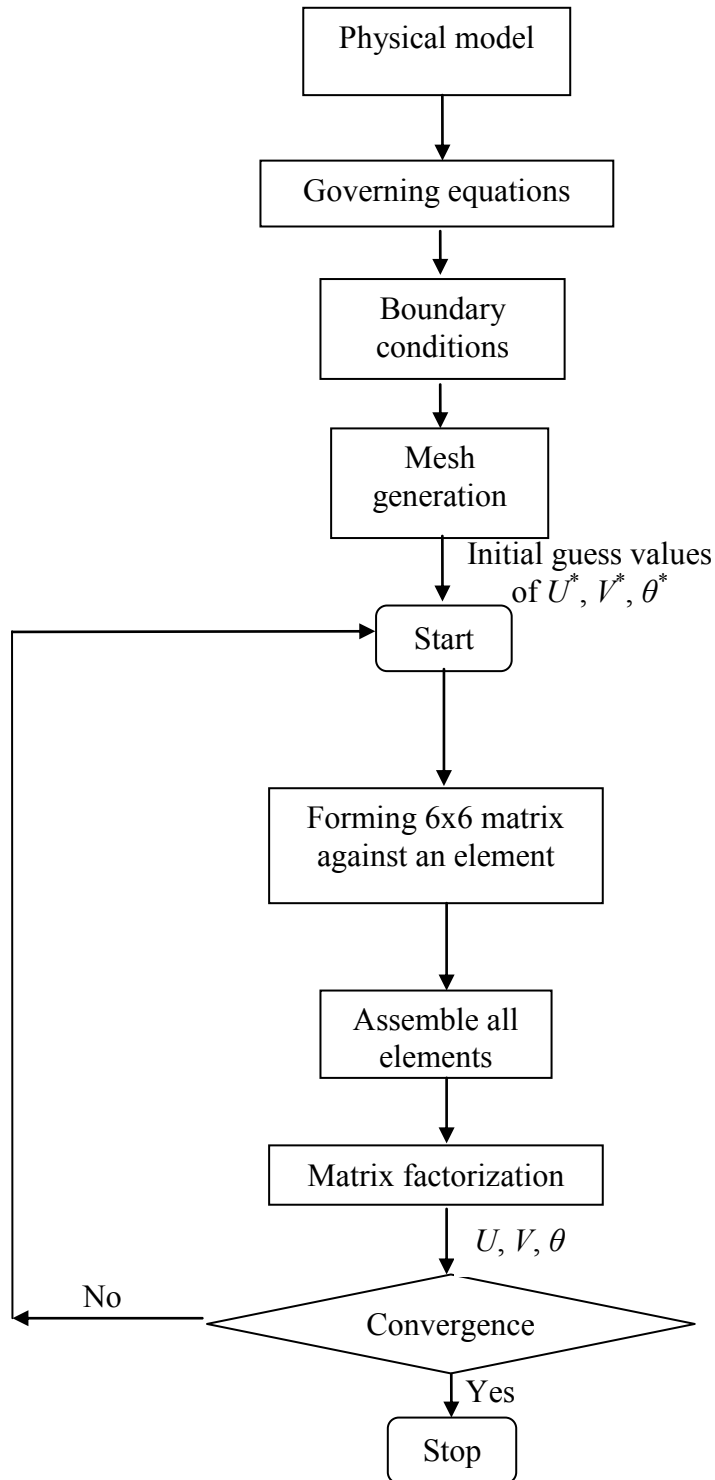
Flow chart of the computational procedure

Chapter 3: Effect of Conjugate Heat Transfer on Flow of Nanofluid

3.1 Introduction

Natural convection inside enclosure has received a noticeable attention of investigation. This is due to their extensive applications in industry like cooling or heating system, energy storage system, heat dissipation from electronic components etc. Recently the natural convection was widely improved by using the technique of nanofluid. Heat transfer in solids and heat transfer in fluids are combined in the majority of applications. This is because fluid flow around solid or between solids walls and solid are usually immersed in a fluid. The term conjugate heat transfer is used to describe processes which involve variation of temperature within the solids and fluids due to thermal interaction between solids and fluids. A typical example is the heating or cooling of a solid object by the flow of air in which it is immersed. The conjugate heat transfer model was developed after computer came into wide use in order to substitute the empirical relation of proportionality of heat flux to temperature difference with heat transfer coefficient which was the only tool in theoretical heat convection. This model, base on strictly mathematically stated problem, describes the heat transfer between a body and a fluid inside it as a result of two object. The physical procedure and solution of the governing equations are considered separately for each object in two sub domains. Matching conditions for these solutions at the interface provide the distribution of velocity, temperature and heat flux along the body and the flow interface. The conjugate convection heat transfer problem is governed by the set of equations consisting two separate systems for solid body and fluid domain, which is done by a set of partial differential equations for both the fluid and solid domain and with corresponding boundary conditions, which allow the simulation of heat transfer between solid and fluid.

The generalized governing equations are used based on the conservation law of mass, momentum and energy. As the fluid velocity and the heat transfer depend upon a number of factors, a dimensional analysis is presented to show the importance of non-dimensional parameters, which will influence the dimensionless heat transfer parameter, i.e. Nusselt number(Nu).

In the present study an analysis is carried out to investigate the effect of conjugate heat transfer on flow of nanofluid in a rectangular enclosure with heat conducting vertical wall and uniform heat flux.

3.2 Physical Model

The schematic diagram of the present study displays in **Figure 3.1**. It consists of two dimensional rectangular enclosure filled with electrically conducting fluid sides of width L and height H under conjugate conduction convection heat transfer. The enclosure expose to a uniform constant heat flux q, which is maintained at the ambient air flow. The left wall has a thickness of $w_1 = \frac{w}{L} = 0.1$, while the thicknesses of the other boundaries of the wall are assumed to be zero. The right wall is kept at a low temperature T_c, while the horizontal walls are assumed adiabatic. A movable conducting divider of length 0.2 and width 0.1 is attached to the horizontal bottom wall of the cavity. The rectangular enclosure is filled with a suspension of copper nanoparticles in water. The nanofluid used in the analysis is assumed to be Newtonian, incompressible and laminar. The shape and the size of the nanoparticles are assumed to be uniform. The base fluid and nanoparticles (Cu) are in thermal equilibrium and there is no slip between them.
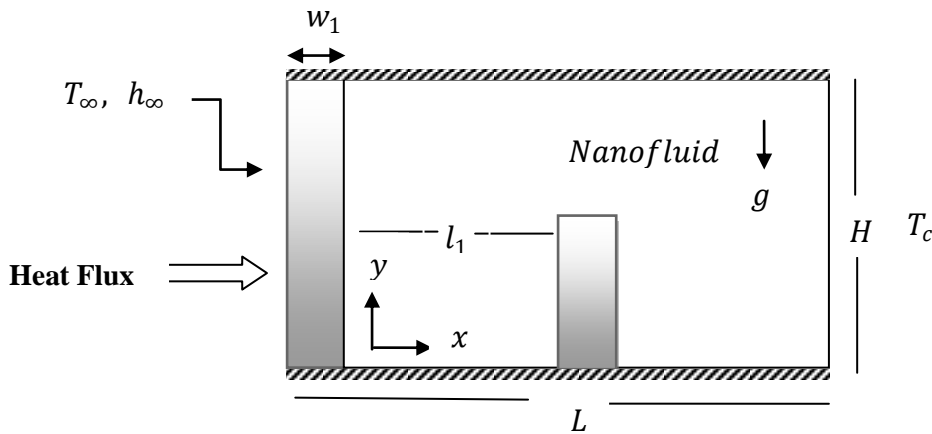

Figure 3.1: Physical Geometry of the Model

The thermo-physical properties of the fluid and nanoparticles are given in Table 3.1. The thermophysical properties of the nanofluid are assumed constant except for the density properties of nanoparticles and fluid are taken to be constant which determine base on Boussinesq approximation. The effect of viscous dissipation is neglected.

3.3 Mathematical Formulation

Several steps for mathematical formulation of the above physical model are as follows.

3.3.1 Governing Equation in Dimensional Form

In the present problem, the flow is considered to be steady, two-dimensional, laminar, incompressible and there is no viscous dissipation. The gravitational force acts in the vertically downward direction. Under the above assumptions, the system of equations governing the flow using conservation of mass, momentum and energy equations for nanofluid and solid in dimensional form can be written as follows:

For Fluid:

Continuity Equation:

$$\frac{\partial u}{\partial x} + \frac{\partial v}{\partial y} = 0 \tag{3.1}$$

Momentum Equations:

$$u\frac{\partial u}{\partial x} + v\frac{\partial u}{\partial y} = \frac{1}{\rho_{nf}}\left[-\frac{\partial p}{\partial x} + \mu_{nf}\left(\frac{\partial^2 u}{\partial x^2} + \frac{\partial^2 u}{\partial y^2}\right)\right] \tag{3.2}$$

$$u\frac{\partial v}{\partial x} + v\frac{\partial v}{\partial y} = \frac{1}{\rho_{nf}}\left[-\frac{\partial p}{\partial y} + \mu_{nf}\left(\frac{\partial^2 v}{\partial x^2} + \frac{\partial^2 v}{\partial y^2}\right) + (\rho\beta)_{nf}\, g(T - T_c)\right] \tag{3.3}$$

Energy Equation:

$$u\frac{\partial T}{\partial x} + v\frac{\partial T}{\partial y} = \alpha_{nf}\left(\frac{\partial^2 T}{\partial x^2} + \frac{\partial^2 T}{\partial y^2}\right) \tag{3.4}$$

For Solid:

Energy Equation:

$$\frac{\partial^2 T_w}{\partial x^2} + \frac{\partial^2 T_w}{\partial y^2} = 0 \tag{3.5}$$

where the effective density of the nanofluid is given as

$$\rho_{nf} = (1 - \phi)\rho_f + \phi\rho_p$$

where ϕ is the solid volume fraction of nanoparticles. In addition the thermal diffusivity of the nanofluid is

$$\alpha_{nf} = \frac{\kappa_{nf}}{(\rho\, C_p)_{nf}}$$

Where $(\rho C_p)_{nf}$ is the heat capacity of the nanofluid and expressed as

$$\left(\rho C_p\right)_{nf} = (1 - \phi)\left(\rho C_p\right)_f + \phi\left(\rho C_p\right)_p$$

additionally, the thermal expansion coefficient of the nanofluid $(\rho\beta)_{nf}$ is expressed as

$$(\rho\beta)_{nf} = (1 - \phi)(\rho\beta)_f + \phi(\rho\beta)_p$$

The effective dynamic viscosity of the nanofluid is given by Brinkmann(1952) is,

$$\mu_{nf} = \frac{\mu_f}{(1 - \phi)^{2.5}}$$

The Maxwell (1904) model for thermal conductivity of solid liquid mixture of relatively large particles (micro/mini size) is good for low solid concentration. The thermal conductivity which for spherical nanoparticles, according to Maxwell (1904) is

$$\kappa_{nf} = \kappa_f \left[\frac{\left(\kappa_p + 2\kappa_f\right) - 2\phi\left(\kappa_f - \kappa_p\right)}{\left(\kappa_p + 2\kappa_f\right) + \phi\left(\kappa_f - \kappa_p\right)} \right]$$

where κ_p is the thermal conductivity of dispersed nanoparticles and κ_f is the thermal conductivity of pure fluid.

3.3.2 Boundary Conditions

The boundary conditions for the present problem are specified as follows:

For all rigid walls: $u = v = 0$

At the right vertical wall: $T = T_c$

At the top and bottom walls: $\frac{\partial T}{\partial y} = 0$

At the left side of thick wall: $q = -\kappa_w \frac{\partial T}{\partial x}|_w + h_\infty (T_w - T_\infty)$

At the divider surface: $u = v = 0$

At the fluid solid wall interfaces: $\kappa_w \frac{\partial T}{\partial x}|_w = \kappa_{nf} \frac{\partial T}{\partial x}|_{nf}$

The average Nusselt number can be used in process for engineering design calculations to estimate the heat transfer from the heated surface. In order to estimate heat transfer enhancement, we have calculated the local Nusselt number and average Nusselt number at the thick wall (hot wall) as

$$Nu_l = -\frac{\kappa_{nf}}{\kappa_f} \frac{H}{(T_w - T_c)} \frac{\partial T}{\partial x}|_{x=0.1}$$

The average Nusselt number is given by $Nu_{av} = \int_0^H Nu_l dy$.

3.3.3 Dimensional Analysis

In our present study the following dimensionless parameters are introduced to obtained the governing equation (3.1-3.5) in non-dimensional forms as follows:

$$X = \frac{x}{L}, \ Y = \frac{y}{L}, \ U = \frac{uL}{\alpha_f}, \ V = \frac{vL}{\alpha_f}, \ P = \frac{\bar{p} L^2}{\rho_{nf} \alpha_f^2}, \ \theta = \frac{T - T_c}{\Delta T} \ \text{and} \ \Delta T = \frac{q'' L}{\kappa_f}$$

Where X and Y are the dimensionless co-ordinates varying along horizontal and vertical directions respectively, U and V are dimensionless velocity component in the x and y directions respectively, θ is the dimensionless temperature and P is the dimensionless pressure.

After substituting these dimensionless variables into the equations (3.1-3.5) the non-dimensional continuity, momentum and energy equations are written as follows:

For Fluid:

Continuity Equation:

$$\frac{\partial U}{\partial X} + \frac{\partial V}{\partial Y} = 0 \tag{3.6}$$

Momentum Equations:

$$U \frac{\partial U}{\partial X} + V \frac{\partial U}{\partial Y} = -\frac{\partial P}{\partial X} + \frac{\mu_{nf}}{\rho_{nf} \alpha_f} \left(\frac{\partial^2 U}{\partial X^2} + \frac{\partial^2 U}{\partial Y^2} \right) \tag{3.7}$$

$$U \frac{\partial V}{\partial X} + V \frac{\partial V}{\partial Y} = -\frac{\partial P}{\partial Y} + \frac{\mu_{nf}}{\rho_{nf} \alpha_f} \left(\frac{\partial^2 V}{\partial X^2} + \frac{\partial^2 V}{\partial Y^2} \right) + \frac{(\rho \beta)_{nf}}{\rho_{nf} \beta_f} Ra \Pr \theta \tag{3.8}$$

Energy Equation:

$$U \frac{\partial \theta}{\partial X} + V \frac{\partial \theta}{\partial Y} = \frac{\alpha_{nf}}{\alpha_f} \left(\frac{\partial^2 \theta}{\partial X^2} + \frac{\partial^2 \theta}{\partial Y^2} \right) \tag{3.9}$$

For Solid:

$$\frac{\partial^2 \theta_w}{\partial X^2} + \frac{\partial^2 \theta_w}{\partial Y^2} = 0 \tag{3.10}$$

The dimensionless parameter appearing in the equations (3.7-3.10) are as follows:

Rayleigh number $Ra = \frac{g \beta_f L^3 \Delta T}{v_f \alpha_f}$ and Prandlt number $Pr = \frac{v_f}{\alpha_f}$, where $\alpha = \frac{\kappa}{\rho C_p}$, the thermal diffusivity of the fluid.

3.3.4 Non Dimensional Boundary Conditions

The non dimensional boundary conditions under consideration can be written as:

For all rigid walls: $U = V = 0$

At the right vertical wall: $\theta = 0$

At the top and bottom walls: $\frac{\partial \theta}{\partial Y} = 0$

At the left side of thick wall: $q = -\frac{\kappa_w}{\kappa_{nf}} \frac{\partial \theta}{\partial X}|_w + \frac{H}{\kappa_{nf}} h_\infty \theta_w = 1$

At the divider surface: $U = V = 0$

At the fluid solid wall interfaces: $\frac{\partial \theta_{nf}}{\partial X} = K_r \frac{\partial \theta_w}{\partial X}$

Where, $K_r = \frac{\kappa_w}{\kappa_{nf}}$ is the solid fluid thermal conductivity ratio.

The local Nusselt number at the thick wall on the enclosure base on the non dimensional variable can be expressed as,

$$Nu_l = -\frac{\kappa_{nf}}{\kappa_f} \frac{\partial \theta}{\partial X}|_{x=0.1}$$

and the average Nusselt number at the left thick wall as

$Nu_{av} = -\frac{\kappa_{nf}}{\kappa_f} \int_0^H \frac{\partial \theta}{\partial X} dy$ and the bulk average temperature is defined as, $\theta_{av} = \int \theta \frac{d\bar{A}}{\bar{A}}$, where $\bar{A}$ is the area of the considered domain. The fluid motion is displayed using the stream functions (ψ) obtained from the velocity components U and V, can be expressed as:

$$U = \frac{\partial \psi}{\partial Y} , \quad V = -\frac{\partial \psi}{\partial X}$$

3.4 Numerical Analysis

In this section Galerkin weighted residual finite element techniques are discussed in detail by which the governing equations along with the boundary conditions are solved numerically.

3.4.1 Finite Element Formulation and Computational Procedure

The method of weighted residuals to derive the finite element equations according to Zienkiewicz (1991) is applied to the equations (3.6) – (3.10) as

$$\int_A N_\alpha \left(\frac{\partial U}{\partial X} + \frac{\partial V}{\partial Y} \right) dA = 0 \tag{3.11}$$

$$\int_A N_\alpha \left(U\frac{\partial U}{\partial X} + V\frac{\partial V}{\partial Y} \right) dA = -\int_A H_\lambda \left(\frac{\partial P}{\partial X} \right) dA + \frac{\mu_{nf}}{\rho_{nf}\alpha_f} \int_A N_\alpha \left(\frac{\partial^2 U}{\partial X^2} + \frac{\partial^2 U}{\partial Y^2} \right) dA \tag{3.12}$$

$$\int_A N_\alpha \left(U\frac{\partial V}{\partial X} + V\frac{\partial V}{\partial Y} \right) dA = -\int_A H_\lambda \left(\frac{\partial P}{\partial Y} \right) dA + \frac{\mu_{nf}}{\rho_{nf}\alpha_f} \int_A N_\alpha \left(\frac{\partial^2 V}{\partial X^2} + \frac{\partial^2 V}{\partial Y^2} \right) dA$$

$$+ \frac{(\rho\beta)_{nf}}{\rho_{nf}\beta_f} RaPr \int_A N_\alpha \theta dA \tag{3.13}$$

$$\int_A N_\alpha \left(U\frac{\partial \theta}{\partial X} + V\frac{\partial \theta}{\partial Y} \right) dA = \frac{\alpha_{nf}}{\alpha_f} \int_A \left(\frac{\partial^2 \theta}{\partial X^2} + \frac{\partial^2 \theta}{\partial Y^2} \right) dA \tag{3.14}$$

$$\int_A N_\alpha \left(\frac{\partial^2 \theta_w}{\partial X^2} + \frac{\partial^2 \theta_w}{\partial Y^2} \right) dA \tag{3.15}$$

where A is the element area, N_α (α = 1, 2, … … , 6) are the element interpolation functions for the velocity components and the temperature, and H_λ(λ = 1, 2, 3) are the element interpolation functions for the pressure.

Gauss's theorem is then applied to equations (3.12)-(3.15) to generate the boundary integral terms associated with the surface tractions and heat flux. Then equations (3.12)-(3.15) become,

$$\int_A N_\alpha \left(U\frac{\partial U}{\partial X} + V\frac{\partial V}{\partial Y} \right) dA + \int_A H_\lambda \left(\frac{\partial P}{\partial X} \right) dA$$

$$+ \frac{\mu_{nf}}{\rho_{nf}\alpha_f} \int_A \left(\frac{\partial N_\alpha}{\partial X}\frac{\partial U}{\partial X} + \frac{\partial N_\alpha}{\partial Y}\frac{\partial U}{\partial Y} \right) dA = \int_{S_o} N_\alpha S_x dS_o \tag{3.16}$$

$$\int_A N_\alpha \left(U\frac{\partial V}{\partial X} + V\frac{\partial V}{\partial Y} \right) dA + \int_A H_\lambda \left(\frac{\partial P}{\partial Y} \right) dA + \frac{\mu_{nf}}{\rho_{nf}\alpha_f} \int_A \left(\frac{\partial N_\alpha}{\partial X}\frac{\partial V}{\partial X} + \frac{\partial N_\alpha}{\partial Y}\frac{\partial V}{\partial Y} \right) dA$$

$$- \frac{(\rho\beta)_{nf}}{\rho_{nf}\beta_f} RaPr \int_A N_\alpha \theta dA = \int_{S_o} N_\alpha S_y dS_o \tag{3.17}$$

$$\int_A N_\alpha \left(U\frac{\partial \theta}{\partial X} + V\frac{\partial \theta}{\partial Y} \right) dA - \frac{\alpha_{nf}}{\alpha_f} \int_A \left(\frac{\partial N_\alpha}{\partial X}\frac{\partial \theta}{\partial X} + \frac{\partial N_\alpha}{\partial Y}\frac{\partial \theta}{\partial Y} \right) dA = \int_{S_w} N_\alpha q_{1w} dS_w \tag{3.18}$$

$$\int_A \left(\frac{\partial N_\alpha}{\partial X}\frac{\partial \theta_w}{\partial X} + \frac{\partial N_\alpha}{\partial Y}\frac{\partial \theta_w}{\partial Y} \right) dA = \int_{S_w} N_\alpha q_{2w} dS_w \tag{3.19}$$

Here (3.16)-(3.19) specify surface tractions (S_x, S_y) along out flow boundary S_0 and (3.18) specify velocity components and fluid temperature or heat flux (q_{1w}, q_{2w}) that flows into or out from the domain along the wall boundary S_w.

The basic unknowns for the above differential equations are the velocity components U, V; the temperature, θ and the pressure, P. The six node triangular element is used in this work for the development of the finite element equations. All six nodes are associated with velocities as well as temperature; only the corner nodes are associated with pressure. This means that a lower order polynomial is chosen for pressure and which satisfies continuity equation. The velocity component and the temperature distributions and linear interpolation for the pressure distribution according to their highest derivative orders in the differential equations (3.6)-(3.10) as

$$U(X,Y) = N_\beta U_\beta \tag{3.20}$$

$$V(X,Y) = N_\beta V_\beta \tag{3.21}$$

$$\theta(X,Y) = N_\beta \theta_\beta \tag{3.22}$$

$$\theta_w(X,Y) = N_\beta \theta_{w\beta} \tag{3.23}$$

$$P(X,Y) = H_\lambda P_\lambda \tag{3.24}$$

Where $\beta = 1,2, \ldots \ldots .6; \lambda = 1,2,3$.

Substituting the element velocity component distributions, the temperature distribution and the pressure distribution from equations (3.20)-(3.24) in equations (3.11) and (3.12)-(3.15)

$$\int_A N_\propto (N_{\beta,x} U_\beta + N_{\beta,y} V_\beta) dA = 0 \tag{3.25}$$

$$\int_A N_\alpha \left[(N_\beta U_\beta)(N_{\gamma,x} U_\gamma) + (N_\beta V_\beta)(N_{\gamma,y} U_\gamma) \right] dA + \int_A H_\lambda H_{\mu,x} P_\mu d +$$
$$\frac{\mu_{nf}}{\rho_{nf} \alpha_f} \int_A \left(N_{\alpha,x} N_{\beta,x} U_\beta + N_{\alpha,y} N_{\beta,y} U_\beta \right) dA = \int_{S_o} N_\alpha S_x dS_o \tag{3.26}$$

$$\int_A N_\alpha \left[(N_\beta U_\beta)(N_{\gamma,x} V_\gamma) + (N_\beta V_\beta)(N_{\gamma,y} V_\gamma) \right] dA + \int_A H_\lambda H_{\mu,y} P_\mu d \frac{\mu_{nf}}{\rho_{nf} \alpha_f}$$
$$\int_A \left(N_{\alpha,x} N_{\beta,x} V_\beta + N_{\alpha,y} N_{\beta,y} V_\beta \right) dA - \frac{(\rho\beta)_{nf}}{\rho_{nf} \beta_f} RaPr \int_A N_\alpha N_\beta \theta_\beta dA = \int_{S_o} N_\alpha S_y dS_o \tag{3.27}$$

$$\int_A N_\alpha \left[(N_\beta U_\beta)(N_{\gamma,x}\theta_\gamma) + (N_\beta V_\beta)(N_{\gamma,y}\theta_\gamma) \right] dA -$$

$$\frac{\alpha_{nf}}{\alpha_f} \int_A \left(N_{\alpha,x} N_{\beta,x} \theta_\beta + N_{\alpha,y} N_{\beta,y} \theta_\beta \right) dA = \int_{S_w} N_\alpha q_{1w} dS_w \tag{3.28}$$

$$\int_A \left(N_{\alpha,x} N_{\beta,x} \theta_{w\beta} + N_{\alpha,y} N_{\beta,y} \theta_{w\beta} \right) dA = \int_{S_w} N_\alpha q_{2w} dS_w \tag{3.29}$$

Then the finite element equations can be written in the form

$$K_{\alpha\beta^x} U_\beta + K_{\alpha\beta^y} V_\beta = 0 \tag{3.30}$$

$$K_{\alpha\beta\gamma^x} U_\beta U_\gamma + K_{\alpha\beta\gamma^y} V_\beta U_\gamma + M_{\lambda\mu^x} P_\mu + \left(\frac{\mu_{nf}}{\rho_{nf}\,\alpha_f} (S_{\alpha\beta^{xx}} + S_{\alpha\beta^{yy}}) U_\beta \right) = Q_{\alpha^u} \tag{3.31}$$

$$K_{\alpha\beta\gamma^x} U_\beta V_\gamma + K_{\alpha\beta\gamma^y} V_\beta V_\gamma + M_{\lambda\mu^y} P_\mu + \left(\frac{\mu_{nf}}{\rho_{nf}\,\alpha_f} (S_{\alpha\beta^{xx}} + S_{\alpha\beta^{yy}}) V_\beta \right)$$

$$- \frac{(\rho\beta)_{nf}}{\rho_{nf}\,\beta_f} RaPr K_{\alpha\beta} \theta_\beta = Q_{\alpha^v} \tag{3.32}$$

$$K_{\alpha\beta\gamma^x} U_\beta \theta_\gamma + K_{\alpha\beta\gamma^y} V_\beta \theta_\gamma - \frac{\alpha_{nf}}{\alpha_f} (S_{\alpha\beta^{xx}} + S_{\alpha\beta^{yy}}) \theta_\beta = Q_{\alpha^\theta} \tag{3.33}$$

$$\left(S_{\alpha\beta^{xx}} + S_{\alpha\beta^{yy}} \right) \theta_\beta = Q_{\alpha^{\theta w}} \tag{3.34}$$

where the coefficients in element matrices are in the form of the integrals over the element area and along the element edges S_o and S_w as

$$K_{\alpha\beta^x} = \int_A N_\alpha N_{\beta,x} \, dA \tag{3.35a}$$

$$K_{\alpha\beta^y} = \int_A N_\alpha N_{\beta,y} \, dA \tag{3.35b}$$

$$K_{\alpha\beta\gamma^x} = \int_A N_\alpha N_\beta N_{\gamma,x} \, dA \tag{3.35c}$$

$$K_{\alpha\beta\gamma^y} = \int_A N_\alpha N_\beta N_{\gamma,y} \, dA \tag{3.35d}$$

$$K_{\alpha\beta} = \int_A N_\alpha N_\beta \, dA \tag{3.35e}$$

$$S_{\alpha\beta^{xx}} = \int_A N_{\alpha,x} N_{\beta,x} \, dA \tag{3.35f}$$

$$S_{\alpha\beta^{yy}} = \int_A N_{\alpha,y} N_{\beta,y} \, dA \tag{3.35g}$$

$$M_{\lambda\mu^x} = \int_A H_\lambda H_{\mu,x} \, dA \tag{3.35h}$$

$$M_{\lambda\mu^y} = \int_A H_\lambda H_{\mu,y} \, dA \tag{3.35i}$$

$$Q_{\alpha^u} = \int_A N_\alpha S_x \, dS_o \qquad (3.35\text{J})$$

$$Q_{\alpha^v} = \int_A N_\alpha S_y \, dS_o \qquad (3.35\text{k})$$

$$Q_{\alpha^\theta} = \int_{S_w} N_\alpha 1 q_w \, dS_w \qquad (3.35\text{l})$$

$$Q_{\alpha^\theta w} = \int_{S_w} N_\alpha 2 q_w \, dS_w \qquad (3.35\text{m})$$

These element matrices are evaluated in closed form ready for numerical simulation. Details of the derivation for these element matrices are omitted herein.

The derived finite element equations (3.30)-(3.34) are nonlinear. These nonlinear algebraic equations are solved by applying the Newton-Raphson iteration technique by first writing the unbalanced values from the set of the finite element equations (3.30)-(3.34) as,

$$F_{\alpha^p} = K_{\alpha\beta^x} U_\beta + K_{\alpha\beta^y} V_\beta \qquad (3.36\text{a})$$

$$F_{\alpha^u} = K_{\alpha\beta\gamma^x} U_\beta U_\gamma + K_{\alpha\beta\gamma^y} V_\beta U_\gamma + M_{\alpha\mu^x} P_\mu$$

$$+ \frac{\mu_{nf}}{\rho_{nf}\alpha_f}\left(S_{\alpha\beta^{xx}} + S_{\alpha\beta^{yy}}\right) U_\beta - Q_{\alpha^u} \qquad (3.36\text{b})$$

$$F_{\alpha^v} = K_{\alpha\beta\gamma^x} U_\beta V_\gamma + K_{\alpha\beta\gamma^y} V_\beta V_\gamma + M_{\alpha\mu^y} P_\mu$$

$$+ \frac{\mu_{nf}}{\rho_{nf}\alpha_f}\left(S_{\alpha\beta^{xx}} + S_{\alpha\beta^{yy}}\right) V_\beta - \frac{(\rho\beta)_{nf}}{\rho_{nf}\beta_f} RaPr K_{\alpha\beta}\theta_\beta - Q_{\alpha^v} \qquad (3.36\text{c})$$

$$F_{\alpha^\theta} = K_{\alpha\beta\gamma^x} U_\beta \theta_\gamma + K_{\alpha\beta\gamma^y} U_\beta \theta_\gamma - \frac{\alpha_{nf}}{\alpha_f}\left(S_{\alpha\beta^{xx}} + S_{\alpha\beta^{yy}}\right)\theta_\beta - Q_{\alpha^\theta} \qquad (3.36\text{d})$$

$$F_{\alpha^\theta w} = \left(S_{\alpha\beta^{xx}} + S_{\alpha\beta^{yy}}\right)\theta_\beta - Q_{\alpha^\theta w} \qquad (3.36\text{e})$$

This leads to a set of algebraic equations with the incremental unknowns of the element nodal velocity components, temperatures and pressures in the form,

$$
\begin{bmatrix}
K_{pu} & K_{pv} & 0 & 0 & 0 \\
K_{uu} & K_{uv} & K_{up} & 0 & 0 \\
K_{vu} & K_{vv} & K_{vp} & K_{v\theta} & 0 \\
K_{\theta u} & K_{\theta v} & 0 & K_{\theta\theta} & 0 \\
0 & 0 & 0 & K_{\theta\theta_w} & 0
\end{bmatrix}
\begin{bmatrix}
\Delta p \\
\Delta u \\
\Delta v \\
\Delta\theta \\
\Delta\theta_w
\end{bmatrix}
=
\begin{bmatrix}
F_{\alpha^p} \\
F_{\alpha^u} \\
F_{\alpha^v} \\
F_{\alpha^\theta} \\
F_{\alpha^\theta w}
\end{bmatrix}
\qquad (3.37)
$$

where Δ represents the vector of nodal velocities, pressure and temperature.

$$K_{uu} = K_{\alpha\beta\gamma^x} U_\beta V_\beta + \left(\frac{\mu_{nf}}{\rho_{nf}\alpha_f}\left(S_{\alpha\beta^{xx}} + S_{\alpha\beta^{yy}}\right)\right)$$

$$K_{uv} = K_{\alpha\beta\gamma^y} U_\gamma$$

$$K_{u\theta} = 0$$

$$K_{up} = M_{\alpha\mu^x}$$

$$K_{vu} = K_{\alpha\beta\gamma^x} V_\gamma$$

$$K_{vv} = K_{\alpha\beta\gamma^y} V_\gamma + + \frac{\mu_{nf}}{\rho_{nf}\,\alpha_f} \left(S_{\alpha\beta^{xx}} + S_{\alpha\beta^{yy}} \right)$$

$$K_{v\theta} = -\frac{(\rho\beta)_{nf}}{\rho_{nf}\,\beta_f}\, RaPrK_{\alpha\beta}$$

$$K_{v\theta_w} = 0$$

$$K_{\theta u} = K_{\alpha\beta\gamma^x} \theta_\gamma$$

$$K_{\theta v} = K_{\alpha\beta\gamma^y} \theta_\gamma$$

$$K_{\theta\theta} = -\frac{\alpha_{nf}}{\alpha_f} \left(S_{\alpha\beta^{xx}} + S_{\alpha\beta^{yy}} \right)$$

$$K_{\theta\theta_w} = 0$$

$$K_{\theta_w p} = 0$$

$$K_{\theta_w u} = 0$$

$$K_{\theta_w v} = 0$$

$$K_{\theta_w\theta_w} = \left(S_{\alpha\beta^{xx}} + S_{\alpha\beta^{yy}} \right)$$

The iteration process is terminated if the percentage of the overall change compared to the previous iteration is less than the specified value.

To solve the sets of the global nonlinear algebraic equations in the form of matrix, the Newton-Raphson iteration technique has been adapted through PDE solver with MATLAB interface. The convergence of solutions is assumed when the relative error for each variable between consecutive iterations is recorded below the convergence criterion ε

such that $|\psi^{n+1} - \psi^n| < \varepsilon$, where n is number of iteration and ψ is the variable u, v or θ, θ_w. The convergence criterion was set to $\varepsilon = 10^{-6}$.

3.4.2 Thermo-physical Properties

The thermophysical properties of the water and nanoparticles are taken from Aminosadati and Ghasemi (2009) and given in Table 3.1

Table 3.1: Thermo-physical properties of fluid and nanoparticles

Physical Properties	Fluid phase (Water)	Solid phase Copper(Cu)
C_p(J/kgK)	4179	385
ρ (kg/m^3)	997.1	8933
k (W/mK)	0.613	401
$\beta \times 10^5$ (K^{-1})	21	1.67

3.4.3 Grid Generation

In the finite element method, the grid or mesh generation is the technique to subdivide a domain into a set of sub-domains, called finite elements. The discrete locations are defined by the numerical grid, at which the variables are to be calculated. It is basically a discrete representation of the geometric domain on which the problem is to be solved. The computational domain with irregular geometries by a collection of finite elements makes
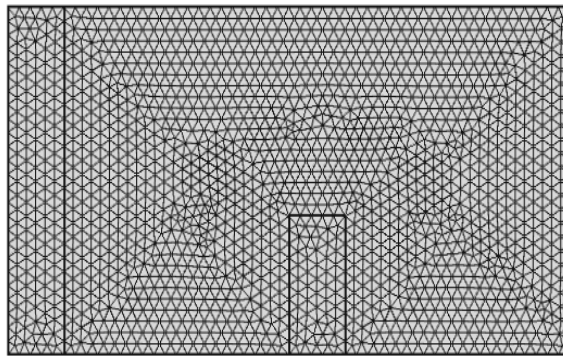

Figure 3.2: Mesh structure of elements for the physical model

the method a valuable practical tool for the solution of boundary value problems arising in various field of engineering. The mesh structure of finite elements for the present physical model displays in Figure 3.2.

3.4.4 Grid Refinement Check

An extensive mesh testing procedure is conducted to guarantee a grid-independent solution for $Ra = 10^6, \phi = 0.05, l_1 = 0.40, \ Pr = 6.2, \ h_\infty = 100 W/m^2 \ K, K_r = 10$ and $w_1 = 0.1$ through a rectangular enclosure. In the present work, five different non-uniform grid systems with the following number of elements within the resolution field: 394, 533, 1058, 3258 and 13020 are examined.
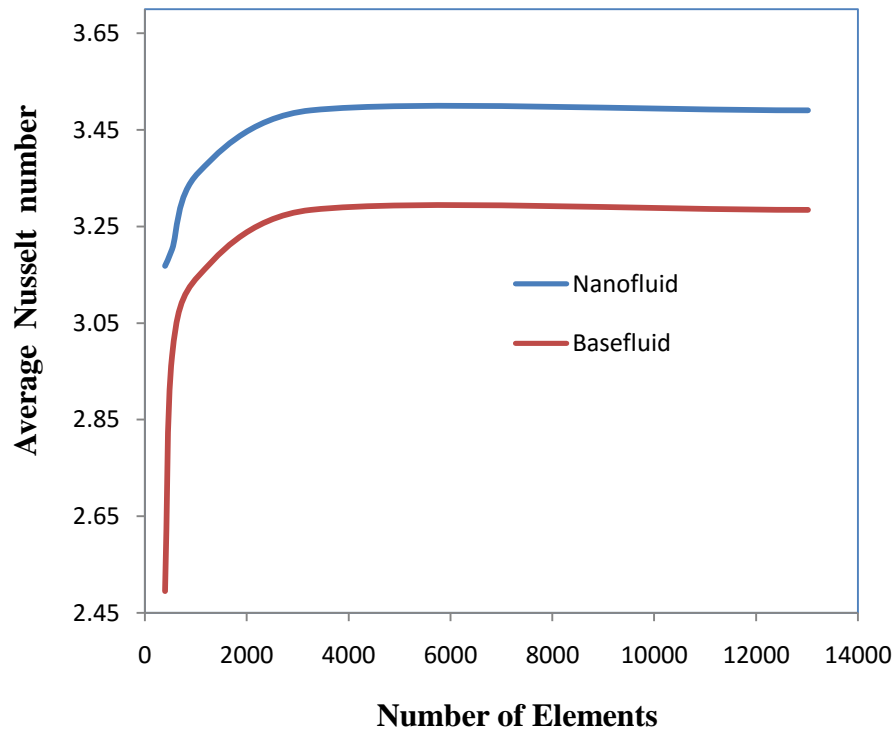

Figure 3.3: Grid Refinement check.

The extreme value of Nu is used as a sensitivity measure of the accuracy of the solution and is selected as the monitoring variable for water-copper nanofluid ($\phi = 5\%$) as well as base fluid ($\phi = 0\%$) for the aforesaid elements to develop an understanding of the grid fineness as shown in Table 3.2 and Figure 3.3. The scale of the average Nusselt number for 3258 elements shows a little difference with the results obtained for the other elements.

Hence, considering the non-uniform grid system of 3258 elements is preferred for the computation.

Table 3.2: Grid Test at $Ra = 10^6, \phi = 0.05, l_1 = 0.40, Pr = 6.2, h_\infty = 100 W/m^2 K$, $K_r = 10$ and $w_1 = 0.1$

Nodes (elements)	6181 (394)	10062 (533)	13922 (1058)	16181 (3258)	28926 (13020)
Nu (nanofluid)	3.16853	3.20314	3.36192	3.49042	3.49057
Nu (basefluid)	2.49469	2.98212	3.14750	3.28430	3.28576
Time [s]	66.265	96.594	122.157	196.328	310.377

3.4.5 Validation of Numerical Procedure

The model validation is an essential part of a numerical investigation. Hence, the outcome of the present numerical procedure is benchmarked against the numerical results of Aminossadati and Ghasemi (2009) which are reported for natural convective cooling of a localized heat source at bottom of a nanofluid filled enclosure in a cavity having relatively low temperature at the top and vertical walls and Rahman and Alim (2010) which are reported for conjugate heat transfer in a lid-driven square enclosure having heat conducting circular cylinder placed at the center. Excellent agreement is achieved, as illustrated in Figure 3.4(a) and Figure 3.4(b), between present results and the numerical results of Aminossadati and Ghasemi (2009) and Rahman and Alim (2010) for both the streamlines and isotherms inside the cavity. These validations boost the confidence in our numerical procedure to carry on with the above stated objectives of the current investigation.
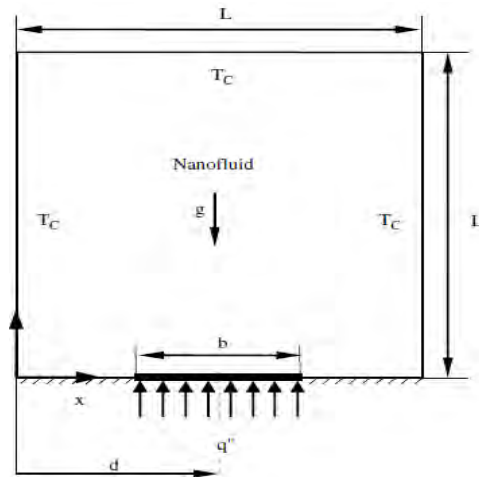
Physical Model

Aminossadati and Ghasemi   Present
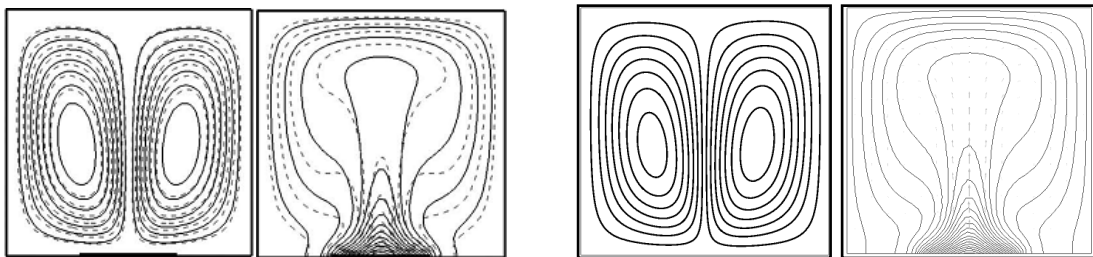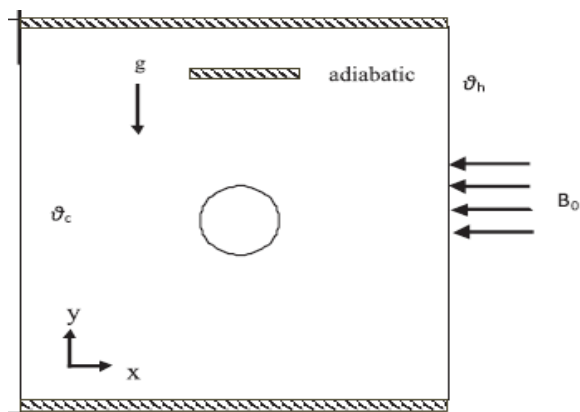

Figure 3.4 (a): Model generation of Aminossadati and Ghasemi(2009)

Physical model
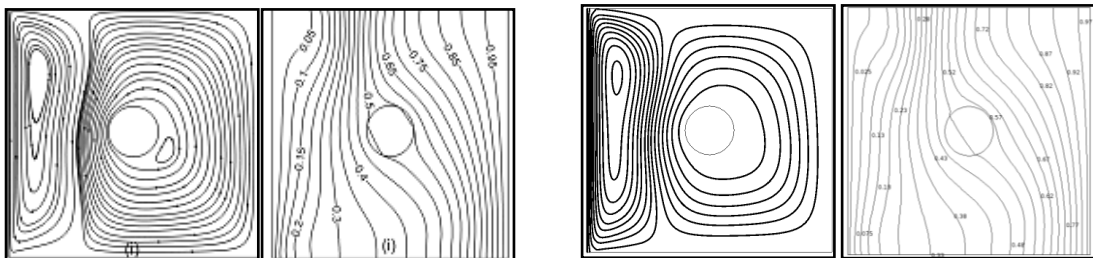
Rahman and Alim   Present

Figure 3.4 (b): Model generation of Rahman and Alim (2010)

3.5 Results and Discussion

Finite element simulation is applied to perform the analysis on the flow and heat transfer of nanofluid filled rectangular enclosure with thick and conducting vertical wall. Effects of the parameters such as Rayleigh number (Ra), convective heat transfer coefficient (h_∞), position of divider (l_1), solid fluid thermal conductivity ratio (K_r) and solid wall thickness (w_1) on heat transfer and fluid flow inside the cavity have been studied for the range of solid volume fraction(ϕ) of 0 to 0.05. The results are generated for different values of governing parameter for this investigation is $Ra = 10^4\text{-}10^7$, h_∞ =0.0- 400, $l_1 = 0.1$ to 0.7, $K_r = 0.5$ - 10.0 and $w_1 = 0.1$- 0.3 respectively. The working fluid is assigned a Prandtl number 6.2 throughout this investigation. The outcomes for the different cases are presented in the following sections.

3.5.1 Effect of Rayleigh number

The influence of Rayleigh number (Ra) from 10^4 to 10^7 on streamlines as well as isotherms for the present configuration at $Pr = 6.2$, $h_\infty = 100W/m^2\ K$, $l_1 = 0.40, K_r = 10$ and $w_1 = 0.1$ for both the pure fluid and nanofluid with $\phi = 0.05$ has been illustrated in Figures 3.5 (a, b). It can be seen from Figure 3.5 (a), the left column shows the stream lines for pure fluid and right column shows the stream lines for the nanofluid and in Figures 3.5 (b) the left column shows the isotherm for pure fluid and the right column shows the isotherm for nanofluid with various value of Rayleigh number (Ra). In each case we see that the flow rises along the left vertical wall, then it get block towards the top wall, which then causes the flow that turn towards the right cold wall then it get blocked again by the bottom wall, which then direct the flow towards the divider then it finally goes again towards the left wall. So a clockwise circulation is located within the rectangular enclosure. We also observe that the centre of recirculation cell is located at the left side of the divider. However, it is observed from the figure that at very low Rayleigh number $(Ra = 10^4)$ the isotherms inside the enclosure seem to be vertical, since the heat flux is along horizontal, so this implies that the heat is transferred by conduction. It is obvious from the Figure 3.5 (a) that the increase in Rayleigh number (Ra) enhances the strength of buoyancy force and hence the natural convection flow, so the value of the stream function at the centre of the enclosure increase with the increase of Rayleigh number (Ra). Also, observe that the stream lines are more clustered towards the walls with the increase of Rayleigh number(Ra). So we can say with the further increase of
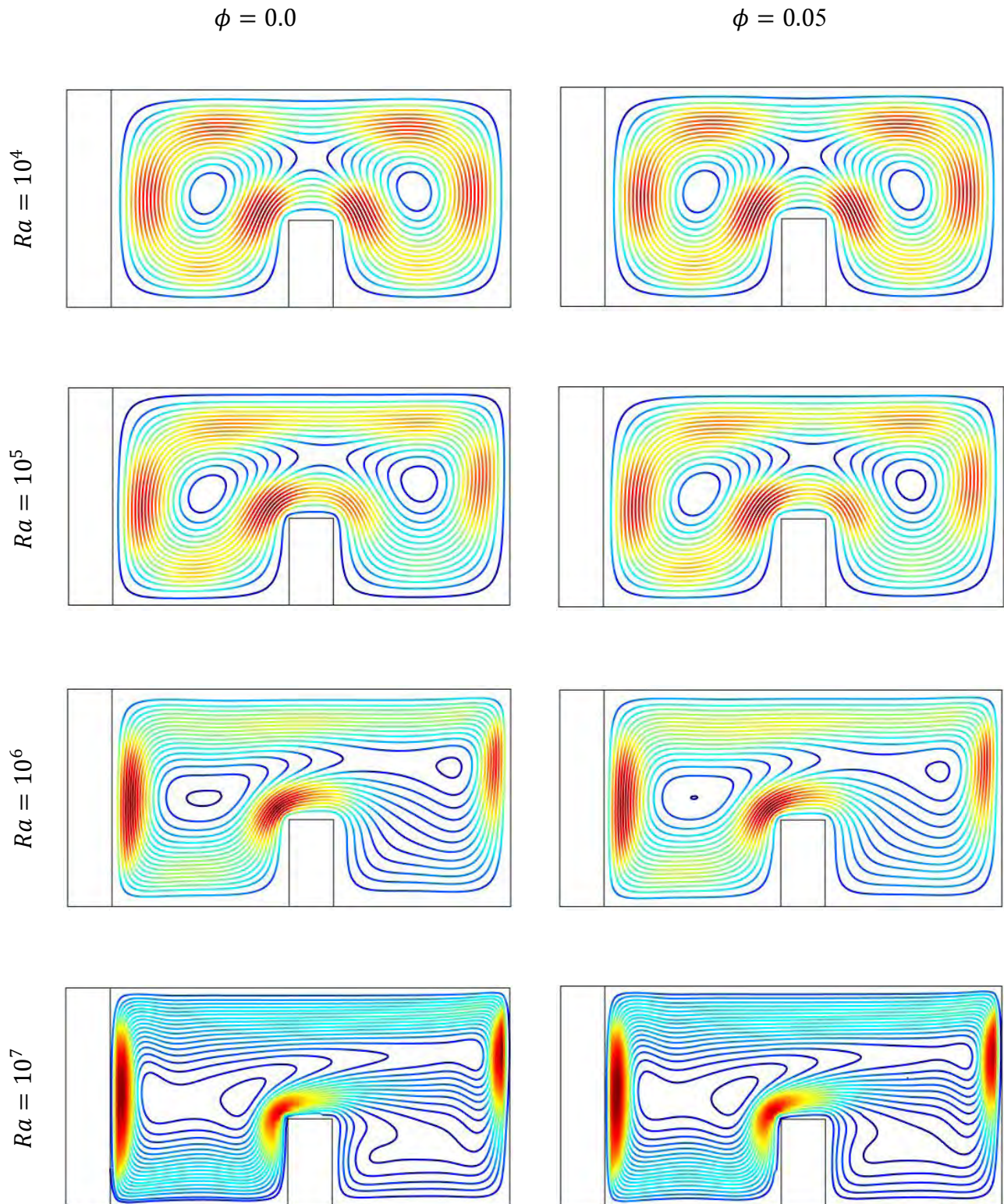
$\phi = 0.0$ $\phi = 0.05$

Figure 3.5: (a) Streamlines at various Ra (at $Pr = 6.2, h_\infty = 100W/m^2\,k$, $l_1 = 0.40$, $K_r = 10$ and $w_1 = 0.1$) for base fluid and nanofluid.

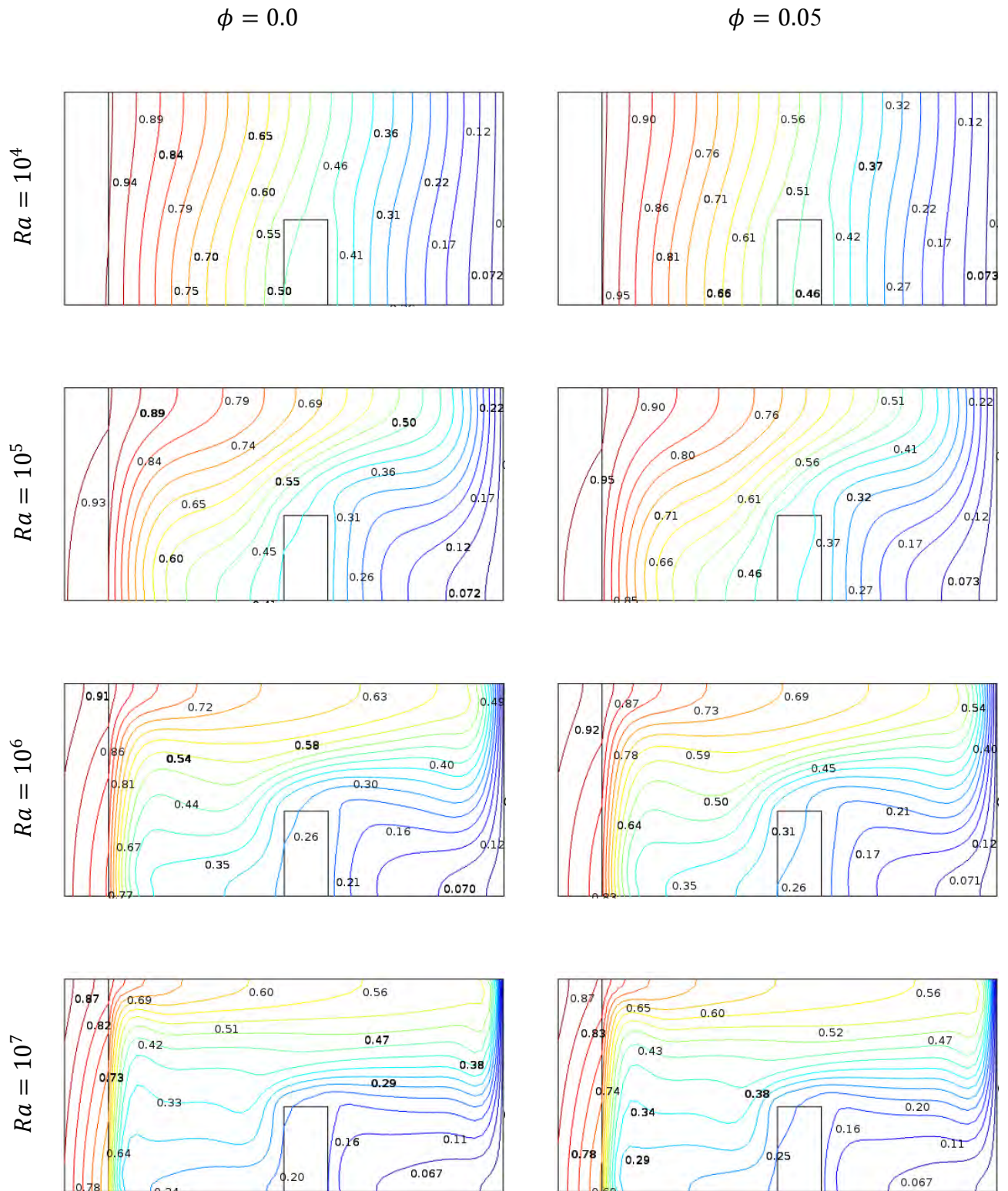$$\phi = 0.0 \qquad\qquad\qquad \phi = 0.05$$

Figure 3.5: (b) Isotherms at various Ra (at $Pr = 6.2$, $h_\infty = 100 W/m^2 k$, $l_1 = 0.40$, $K_r = 10$ and $w_1 = 0.1$) for base fluid and nanofluid.

contact between the fluid and the wall the heat transfer rate increase and we also noticed that with the further increase of Rayleigh number (Ra) less flows go down and enters to the region between the right wall and divider, so minimum level of temperature are observed there, and flow mostly turn towards the left wall. The mechanism of forming stream lines is as follows, the fluid adjacent to the left hot wall (interface) is heated, and moves up due to convection (buoyancy force) which moves to the right cold wall (due to heating) and falls downwards to the lower adiabatic wall.

With the increase of solid volume fraction (ϕ) of nanofluid, thermal conductivity of the nanofluid will be increased, hence the buoyancy force and flow strength will be increased with the increase of Rayleigh number (Ra).It is interesting to observe that the increase in Rayleigh number (Ra), enhanced the heat transfer rate that leads to the decreases in both the flow and the wall temperatures, which is an indication of enhancing the enclosure cooling performance. So in the case of pure fluid we see that the maximum wall temperature decreases from 0.95 for $Ra = 10^4$ to 0.87 for $Ra = 10^7$ in the case of pure fluid. It is also noticeable from Figure 3.4 (b) that for higher Rayleigh number (Ra) the isotherms in the middle section of the enclosure are smooth curves, which are parallel to the horizontal walls, where near the side walls we see the isotherm are more strictly parallel to the vertical wall.

We also see that the increase of solid volume fraction (ϕ) of nanofluid, enhance the thermal conductivity and hence the heat transfer rate is increase, which leads to the temperature reduction within the thick wall.

Figure 3.5 (c) displays the average Nusselt number along the hot wall for various values of Rayleigh number (Ra) and solid volume fraction(ϕ). We see here a linear variation of average Nusselt number with the increase of solid volume fraction. It is seen that the average Nusselt number increases with the increase of Rayleigh number(Ra). The effect of nanoparticles can be more observed at lower Rayleigh number (Ra) because in this case conduction is the dominant mode of heat transfer. When the solid volume fraction increases the heat transfer rate as well as average Nusselt number enhance, from this we can say adding copper nanoparticles to the base fluid leads to enhancement in the heat transfer which shows the ability of heat absorption by the inner flow.
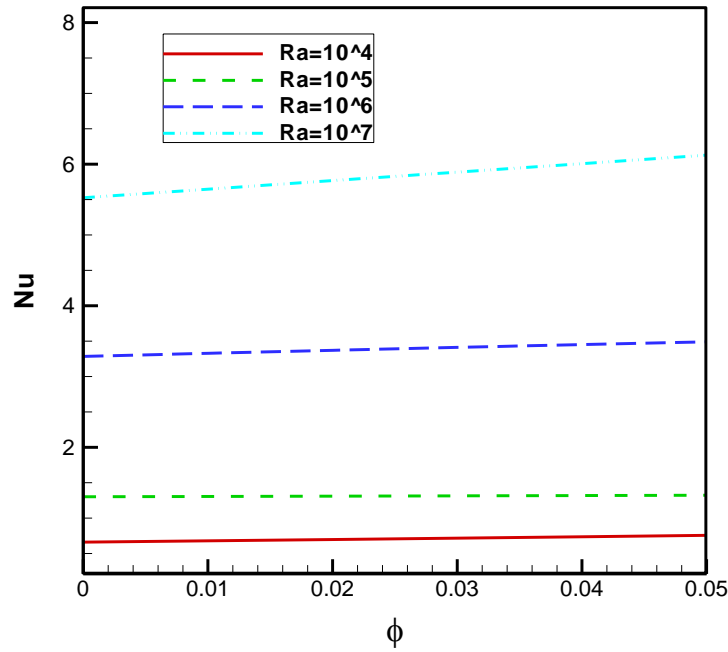
Figure 3.5 (c): Average Nusselt number at various Ra (for $Pr = 6.2,\ h_\infty = 100\text{W/m}^2 k$, $l_1 = 0.40$, $K_r = 10$ and $w_1 = 0.1$).

3.5.2 Effect of Convective Heat Transfer Coefficient

We now discuss the effect of convective heat transfer coefficient (h_∞) on the flow and temperature field in Figures 3.6 (a, b) for $Pr = 6.2,\ Ra = 10^6$, $l_1 = 0.40, K_r = 10$ and $w_1 = 0.1$ for both the pure fluid and nanofluid. A zero value of convective heat transfer coefficient (h_∞) indicates the fact that the submitted heat is completely transfered from the left wall to the inner flow. So, in the case of $h_\infty = 400W/m^2\ k$ the maximum value of the stream function decrease with respect to the case $h_\infty = 100W/m^2\ k$. The buoyancy force and flow strength are more pronounced for higher values of convective heat transfer coefficient (h_∞). The increase of convective heat transfer coefficient (h_∞) reduces the thick wall temperature, thereby heat is less absorbed by the inner flow which leads to decrease the maximum temperature. We also see in the case $h_\infty = 0$, the isotherms near the vertical side walls are more clustered; however the increase in convective heat transfer coefficient (h_∞) cause the decrease in the temperature gradient in the region. We notice here that isotherms are almost parallel to the vertical walls, which indicates the reduction of heat transfer. This point can be explained as when the ambient convective heat transfer coefficient (h_∞) is increased, the input heat flux is absorbed by ambient rather than inner flow. However the increase in h_∞ causes decreases in the temperature gradients in the inner flow, which is also an indication of enhancing of cooling performance.
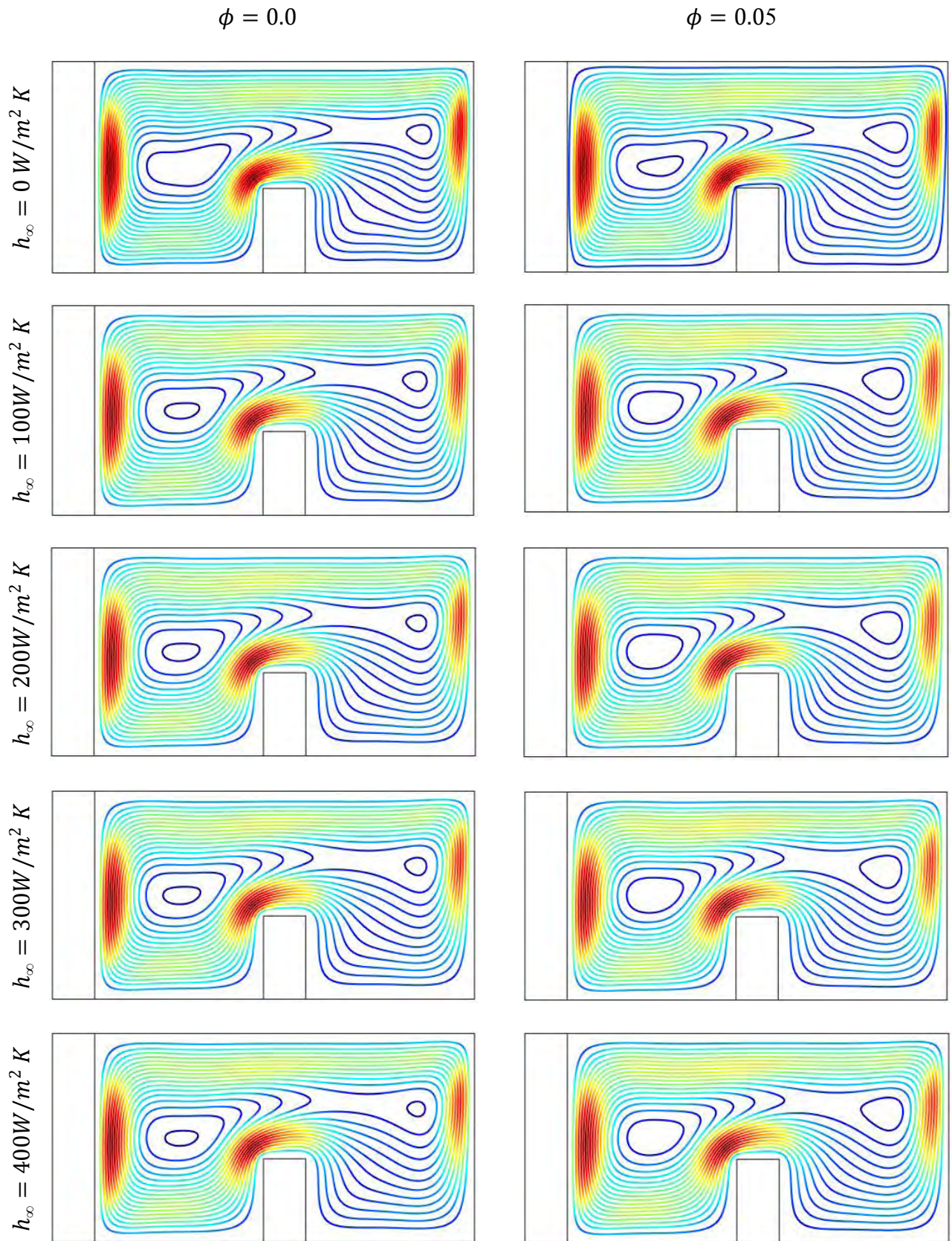
41

$\phi = 0.0$ $\phi = 0.05$

Figure 3.6: (a) Streanlines at various convective heat transfer coefficient (h_∞) (at $Ra = 10^6$, $Pr = 6.2$, $l_1 = 0.40$, $K_r = 10$ and $w_1 = 0.1$) for base fluid and nanofluid.
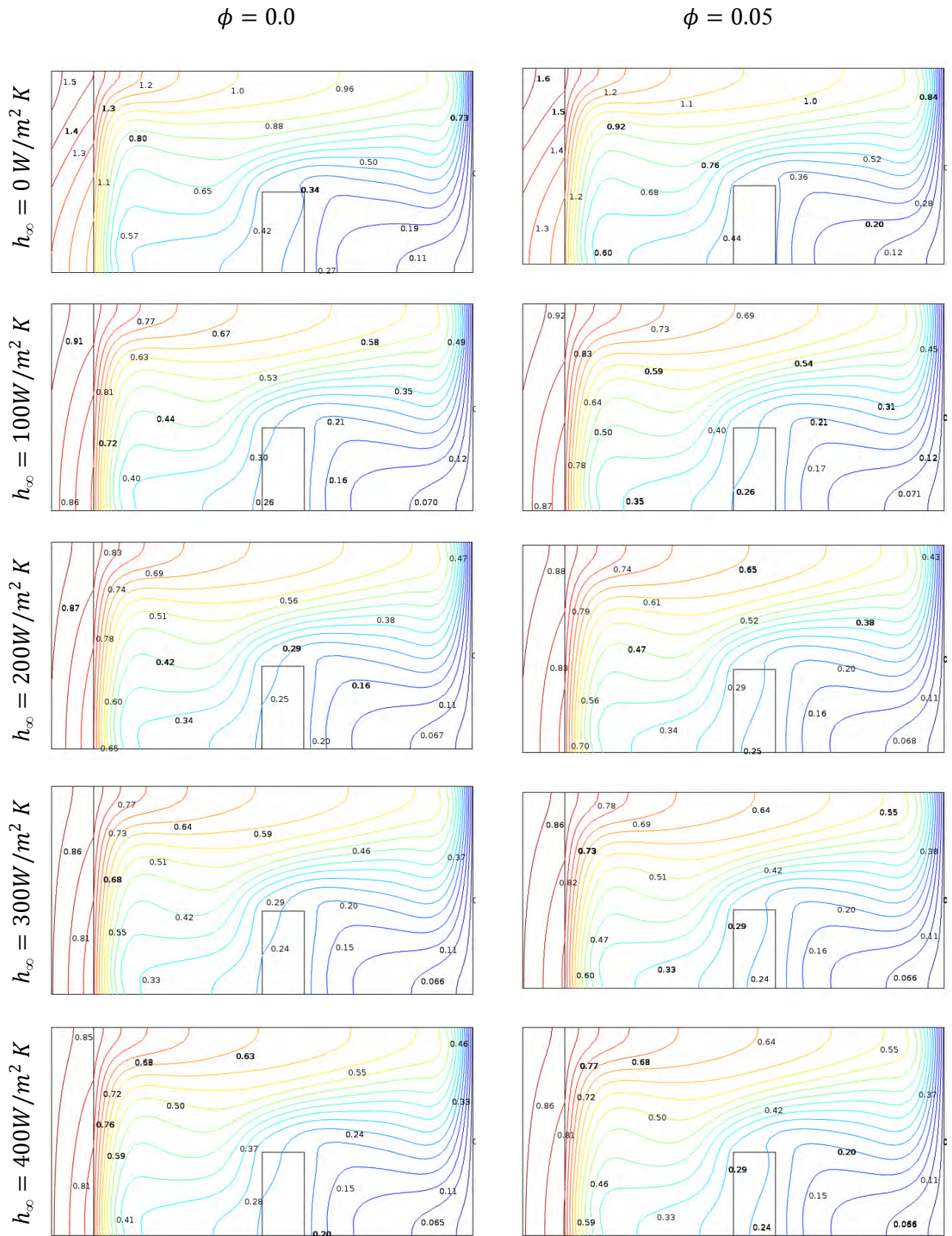
Figure 3.6: (b) Isotherms at various convective heat transfer coefficient (h_∞) $(at\ Ra = 10^6, Pr = 6.2, l_1 = 0.40,\ K_r = 10\ and\ w_1 = 0.1)$ for base fluid and nanofluid.

The variation of average Nusselt number (Nu) is displayed in Figure 3.6 (c) along the hot wall against the solid volume fraction for different values of ambient convective heat transfer coefficient (h_∞). We see that when convective heat transfer coefficient (h_∞) increase the input heat flux is less absorbed by the inner flow, which point the reduction in the average Nusselt number (Nu) .
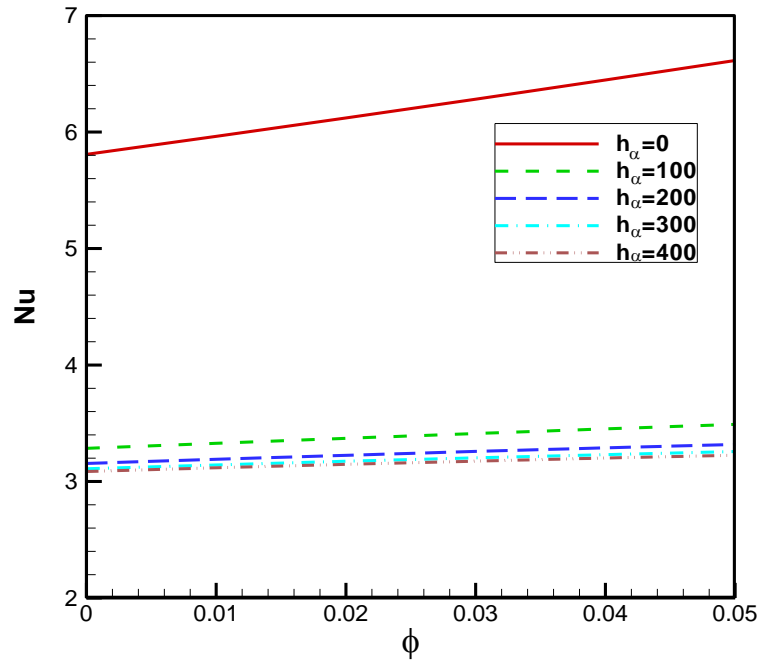

Figure 3.6 (c): Average Nusselt number at various h_∞ (for $Ra = 10^6, Pr = 6.2,$ $h_\infty = 100W/m^2\ K$, $l_1 = 0.40, K_r = 10$ and $w_1 = 0.1$).

3.5.3 Effect of Divider Position

The effect of divider position (l_1) on streamlines and isotherms are shown in Figures 3.7 (a, b) for $Ra = 10^6, Pr = 6.2, h_\infty = 100\ W/m^2 K, K_r = 10$ and $w_1 = 0.1$ for both the pure fluid and nanofluid with 5% concentration.

We see in Figure 3.7 (a), when $l_1 = 0.1$ a clockwise circulation is observed with one core which covers the whole cavity. In this case we notice that there is a weak flow between the divider and the left wall. So, the temperature of this region increases which cause from the reduction of the convective heat transfer. As the divider position (l_1) increases from the left wall the resistance of circulating flow decrease, which leads to increase in the flow strength. For $l_1 = 0.45$ we see again a clockwise circulation with one cores. With further

increase of position of divider i.e. for $l_1 = 0.7$ we observe that the flow strength increases between the left wall and the divider. It is also noticeable that the center of the core location changes with the divider positions. We also see decrease in the distance between the left wall and divider cause the cold flow down. Through the increase in l_1 enhanced the heat transfer, so energy absorption by the inner flow occurs, which indicate the fact that heat is more transferred from the hot wall to the cold region. So the temperature of the thick wall reduces. It is also observed from the Figure 3.7 (b) that for smaller l_1 the isotherms are clustered near the wall and with the increase in distance between the left wall and the divider isotherms is parallel to the horizontal walls.

Figure 3.7 (c) displays the variation of average Nusselt number (Nu) along the hot wall for various position of divider against the solid volume fraction. We see the increase in l_1 , leads to the increase in the flow strength and hence the heat transfer rate enhance, so the average Nusselt number clearly increases with the increase of distance between the hot wall and the divider. When the divider move from $x = 0.1$ to $x = 0.45$ the average Nusselt number increases faster because in this case convection dominate the conduction mode, but the rate of increasing average Nusselt number(Nu) decreases when the divider gets closure to the right wall, which is noticeable at $\phi = 5\%$ more effectively.
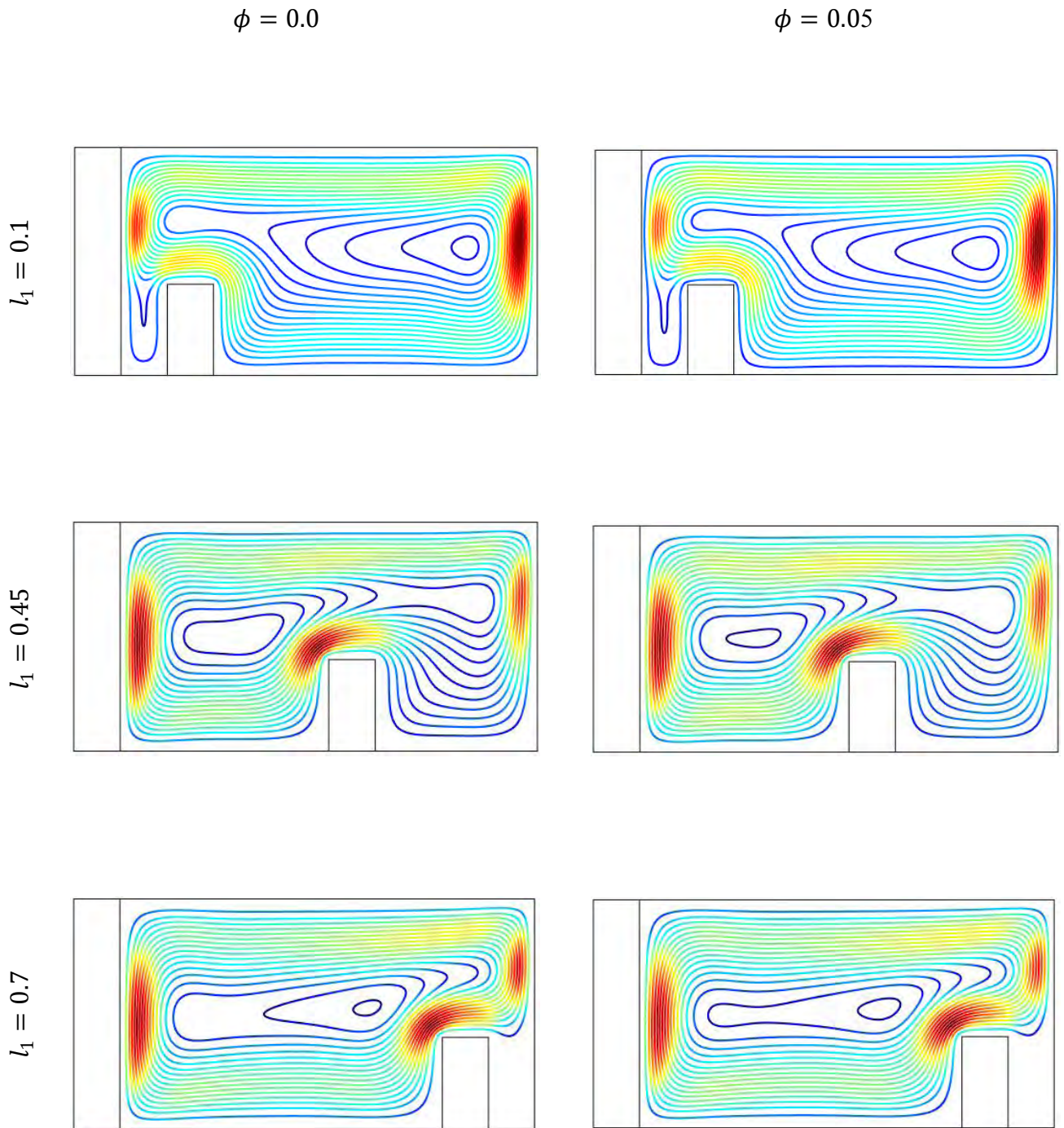
$\phi = 0.0$ $\phi = 0.05$

Figure 3.7: (a) Streamlines at various Divider Position (l_1) (at $Ra = 10^6$, $Pr = 6.2$, $h_\infty = 100W/m^2K$, $K_r = 10$ and $w_1 = 0.1$) for base fluid and nanofluid.
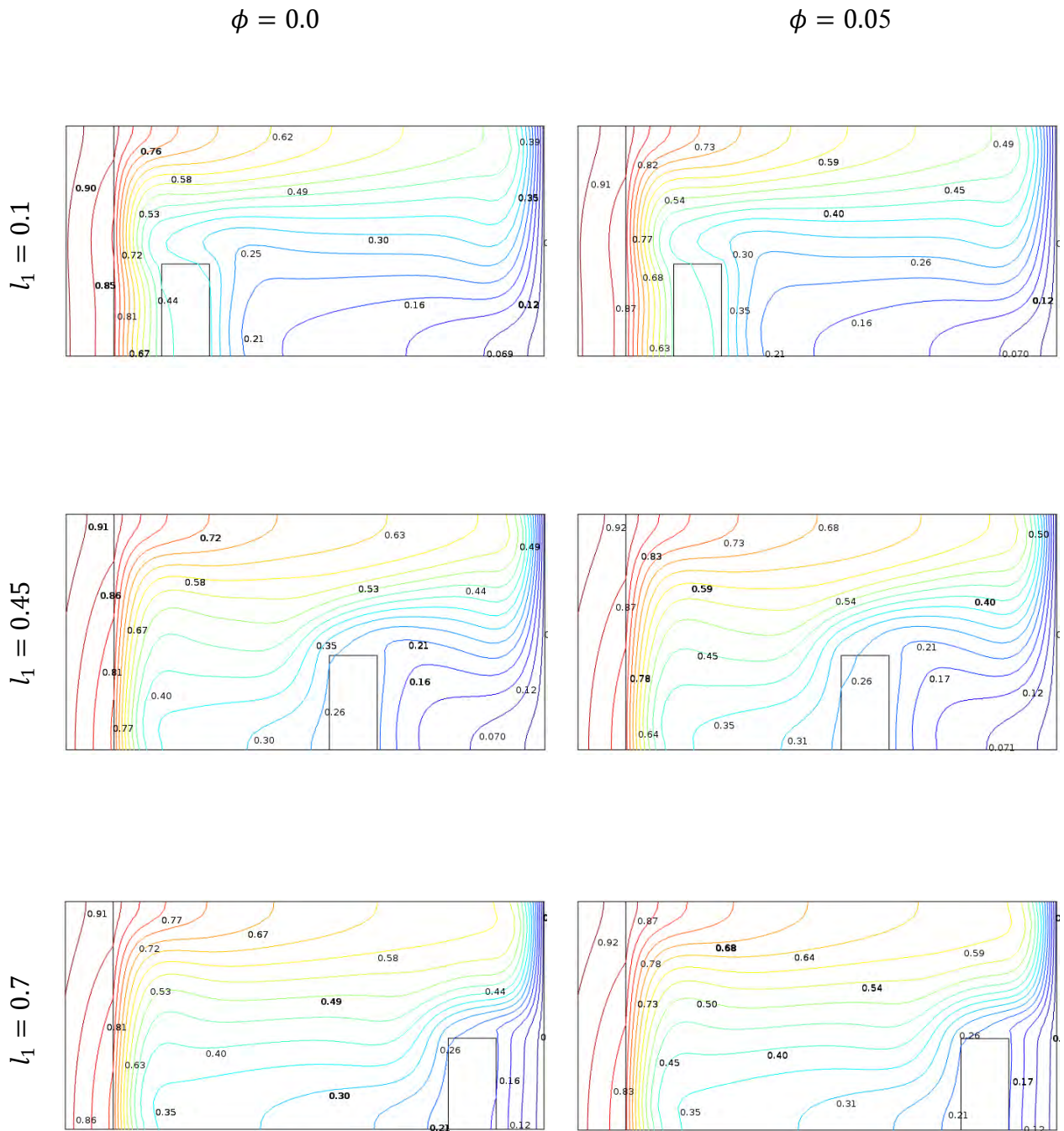
$$\phi = 0.0 \qquad\qquad\qquad \phi = 0.05$$

Figure 3.7 (b): Isotherms at various Divider Position (l_1) (at $Ra = 10^6$, $Pr = 6.2$, $h_\infty = 100W/m^2 K$, $K_r = 10$ and $w_1 = 0.1$) for base fluid and nanofluid.
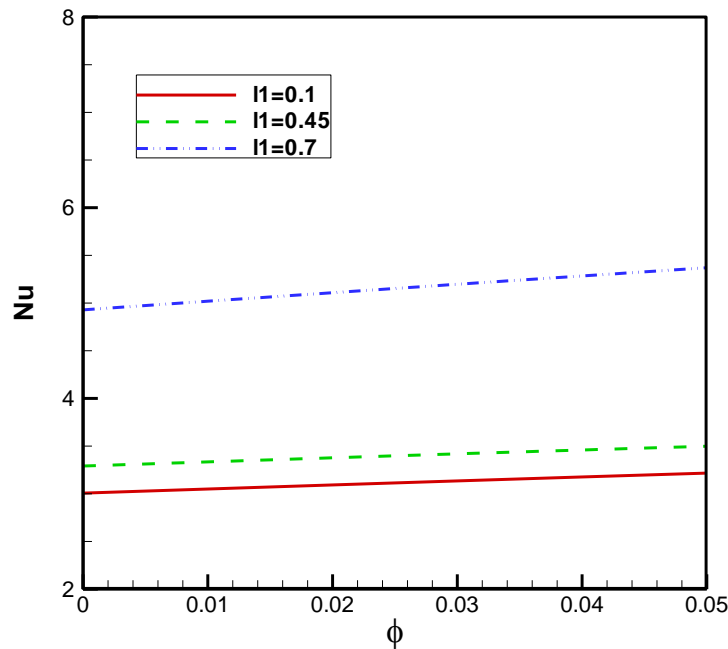
Figure 3.7 (c): Average Nusselt number at various l_1 (for $Ra = 10^6, Pr = 6.2,$ $h_\infty = 100 W/m^2 k , K_r = 10$ and $w_1 = 0.1$).

3.5.4 Effect of Solid Fluid Thermal Conductivity Ratio

Figures 3.8 (a, b) show the effect of solid fluid thermal conductivity ratio (K_r) on the flow and temperature field for $Ra = 10^6, Pr = 6.2, h_\infty = 100 W/m^2 K, l_1 = 0.4$ and $w_1 = 0.1$ for both the pure fluid and nanofluid with $\phi = 5\%$. We observe that at very low wall conductivity ratio $(K_r = 0.5)$ the wall thermal resistance is very high, hence a steeper gradient of isotherm within the wall is seen, which indicates less amount of heat is transferred to the enclosure. Further increase of K_r, leads to reduce the wall thermal resistance. This can be characterized by the reduction of isotherm gradient within the wall and the convection activities within the enclosure. It is observed that two cores are formed as shown in the figure 3.8 (a). As the conduction ration (K_r) increases, the magnitude of the left cell increases, while the magnitude of the right core decreases. This indicates the facts that with the increase of conductivity ratio (K_r), the flow strength between the left wall and the divider increase. This phenomenon is due to the temperature gradient near the wall increase with increase of the parameter K_r. Thus much amount of heat transfer from the thick wall to the fluid is obtained for the higher value of solid fluid thermal conductivity ratio (K_r)(good conductivity solid wall). It is also observed that convection effect in the fluid become stronger for higher value of thermal conductivity ratio (K_r) .
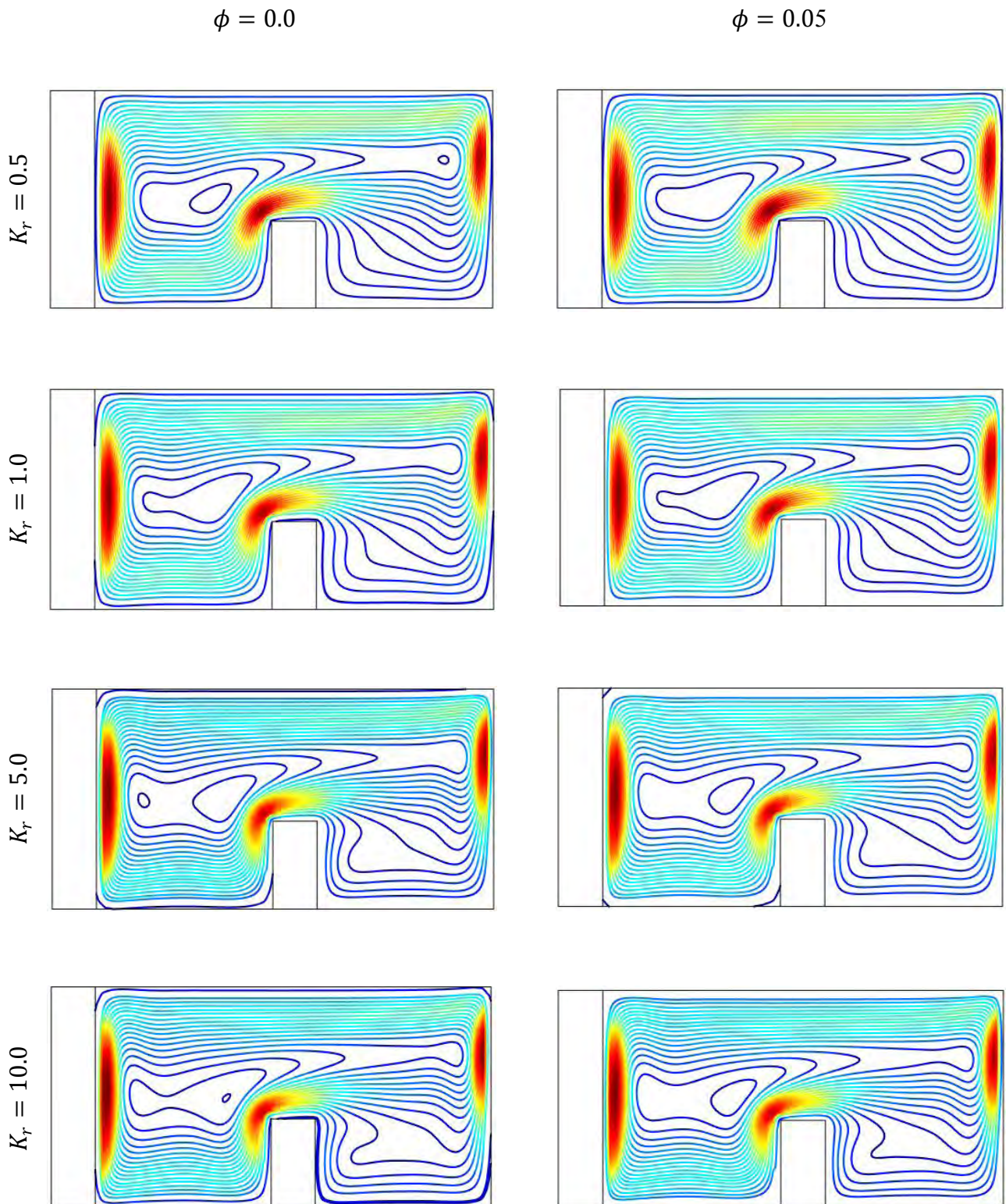
Figure 3.8: (a) Streamlines at various solid fluid thermal conductivity ration (K_r)(at $Ra = 10^6$, $Pr = 6.2$, $h_\infty = 100W/m^2K$, $l_1 = 0.40$ and $w_1 = 0.1$) for base fluid and nanofluid.

$\phi = 0.0$ $\phi = 0.05$

$K_r = 0.5$
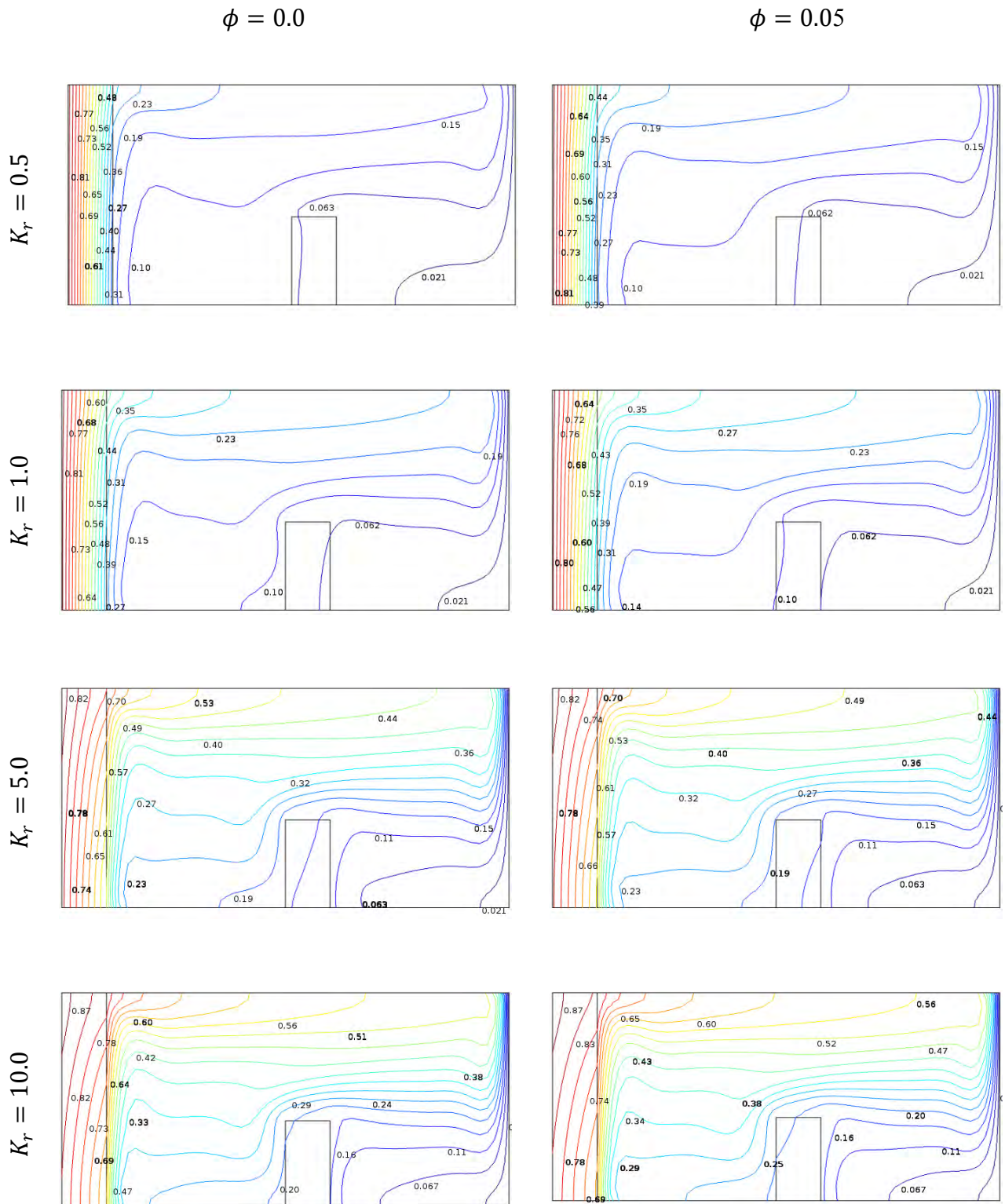
$K_r = 1.0$

$K_r = 5.0$

$K_r = 10.0$

Figure 3.8: (b) Isotherms at various solid fluid thermal conductivity ration (K_r) (at $Ra = 10^6$, $Pr = 6.2$, $h_\infty = 100 W/m^2 K$, $l_1 = 0.40$ and $w_1 = 0.1$) for base fluid and nanofluid.

50

Figure 3.8 (c) displays the variation of average Nusselt number (Nu) with the solid volume fraction for different values of wall thermal conductivity ratio (K_r) for $Ra = 10^6, Pr = 6.2, h_\infty = 100 \, w/m^2k$, $l_1 = 0.4$ and $w_1 = 0.1$ with the solid volume fraction $\phi = 5\%$. We observe that the heat transfer rate increases with the increase of conductivity ratio. This is due to the temperature gradient near the solid wall increase with the increase of conductivity ratio and this mechanism enhances the heat transfer rate
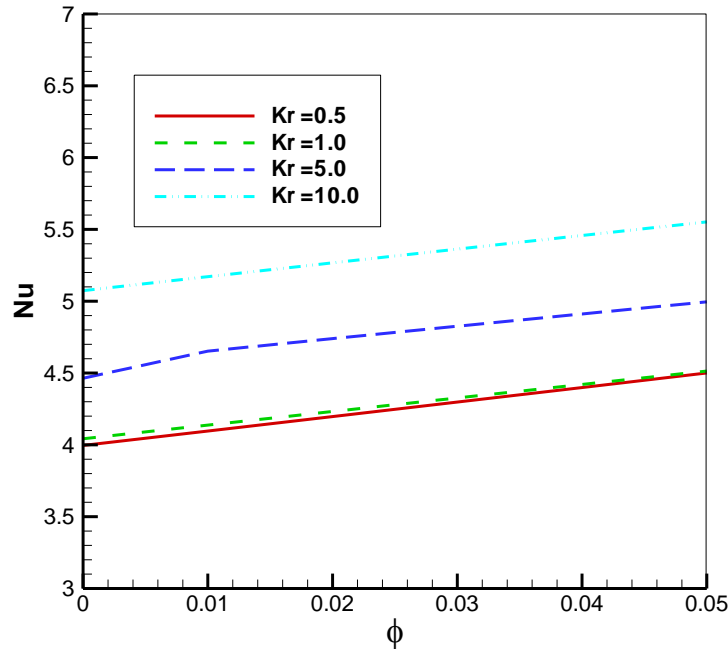

Figure 3.8 (c): Average Nusselt number at various k_r (for $Ra = 10^6, Pr = 6.2,$ $l_1 = 0.4, \; h_\infty = 100W/m^2K$ and $w_1 = 0.1$).

3.5.5 Effect of Solid Wall Thickness

The effect of wall thickness (w_1) is depicted in Figures 3.9 (a, b) for $Ra = 10^6, \; Pr = 6.2, h_\infty = 100 \, w/m^2k$, $K_r = 10$ and $l_1 = 0.4$ for both pure fluid and nanofluid with $\phi = 5\%$. We see that the parameter wall thickness (w_1) affects the fluid and solid wall temperature as well as the flow characteristics. We notice here that the strength of the flow circulation is much higher for a thin solid wall. For thick solid wall $(w_1 = 0.1)$ we observe that a circular main cell with two cores is formed within the enclosure, with the increasing of wall thickness the shape of the circulating cell becomes elliptical. This is because the fluid adjacent to the hotter wall has lower density than the fluid at the middle of the enclosure. As a result the fluid moves upwards from the middle section of hot wall, and reach at the upper part of the enclosure, and then it is cooled, so its density increase, then the fluid flows downwards at the right side, and finally it directed to the left wall.

$\phi = 0.0$ $\phi = 0.05$

Figure 3.9: (a) Streamlines at various solid wall thickness (w_1) (at $Ra = 10^6$, $Pr = 6.2$, $h_\infty = 100 W/m^2 \text{K}$, $K_r = 10$ and $l_1 = 0.40$) base fluid and nanofluid.

$$\phi = 0.0 \qquad\qquad \phi = 0.05$$
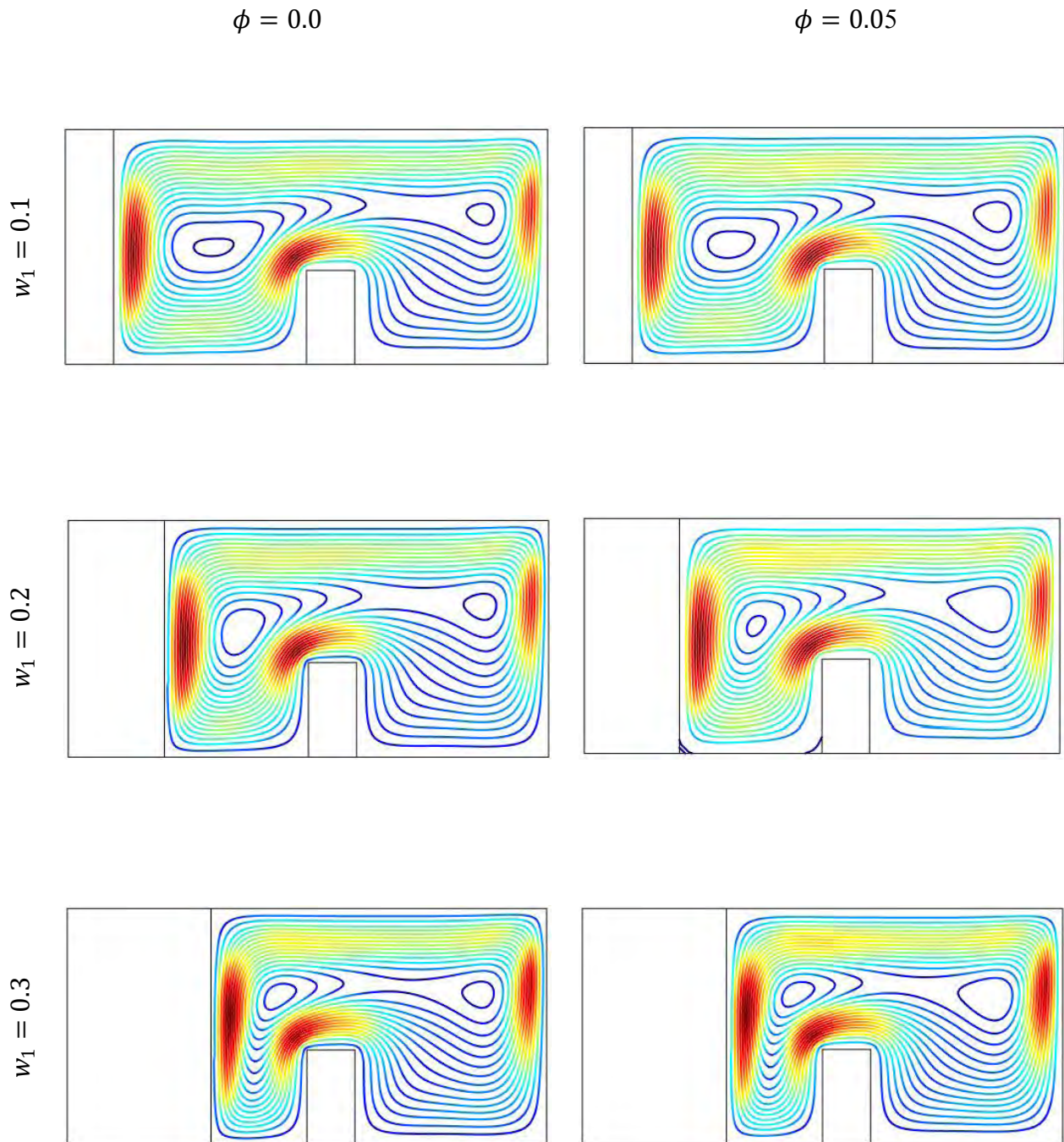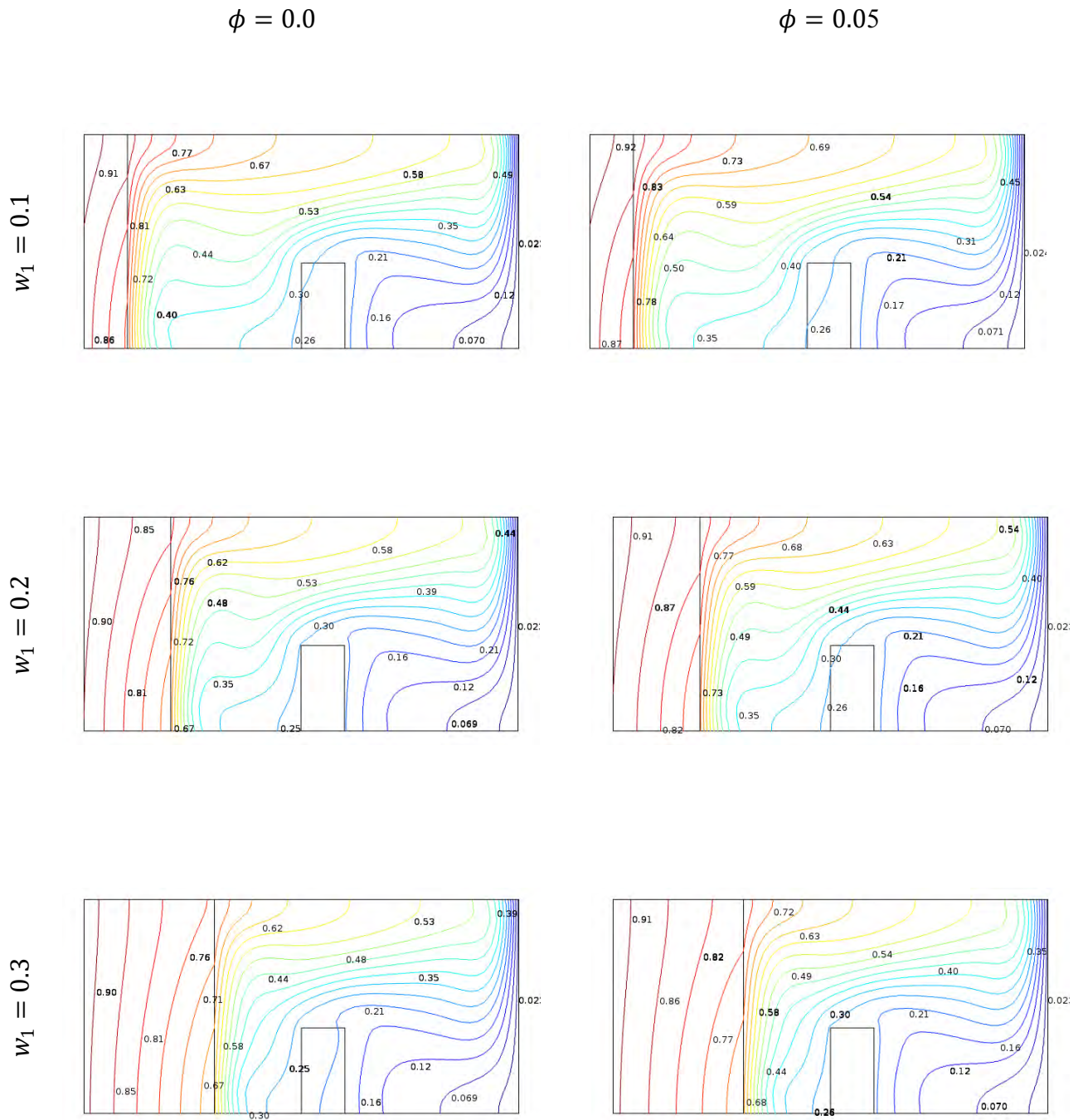

Figure 3.9: (b) Isotherms at various solid wall thickness (w_1) (at $Ra = 10^6$, $Pr = 6.2$, $h_\infty = 100 W/m^2 \, K$, $K_r = 10$ and $l_1 = 0.40$) for base fluid and nanofluid.

So a clockwise circulation is observed. We also notice here that for small wall thickness $(w_1 = 0.1)$ the strength of flow between the solid wall and the divider is higher than the larger value of wall thickness (w_1). On the other hand the effect of wall thermal resistance is directly proportional with wall thickness, so when wall thickness (w_1) increase from $w_1 = 0.1$ to $w_1 = 0.3$, the temperature (isotherm) gradient within the wall decreases, with less convection amount within the enclosure. This is because with the increase of solid wall thickness (w_1), it behaves as an insulated material in this case. So we can say the thermal resistance of the wall is inversely proportional with its thermal conductivity and directly with its wall thickness.

The effect of wall thickness (w_1) on Nusselt number (Nu) is depicted in Figure 3.9 (c) with the various values of solid volume fraction(ϕ). In general increasing wall thickness (w_1) decrease Nusselt number (Nu), because of the increased of thermal wall resistance which resist the heat transfer rate to the cavity.
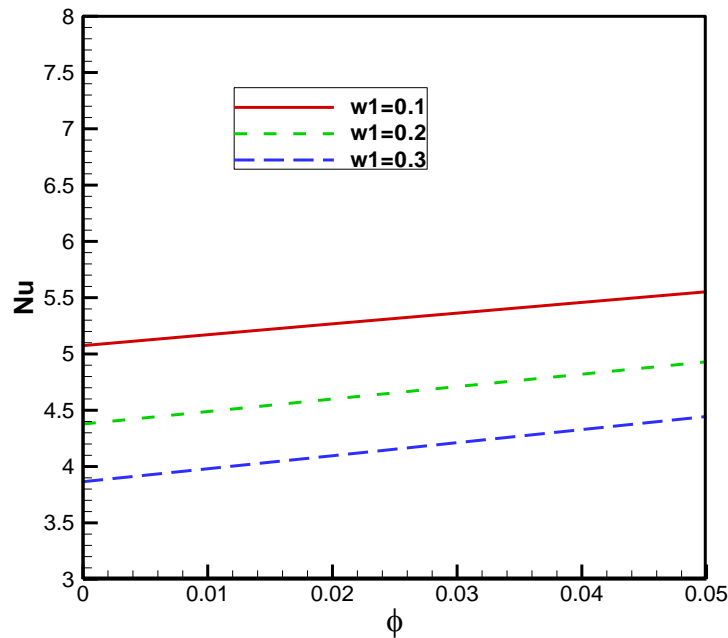

Figure 3.9 (c): Average Nusselt number at various w_1 (for $Ra = 10^6, Pr = 6.2$, $h_\infty = 100W/m^2 K$, $K_r = 10$ and $l_1 = 0.4$).

54

3.6 Conclusion of Chapter Three

Based on the results and discussion as furnished in this chapter of conjugate effect on fluid flow and heat transfer in a cavity with finite vertical thick walled enclosure the following conclusions are drawn.

1) There is a significant effect of Rayleigh number on the pattern of streamlines and isotherms in the cavity. Both increasing the value of Rayleigh number and solid volume fraction of nanparticles arguments the flow strength keeping other parameter fixed. A remarkable effect of Ra on the average heat transfer rate (Nesselt number) is observed which indicate enhanced rate of heat transfer and increase the cooling performance of the enclosure. i.e. Nusselt number is an increasing function of Rayleigh number.

2) The increase in the convective heat transfer coefficient leads to the decrease in the heat transfer. The presence of the nanoparticles is more effective at a higher h_∞.

3) The location of the divider position has a remarkable effect on the thermal behavior and flow pattern. When the divider gets closure to the cold wall, the heat transfer is enhanced.

4) Conduction in the wall makes a strong effect on natural convection in the fluid part. It is found that the rate of heat transfer increases and the fluid moves with greater velocity when the value of Rayleigh number and conductivity ratio increase. It is observed that the temperature difference between the interface and the cold boundary reduces with decreasing the solid fluid thermal conductivity ratio, therefore reducing the average Nusselt number. For lower value of k_r, where solid wall is insulation material, Nu has low values comparing with those at high value of k_r because of the increase in the thermal resistance of the overall system and vice versa.

5) The strength of the flow circulation of the fluid is much higher with thin wall. The strength of the circulation cell can be controlled by the thickness of the solid wall. The natural convection inside the nanofluid filled cavity decreases with increasing its wall thickness. The average Nuselt number decreases by increasing the wall thickness and Nu becomes constant for the highest values of the thickness parameter of the solid vertical wall.

Chapter 4: MHD Effect on Conjugate Heat Transfer

4.1 Introduction

The influence of the magnetic field on convective conjugate heat transfer flow of the nanofluid is of paramount importance in engineering. A free convection flow of an electrically conducting fluid in a cavity in the presence of magnetic field is of special technical significance because of its frequent occurrence in many industrial applications such as geothermal reservoirs, cooling of nuclear reactors, thermal insulations and petroleum reservoirs. These types of problems also arise in electronic packages, microelectronic devices during their operations.

In this chapter, the present work is devoted to the numerical study of laminar magneto hydrodynamic (MHD) conjugate natural convection flow on an incompressible, viscous and electrically conducting fluid with heat conducting vertical wall and uniform heat flux.

The objective of the present study is to examine the momentum and energy transport processes in a rectangular enclosure in presence of magnetic field. The results are shown in terms of parametric presentations of streamlines and isotherms for various pertinent dimensionless parameters. This dimensionless group includes the Rayleigh number (Ra), convective heat transfer coefficient (h_∞), position of divider (l_1), solid fluid thermal conductivity ratio (K_r), solid wall thickness (w_1) and solid volume fraction(ϕ) on heat transfer and fluid flow inside the cavity for the range of Hartmann number (Ha) of 0 to 60. Results are presented graphically with detailed discussion. Finally, the implications of the above parameters are depicted on the average Nusselt number (Nu) of the fluid. . The current numerical results have an excellent agreement on heat transfer flow for a Newtonian fluid in a cavity in the presence of magnetic field.

4.2 Physical Model

The schematic diagram of the present study is displayed in **Figure** 4.1. It consists of two dimensional rectangular enclosure filled with electrically conducting fluid with sides of width L and height H under conjugate conduction convection heat transfer. The enclosure exposes to a uniform and constant heat flux q, which is maintained at the ambient air flow. The left wall has a thickness of width $w_1 = \frac{w}{L} = 0.1$, while the thicknesses of the other boundaries of the wall are assumed to be zero. The right wall is kept at a low

temperature T_c , while the horizontal walls are assumed adiabatic. A movable conducting divider is attached to the horizontal bottom wall of the cavity. The rectangular enclosure is filled with a suspension of copper nanoparticles in water. The nanofluids used in the analysis are assumed to be Newtonian, incompressible and laminar. The shape and the size of the nanoparticles are assumed to be uniformed. The base fluid and nanoparticles (Cu) are in thermal equilibrium and there is no slip between them. A magnetic field of strength B_0 is applied horizontally normal to the side walls.
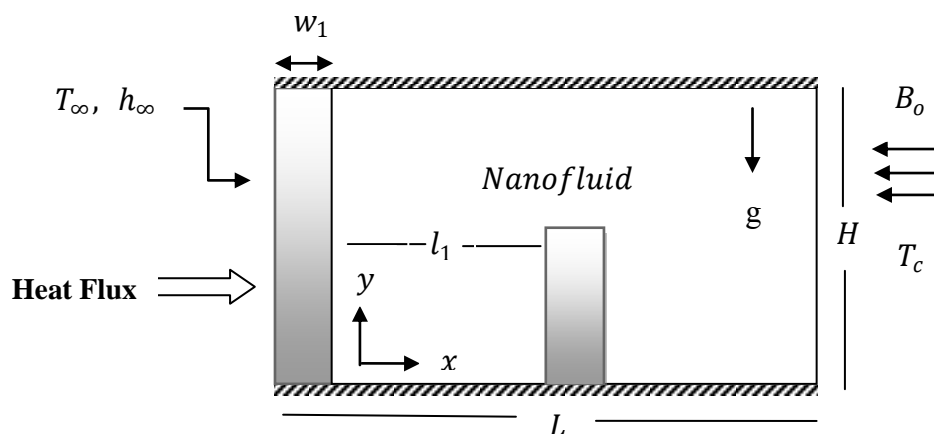

Figure 4.1:Physical Geometry of the model

4.3 Mathematical Formulation

The working fluid is assumed to be Newtonian and incompressible. The flow is set to operate in the laminar natural convection regime. The fluid properties are assumed constant except for the density variation which is treated according to Boussinesq approximation while viscous dissipation effects are considered negligible. The viscous incompressible flow and the temperature distribution inside the cavity are described by the Navier–Stokes and the energy equations, respectively. The governing equations of the present problem are as follows:

4.3.1 Governing Equation

For Fluid:

Continuity Equation:

$$\frac{\partial u}{\partial x} + \frac{\partial v}{\partial y} = 0 \tag{4.1}$$

Momentum Equations:

$$u\frac{\partial u}{\partial x} + v\frac{\partial u}{\partial y} = \frac{1}{\rho_{nf}}\left[-\frac{\partial p}{\partial x} + \mu_{nf}\left(\frac{\partial^2 u}{\partial x^2} + \frac{\partial^2 u}{\partial y^2}\right)\right] \tag{4.2}$$

$$u\frac{\partial v}{\partial x} + v\frac{\partial v}{\partial y} = \frac{1}{\rho_{nf}}\left[-\frac{\partial p}{\partial y} + \mu_{nf}\left(\frac{\partial^2 v}{\partial x^2} + \frac{\partial^2 v}{\partial y^2}\right) + (\rho\beta)_{nf}\,g(T - T_c) - \sigma_{nf}B_o^2 v\right] \tag{4.3}$$

Energy Equation:

$$u\frac{\partial T}{\partial x} + v\frac{\partial T}{\partial y} = \alpha_{nf}\left(\frac{\partial^2 T}{\partial x^2} + \frac{\partial^2 T}{\partial y^2}\right) \tag{4.4}$$

For Solid:

Energy Equation:

$$\frac{\partial^2 T_w}{\partial x^2} + \frac{\partial^2 T_w}{\partial y^2} = 0 \tag{4.5}$$

4.3.2 Boundary Conditions

The boundary conditions for the present problem are specified as follows:

For all rigid walls: $u = v = 0$

At the right vertical wall: $T = T_c$

At the top and bottom walls: $\frac{\partial T}{\partial y} = 0$

At the left side of thick wall: $q = -\kappa_w \frac{\partial T}{\partial x}|_w + h_\infty(T_w - T_\infty)$

At the divider surface: $u = v = 0$

At the fluid solid wall interfaces: $\kappa_w \frac{\partial T}{\partial x}|_w = \kappa_{nf}\frac{\partial T}{\partial x}|_{nf}$

In order to estimate heat transfer enhancement, we have calculated the local Nusselt number and average Nusselt number at the thick wall (hot wall) as

$$Nu_l = -\frac{\kappa_{nf}}{\kappa_f}\frac{H}{(T_w - T_c)}\frac{\partial T}{\partial x}|_{x=0.1}$$

The average Nusselt number is given by $Nu_{av} = \int_0^H Nu_l\,dy$.

4.3.3 Dimensional Analysis

The above equations are non-dimensionalized upon incorporating the following dimensionless variables:

$$X = \frac{x}{L} \ , \ Y = \frac{y}{L} \ , \ U = \frac{uL}{\alpha_f} \ , \ V = \frac{vL}{\alpha_f} \ , \ P = \frac{\bar{p}\,L^2}{\rho_{nf}\,\alpha_f^2} \ , \ \theta = \frac{T-T_c}{\Delta T} \ \text{and} \ \Delta T = \frac{q''L}{\kappa_f}.$$

After substituting these dimensionless variables into the equations (4.1-4.5) the non-dimensional continuity, momentum and energy equations are written as follows:

For Fluid:

Continuity Equation:

$$\frac{\partial U}{\partial X} + \frac{\partial V}{\partial Y} = 0 \tag{4.6}$$

Momentum Equations:

$$U\frac{\partial U}{\partial X} + V\frac{\partial U}{\partial Y} = -\frac{\partial P}{\partial X} + \frac{\mu_{nf}}{\rho_{nf}\,\alpha_f}\left(\frac{\partial^2 U}{\partial X^2} + \frac{\partial^2 U}{\partial Y^2}\right) \tag{4.7}$$

$$U\frac{\partial V}{\partial X} + V\frac{\partial V}{\partial Y} = -\frac{\partial P}{\partial Y} + \frac{\mu_{nf}}{\rho_{nf}\,\alpha_f}\left(\frac{\partial^2 V}{\partial X^2} + \frac{\partial^2 V}{\partial Y^2}\right) + \frac{(\rho\beta)_{nf}}{\rho_{nf}\,\beta_f}\,Ra\,\Pr\theta - Ha^2\,\Pr V \tag{4.8}$$

Energy Equation:

$$U\frac{\partial \theta}{\partial X} + V\frac{\partial \theta}{\partial Y} = \frac{\alpha_{nf}}{\alpha_f}\left(\frac{\partial^2 \theta}{\partial X^2} + \frac{\partial^2 \theta}{\partial Y^2}\right) \tag{4.9}$$

For Solid:

$$\frac{\partial^2 \theta_w}{\partial X^2} + \frac{\partial^2 \theta_w}{\partial Y^2} = 0 \tag{4.10}$$

The dimensionless parameter appearing in the equations (4.7-4.10) are as follows:

Rayleigh numbe $Ra = \frac{g\,\beta_f L^3 \Delta T}{\nu_f \alpha_f}$, Hartmann number $Ha = B_o L\sqrt{\frac{\sigma_{nf}}{\rho_{nf}\,\nu_f}}$, B_o is the magnitude of the magnetic field and σ is the electrical conductivity and Prandlt number $Pr = \frac{\nu_f}{\alpha_f}$,where $\alpha = \frac{\kappa}{\rho C_p}$, is the thermal diffusivity of the fluid.

4.3.4 Non Dimensional Boundary Conditions

The non dimensional boundary conditions under consideration can be written as:

For all rigid walls: $U = V = 0$

At the right vertical wall: $\theta = 0$

At the top and bottom walls: $\frac{\partial \theta}{\partial Y} = 0$

At the left side of thick wall: $q = -\frac{\kappa_w}{\kappa_{nf}}\frac{\partial \theta}{\partial X}\big|_w + \frac{H}{\kappa_{nf}}h_\infty \theta_w = 1$

At the divider surface: $U = V = 0$

At the fluid solid wall interfaces: $\frac{\partial \theta_{nf}}{\partial X} = K_r \frac{\partial \theta_w}{\partial X}$

Where, $K_r = \frac{\kappa_w}{\kappa_{nf}}$ is the solid fluid thermal conductivity ratio.

The local Nusselt number at the thick wall on the enclosure base on the non dimensional variable can be expressed as,

$$Nu_l = -\frac{\kappa_{nf}}{\kappa_f} \frac{\partial \theta}{\partial X} |_{x=0.1}$$

and the average Nusselt number at the right thick wall as

$$Nu_{av} = -\frac{\kappa_{nf}}{\kappa_f} \int_0^H \frac{\partial \theta}{\partial X} dy \ .$$

4.4 Numerical Validation

4.4.1 Grid Generation

Grid or mesh generation is the partition of the geometry model into small units of simple shapes named finite elements, control volume etc that approximates the physical domain in finite element method. Dependent variables are approximated at the local element coordinates defined by the numerical grid. It is mainly a disconnected demonstration of the physical domain where the solutions are to be carried out. Meshing the complicated geometry make the finite element method a powerful technique to solve boundary value problems occurring in a range of engineering applications. Figure 4.2 shows the mesh configuration of present physical domain with triangular finite elements.
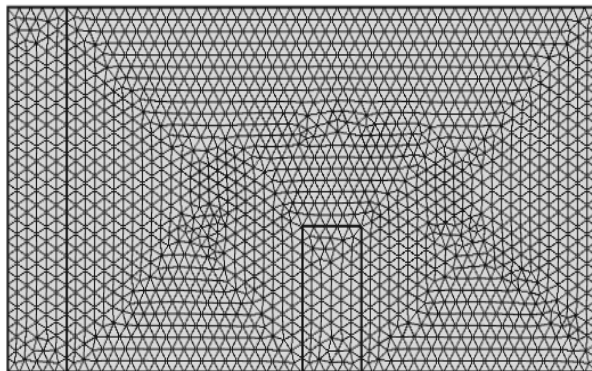

Figure 4.2: Mesh Structure of elements for the physical model

4.4.2 Grid Refinement Check

In order to determine the proper grid size for this study, a grid independence test is conducted with five types of mesh for $Ra = 10^6$, $Ha = 30$, $\phi = 0.05$, $l_1 = 0.40$, $Pr = 6.2$ and $h_\infty = 100\ W/m^2K$, $K_r = 10$ and $w_1 = 0.1$ through an rectangular enclosure. In the present work, five different non-uniform grid systems with the following number of elements within the resolution field: 394, 533, 1058, 3258 and 13020 are examined.
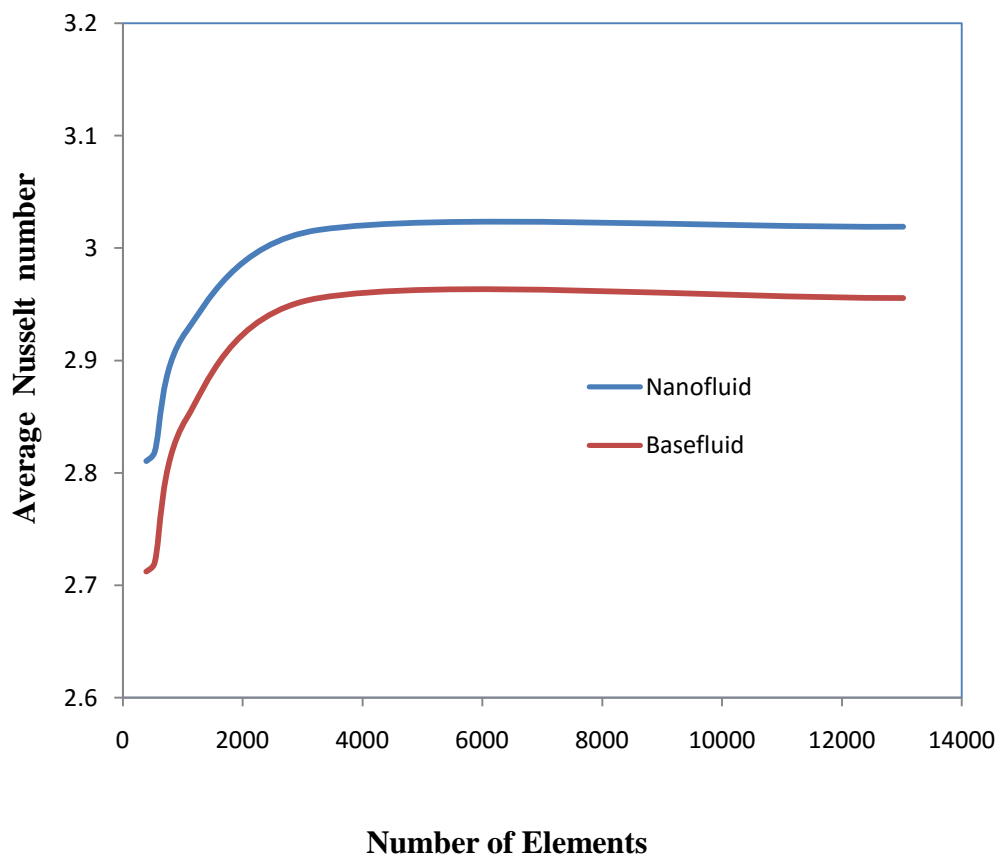

Figure 4.3: Grid refinement check.

The numerical scheme is carried out for highly precise key in the average Nusselt number for water-copper nanofluid ($\phi = 5\%$) as well as base fluid ($\phi = 0\%$) for the aforesaid elements to develop an understanding of the grid fineness as shown in Table 4.2 and Figure.4.3. The scale of the average Nusselt number for 3258 elements shows a little difference with the results obtained for the other elements. Hence, considering the non-

uniform grid system of 3258 elements is preferred for the computation. Since, it is noticed from Table 4.2 and Figure 4.3 that no further improvement is found for higher values.

Table 4.2: Grid Test at $Ra = 10^6, \phi = 0.05, l_1 = 0.40, Pr = 6.2, Ha = 30, h_\infty = 100\ W/m^2K$, $K_r = 10$ and $w_1 = 0.1$

Nodes (elements)	6181 (394)	10062 (533)	13922 (1058)	16181 (3258)	28926 (13020)
Nu (nanofluid)	2.81063	2.81877	2.92582	3.01603	3.01899
Nu (basefluid)	2.71233	2.72012	2.84810	2.95562	2.95577
Time [s]	96.265	106.594	192.157	256.328	390.377

4.5 Results and Discussion

In this section, the effects of MHD on conjugate natural convection heat transfer in a rectangular enclosure with heat conducting vertical wall and uniform heat flux are explored with solid volume fraction $\phi = 5\%$. Numerical results in terms of streamlines, isotherms for various Rayleigh number (Ra),convective heat transfer coefficient (h_∞), position of divider (l_1), solid fluid thermal conductivity ratio (K_r), solid wall thickness (w_1) and solid volume fraction(ϕ) on heat transfer and fluid flow inside the cavity have been studied for the range of Hartmann number (Ha) of 0 to 60. The ranges of Ra, h_∞, l_1, K_r and w_1 for this investigation vary from 10^4 to 10^7, 0.0 to 400, 0.1 to 0.7, 0.5 to 10.0, 0.1 to 0.3 respectively. In addition, the values of the average Nusselt number (Nu) in the domain have been calculated for the above mentioned parameters. The outcomes for the different cases are presented in the following sections.

4.5.1 Effect of Hartmann number on Rayleigh number

The effect of Hartmann number (Ha) on the streamlines and isotherms for the present configuration at $Pr = 6.2$, $h_\infty = 100W/m^2\ K$, $l_1 = 0.40$,$w_1 = 0.1$ and $\phi = 0.05$ are presented in Figures 4.4 (a, b) respectively for four values of the Rayleigh number $(Ra = 10^4, 10^5, 10^6, 10^7)$. The enclosure is filled with nanofluid, which has the solid volume fraction$(\phi = 0.05)$. We here notice that the buoyancy driven clockwise circulating flows are evident for all values of the Rayleigh number (Ra) and Hartmann

number (Ha).We see that the strength of these circulating increases as the Rayleigh number (Ra) increases and decreases as the Hartmann number (Ha) increase. The result also shows a conducting dominating regime at low Rayleigh number (Ra) with vertical isotherms and convective dominating regime at high Rayleigh number (Ra) with horizontal isotherms. We also observe here that the strength of the flow circulation and the streamlines are affected by different values of Hartmann number (Ha). This effect is more pronounced at $Ra = 10^5$, where an increasing in Hartmann number (Ha), the isotherms goes from horizontal to vertical. Because at $Ra = 10^5$, where the convective flow field is not very strong and can be influence by the magnetic field. This is an indication of weaker convection flows at higher Hartmann number (Ha) due to influence of magnetic field on the convective flows.

Figure 4.4 (c) , displays the effect of Hartmann number (Ha) on the average Nusselt number (Nu) along the hot wall at four different values of Rayleigh number $(Ra = 10^4, 10^5, 10^6, 10^7)$, with $\phi = 0.05$. The result shows that due to the strong buoyancy flow the average Nusselt number (Nu) increases as the Rayleigh number (Ra) increases and due to the suppression of the convective circulating flows by the magnetic fields, it decreases as the Hartmann number (Ha) increases. We also notice that for lower Rayleigh number (Ra) where the heat transfer is only due to conduction and in this case magnetic field does not have a considerable effect on the heat transfer performance, we see the change of average Nusselt number (Nu) remains same, but the average Nusselt number decreases faster when the Hartmann number (Ha) increase for higher value of Rayleigh number (Ra), where heat transfer occurs mainly for convection and the magnetic field can suppress the convective flow.
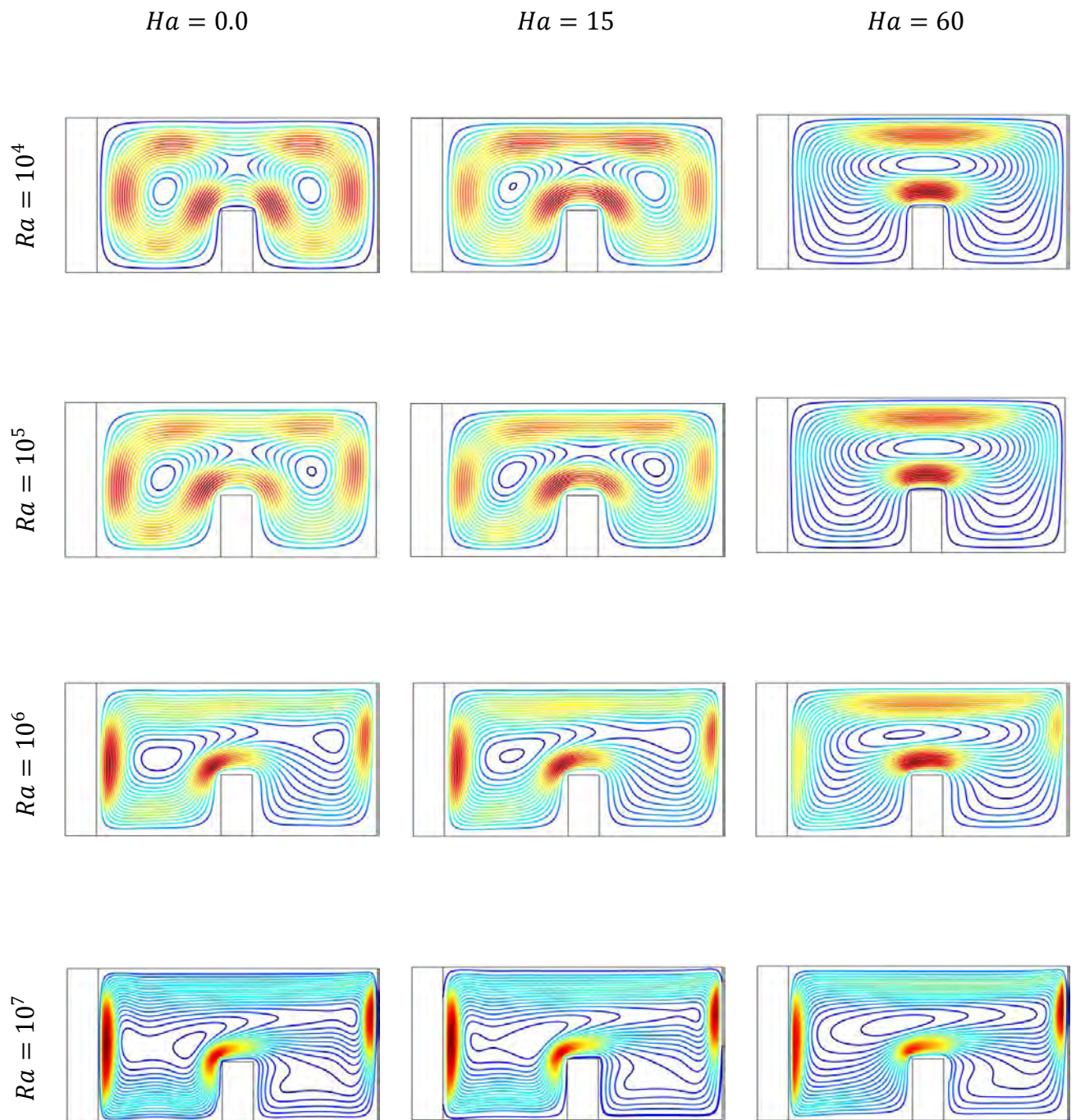
Figure 4.4: (a) Effect of Hartmann number ($Ha = 0.0, 15, 60$) on Streamlines at various Rayleigh number for $Pr = 6.2$, $h_\infty = 100W/m^2$K, $l_1 = 0.40$,$w_1 = 0.1$, $K_r = 10$ and $\phi = 0.05$.
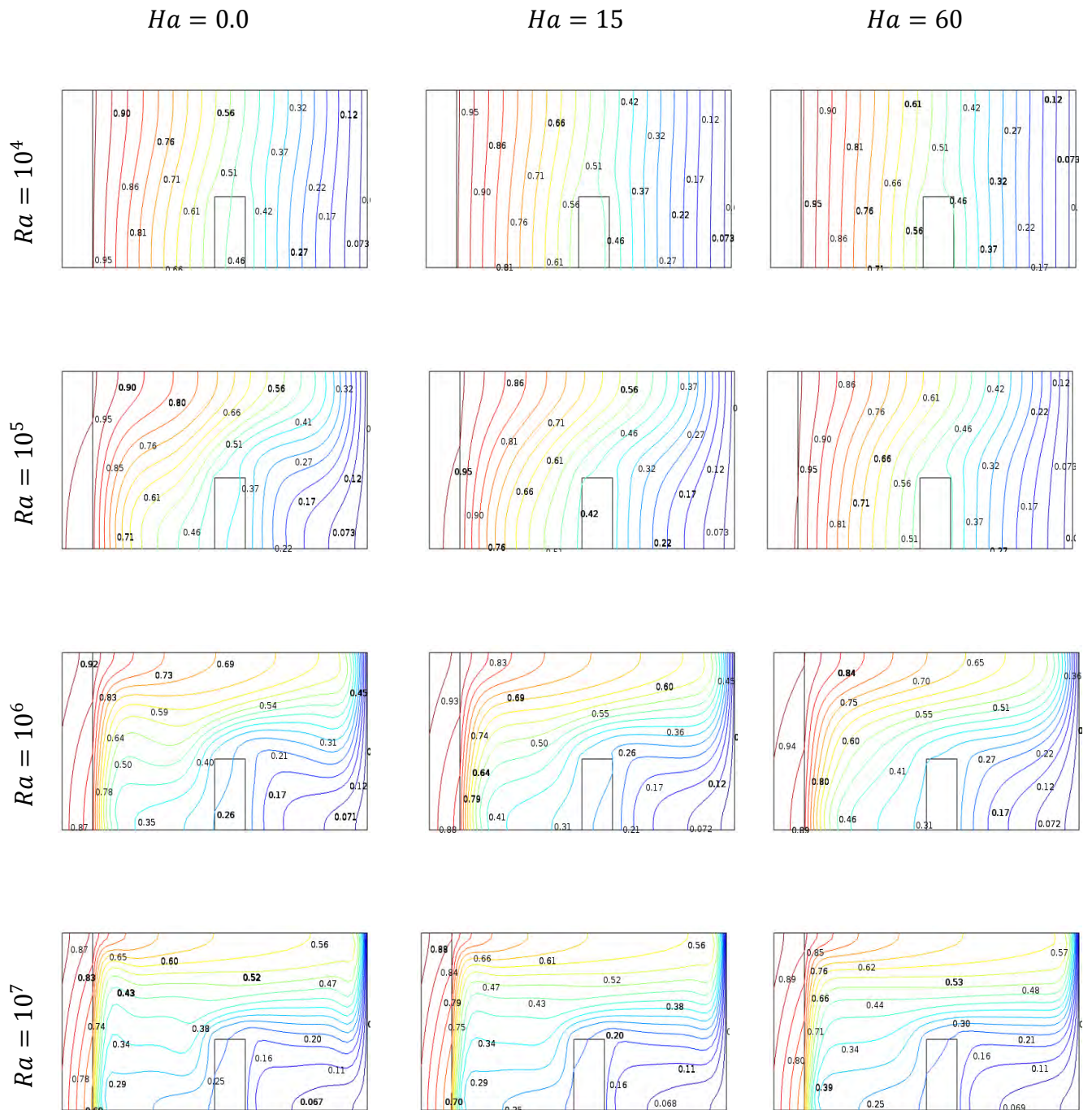
Figure 4.4: (b) Effect of Hartmann number ($Ha = 0.0, 15, 60$) on Isotherms at various Rayleigh number for $Pr = 6.2$, $h_\infty = 100 W/m^2 K$, $l_1 = 0.40$, $w_1 = 0.1$, $K_r = 10$ and $\phi = 0.05$.
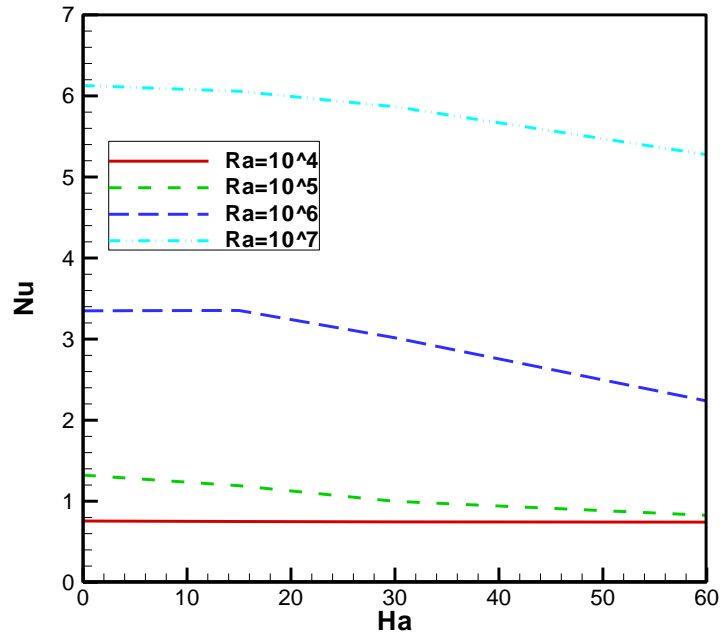
Figure 4.4 (c): Average Nusselt number at various Ra (for $Ha = 0, 15, 30, 60$, $Pr = 6.2$, $h_\infty = 100W/m^2$ K, $l_1 = 0.40, K_r = 10$ and $w_1 = 0.1$).

4.5.2 Effect of Hartmann number on Convective Heat Transfer Coefficient

Figures 4.5 (a, b) represent the effect of Hartmann number (Ha) on fluid flow and temperature field for various values of convective heat transfer coefficient (h_∞) with $Ra = 10^6, l_1 = 0.40, w_1 = 0.1, Pr = 6.2 , K_r = 10$ and $\phi = 0.05$. We observe that strength of the flow circulation decreases as the convective heat transfer coefficient (h_∞) and the Hartmann number (Ha) increase. We also notice in Figure 4.5 (a) that in the case of $h_\infty = 400W/m^2$K the maximum value of stream function decreases with respect to the case $h_\infty = 100W/m^2$K. We know that the increase of convective heat transfer coefficient (h_∞) reduces the thick wall thermal temperature, so heat will less absorbed by inner flow. We also notice due to magnetic field, the strength of convective circulation reduces, so with the increases of Hartmann number (Ha) we see weaker flow strength. We also observe in Figure 4.5 (b) that at lower Hartmann number (Ha) the isotherms near the vertical wall are more clustered for the lower values of convective heat transfer coefficient(h_∞).

Figure 4.5: (a) Effect of Hartmann number ($Ha = 0.0, 15, 60$) on Streamlines at various Convective heat transfer coefficient for $Ra = 10^6, Pr = 6.2, l_1 = 0.40, w_1 = 0.1$, $K_r = 10$ and $\phi = 0.05$.
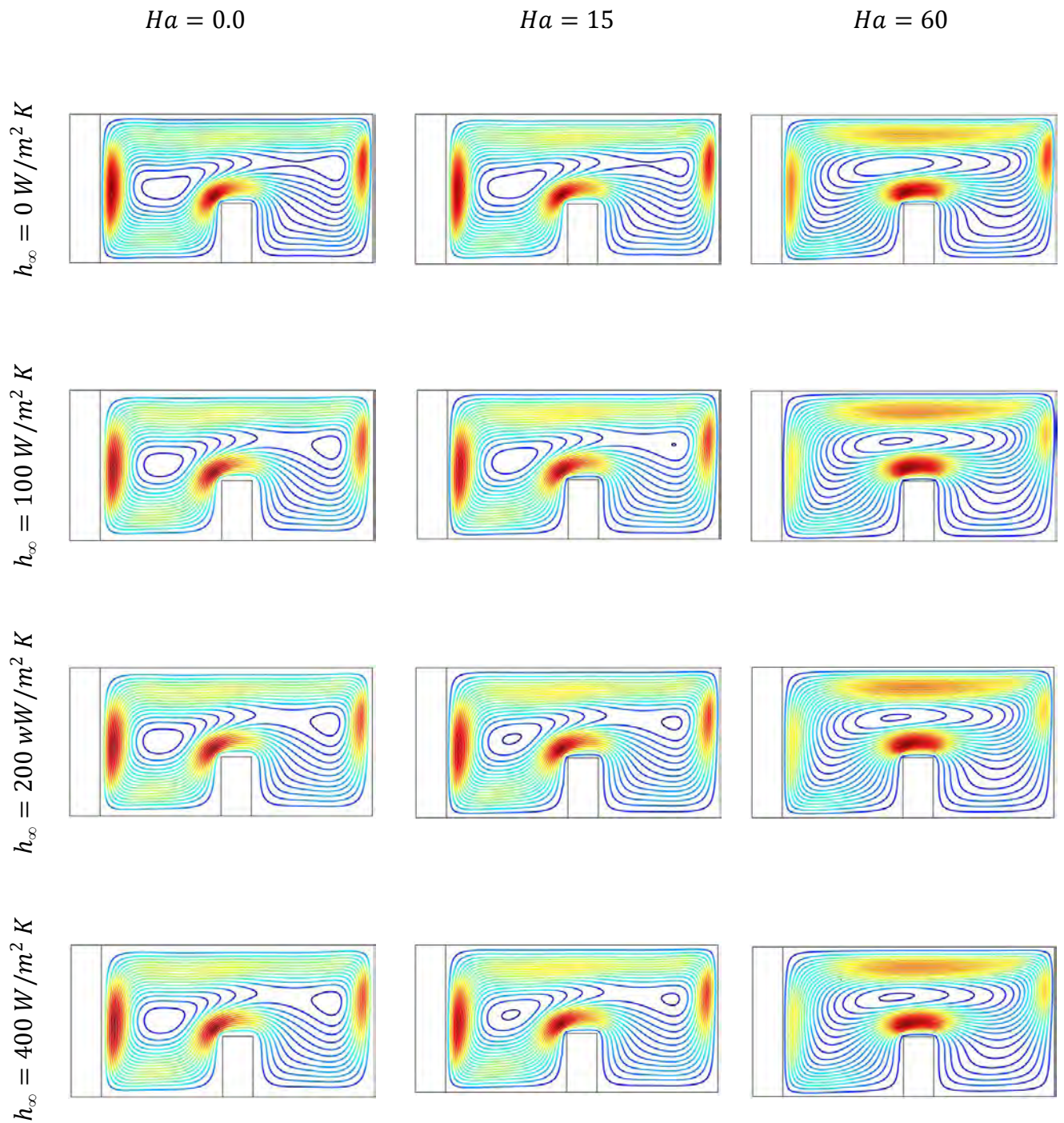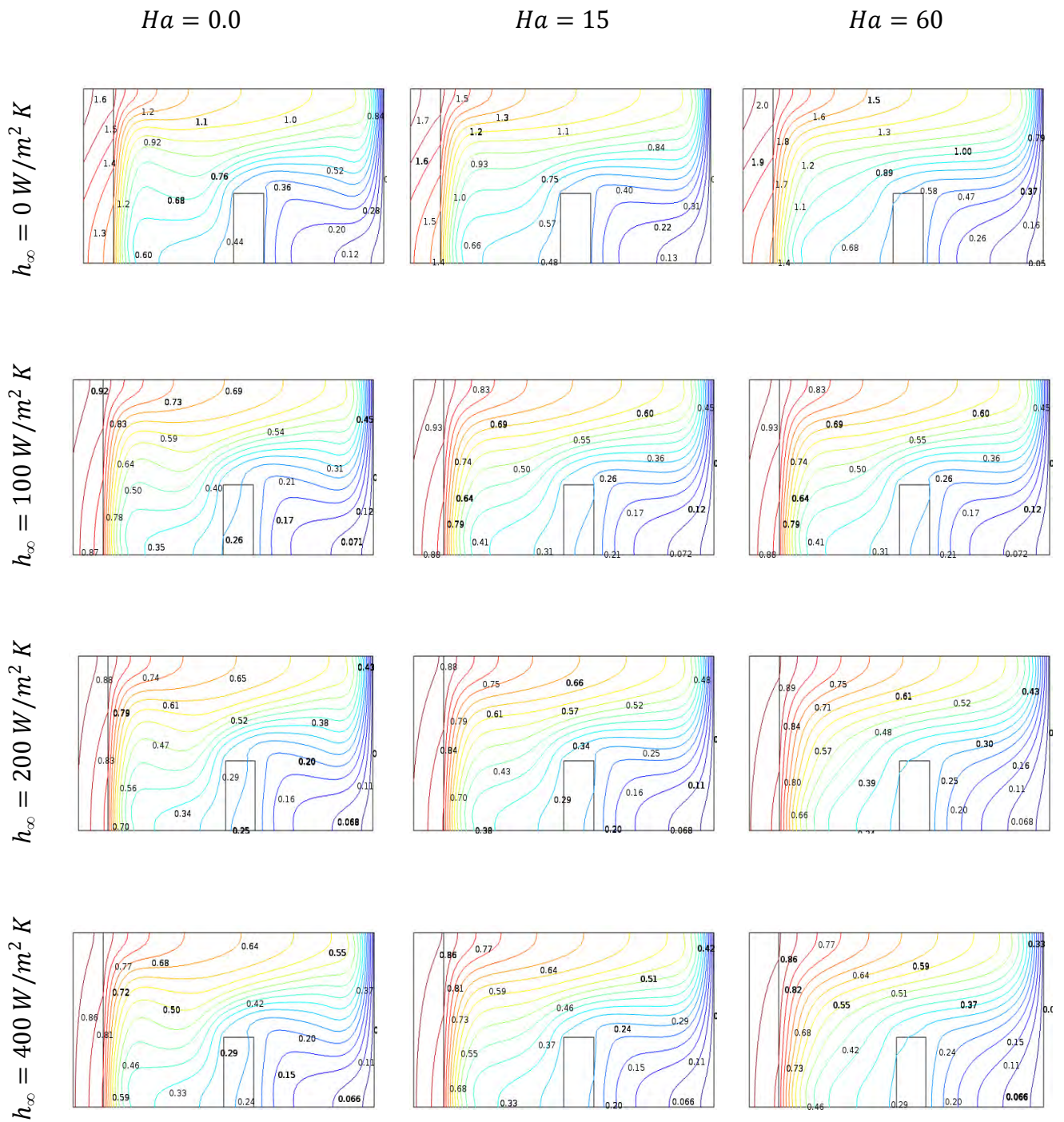
Figure 4.5: (b) Effect of Hartmann number ($Ha = 0.0, 15, 60$) on Streamlines at various Convective heat transfer coefficient for $Ra = 10^6, Pr = 6.2$, $l_1 = 0.40, w_1 = 0.1,$ $K_r = 10$ and $\phi = 0.05$.

It is also evident that for the influence of magnetic field, we see that with the increase of Hartmann number (Ha) isotherms goes from horizontal to vertical direction, which is an indication of weaker convection.

The effect of Hartmann number (Ha) on the average Nusselt number (Nu) along the hot wall for different values of convective heat transfer coefficient (h_∞) depicted in Figure 4.5 (c) on taking $Ra = 10^6, l_1 = 0.40, w_1 = 0.1, Pr = 6.2$ and $\phi = 0.05$. We see that with the increase of convective heat transfer coefficient (h_∞) the input heat flux is less absorbed by the inner flow, and due to the effect of magnetic field, the flow strength reduces as the Hartmann number (Ha) increases. We also notice that at $h_\infty = 0.0\text{W}/m^2\text{K}$, heat transfer rate is high, because in that case input heat flux is fully absorbed by the inner flow.
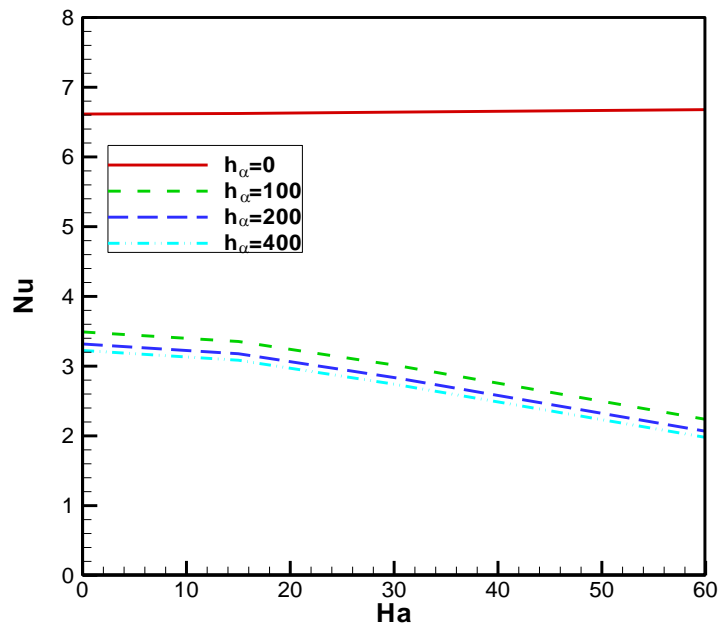

Figure 4.5 (c): Average Nusselt number at various h_∞ (for $Ha = 0, 15, \ 30, \ 60$, $Ra = 10^6, Pr = 6.2, \ , l_1 = 0.40, \ K_r = 10$ and $w_1 = 0.1$).

4.5.3 Effect of Hartmann number on Solid Volume Fractions

The effect of Hartmann number (Ha) on stream lines and isotherms for various values of solid volume fraction (ϕ) is depicted in Figures 4.6 (a, b) with $Ra = 10^6, l_1 = 0.40, w_1 = 0.1, Pr = 6.2$ and $h_\infty = 100\text{W}/m^2\text{K}$. The addition of nanoparticles results in an increasing of the maximum stream function. The reason for this is that the addition of

solid nanoparticles with higher thermal conductivity enhances the conduction heat transfer process at low Rayleigh number(Ra) and with the increase in Rayleigh number (Ra) due to increasing the strength of the buoyancy driven flow within the enclosure, we see stronger flow pattern. But in present of the Hartmann number (Ha) due to magnetic field the strength of convective circulation decreases. The mechanism is that the enclosure that are filled with electrically conducting fluid, are in the influence of magnetic field. The finding of these studies is that the fluid within the enclosure, which is under the magnetic effects, experiences a Lorentz force, which affects the buoyancy flow field and reduces the flow velocities, which in turn affects in the heat transfer. We observe here that the addition of nanoparticles results in an increasing of the maximum stream function in the absence of the magnetic field; however the strength of the convective circulation decreases when the magnetic field is applied. It is because the addition of nanoparticle in the presence of the magnetic field, produce a weaker buoyancy driven circulation and make lower value of the stream functions. On the other hand we notice that the increase of the solid volume fraction (ϕ) the temperature gradient in the thick wall increases, and due to the suppression of the convection circulation flows by the influence of stronger magnetic field, it decreases as a Hartmann number (Ha) increases, which is noticed in the isotherm line, as it is found more clustered near the thick wall for the lower value of Hartmann number (Ha), this is an indication of higher convection flow at lower Hartmann number (Ha).
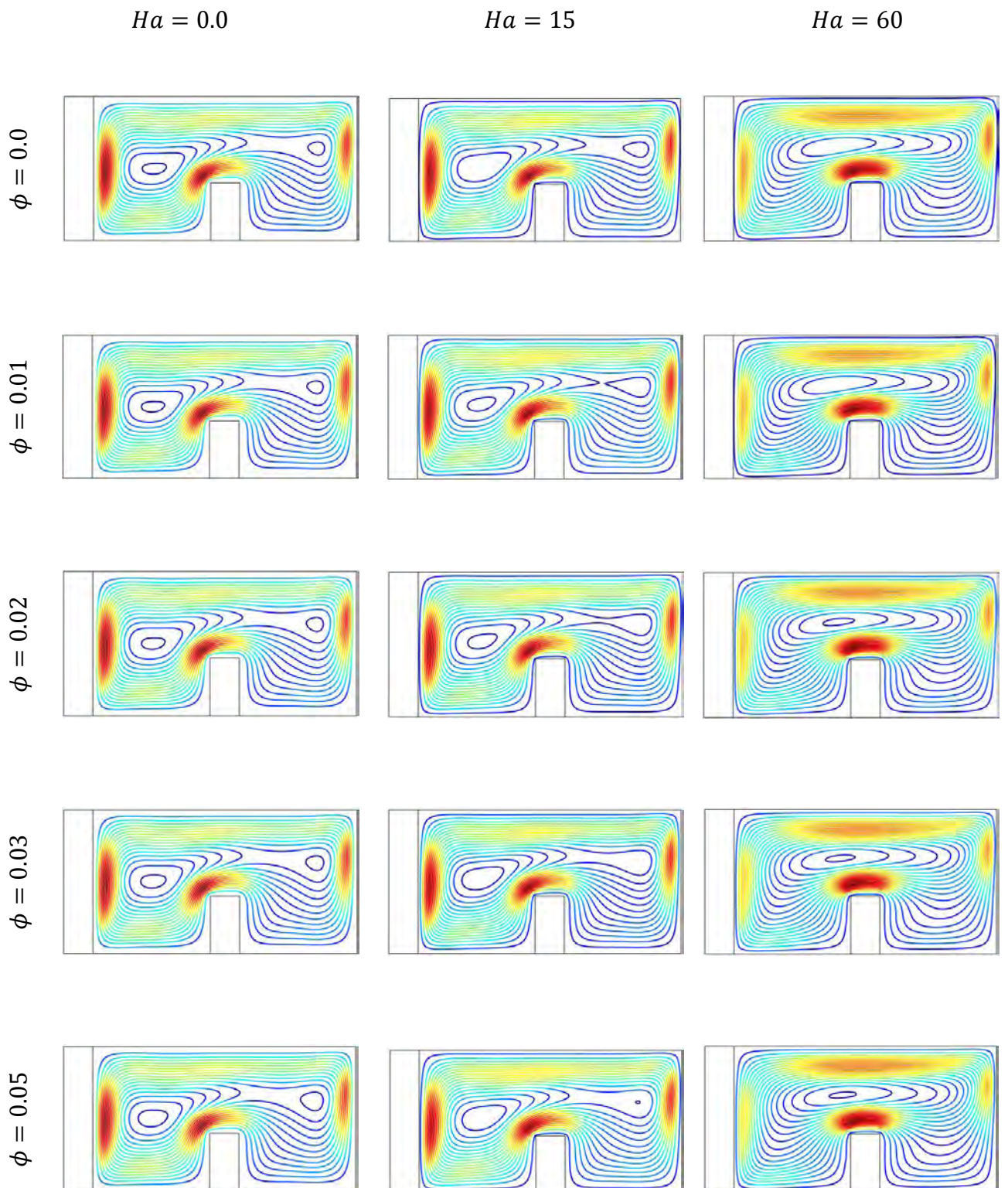
Figure 4.6: (a) Effect of Hartmann number ($Ha = 0.0, 15, 60$) on Streamlines at various Solid volume fraction for $Ra = 10^6, Pr = 6.2, h_\infty = 100 W/m^2 \text{K}, l_1 = 0.40, K_r = 10$ and $w_1 = 0.1$.
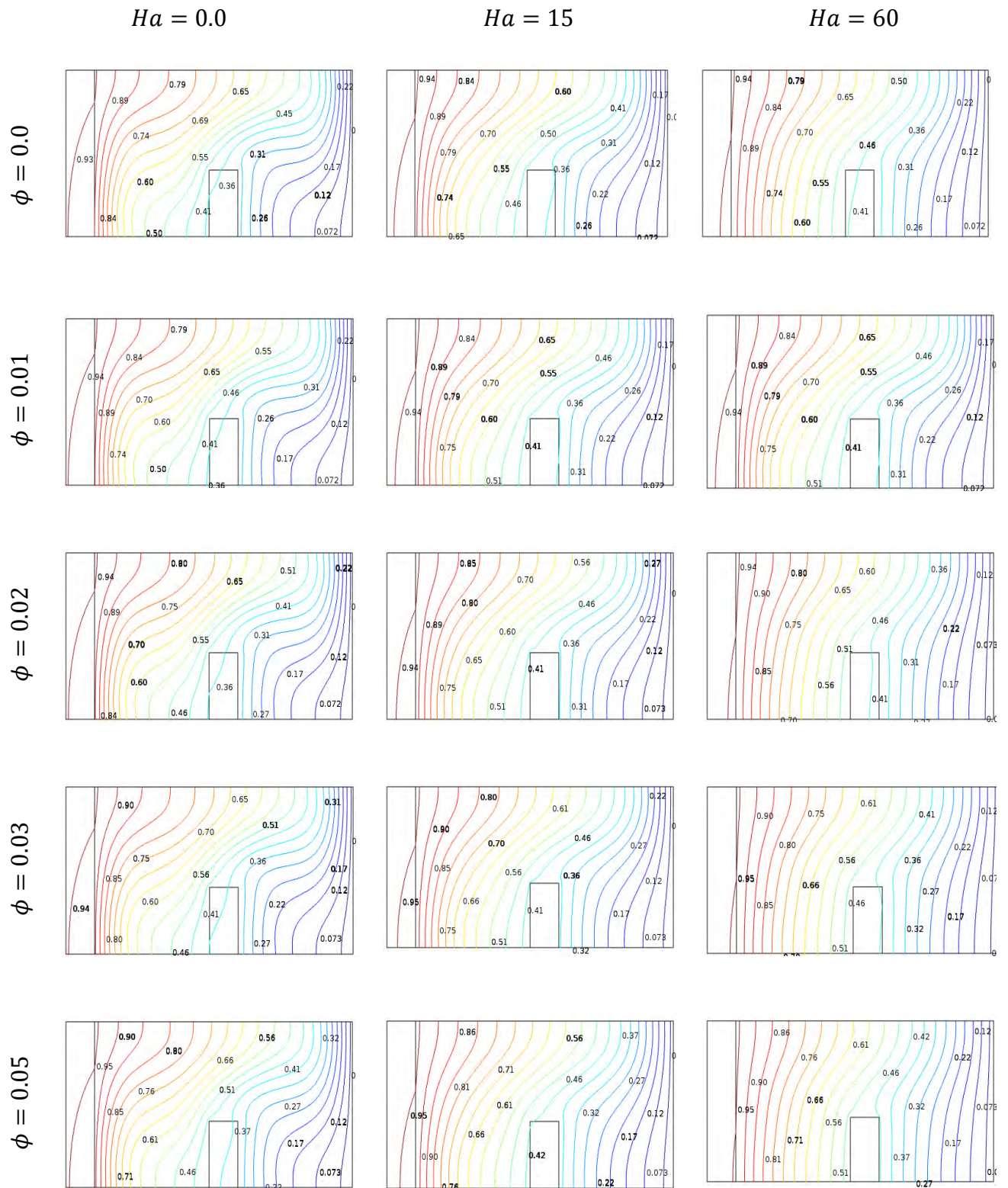
Figure 4.6: (b) Effect of Hartmann number ($Ha = 0.0, 15, 60$) on Isotherms at various Solid volume fraction for $Ra = 10^6, Pr = 6.2$, $h_\infty = 100 W/m^2 \text{K}$, $l_1 = 0.40$, $K_r = 10$ and $w_1 = 0.1$.

Figure 4.6 (c) shows the effect of Hartmann number (Ha) on the average Nusselt number (Nu) along the hot wall of the enclosure at five different values of solid volume fraction $(\phi = 0.0, 0.01, 0.02, 0.03, 0.04, 0.05)$ with $Ra = 10^6, l_1 = 0.40, w_1 = 0.1, Pr = 6.2$ and $h_\infty = 100$W/m^2K. This shows that the Hartmann number (Ha) plays a critical role in the study of the heat transfer performance of the enclosure at various value of solid volume fraction(ϕ) of nanoparticles. We see that the strength of the buoyancy flow and heat transfer rate increases as the solid volume fraction (ϕ)increases, however an increasing in Hartmann number (Ha) reduces the heat transfer rate, since magnetic field suppress the convective flow and heat transfer rate. So we can control convective heat transfer by the magnetic field.
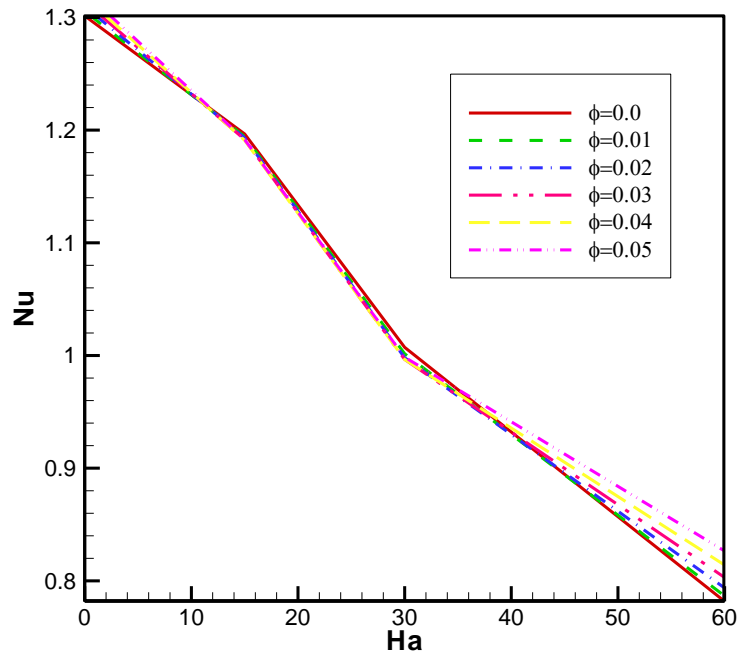

Figure 4.6 (c): Average Nusselt number at various ϕ (for $Ha = 0, 15, \ 30, \ 60$, $Ra = 10^6, Pr = 6.2, \ , l_1 = 0.40, \ w_1 = 0.1, K_r = 10$ and $h_\infty = 100$W/m^2K).

4.5.4 Effect of Hartmann number on Divider Position

The flow and temperature field due to various values of Hartmann number (Ha) on different divider positions (l_1) is shown in Figures 4.7(a, b) on taking $Ra = 10^6, w_1 = 0.1, \ Pr = 6.2$ and $h_\infty = 100$W/m^2K with $\phi = 0.05$. We observe that an increasing in divider position (l_1) from the solid wall leads to increase the flow strength, but it retards the flow strength with the higher values of Hartmann number (Ha) due to the effect of

magnetic field. We also see that when the distance between the solid wall and the divider increases the isotherms show more convective dominating mode, and its go to horizontal from vertical position. It is an indication of higher convection. But it reduces with the increase of Hartmann number at $Ha = 30, 60$, due to the influence of higher effect of magnetic field.
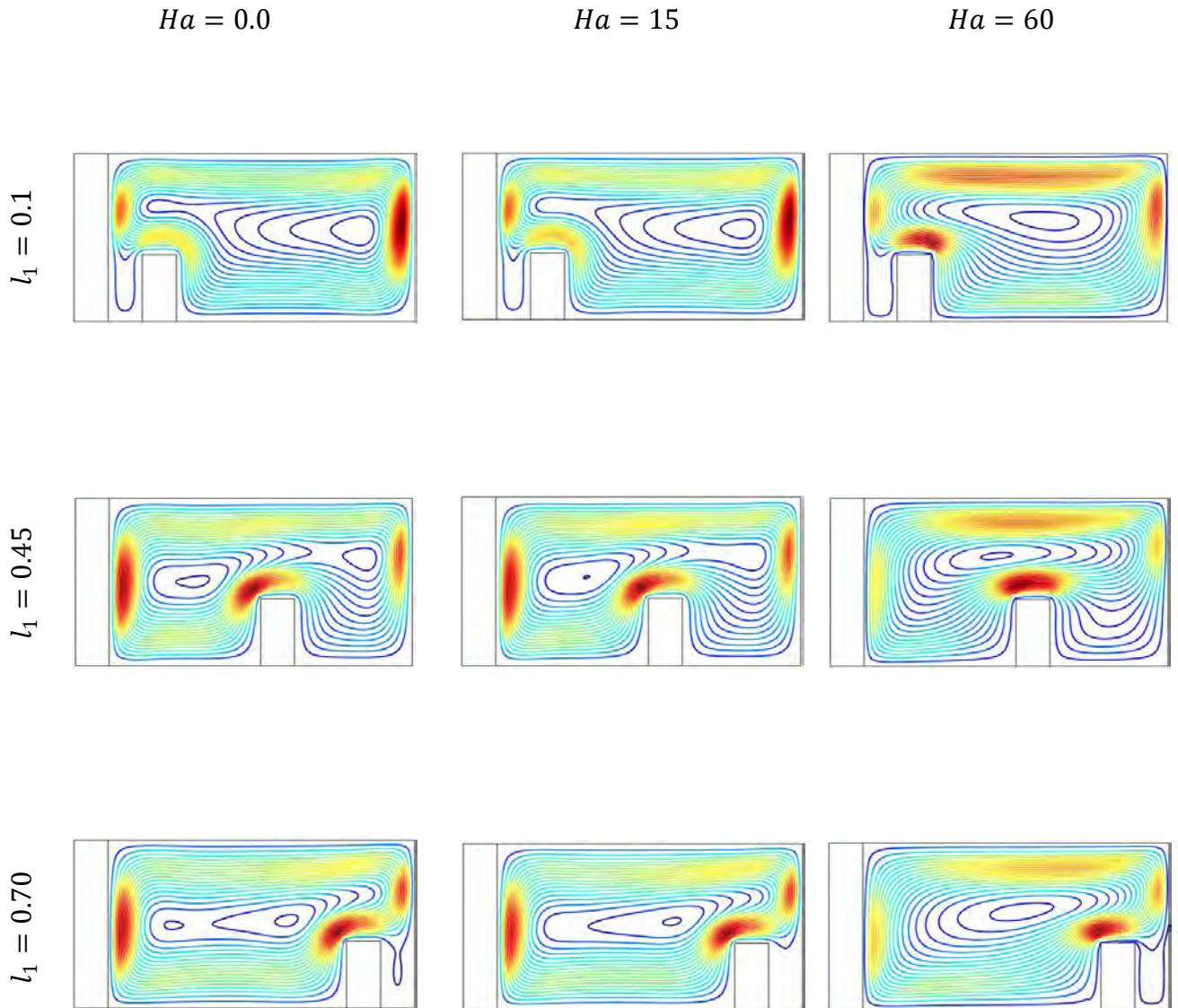

Figure 4.7: (a) Effect of Hartmann number ($Ha = 0.0, 15, 60$) on Streamlines at various Divider Position for $Ra = 10^6, Pr = 6.2, h_\infty = 100W/m^2\text{K}, K_r = 10$ and $w_1 = 0.1$.
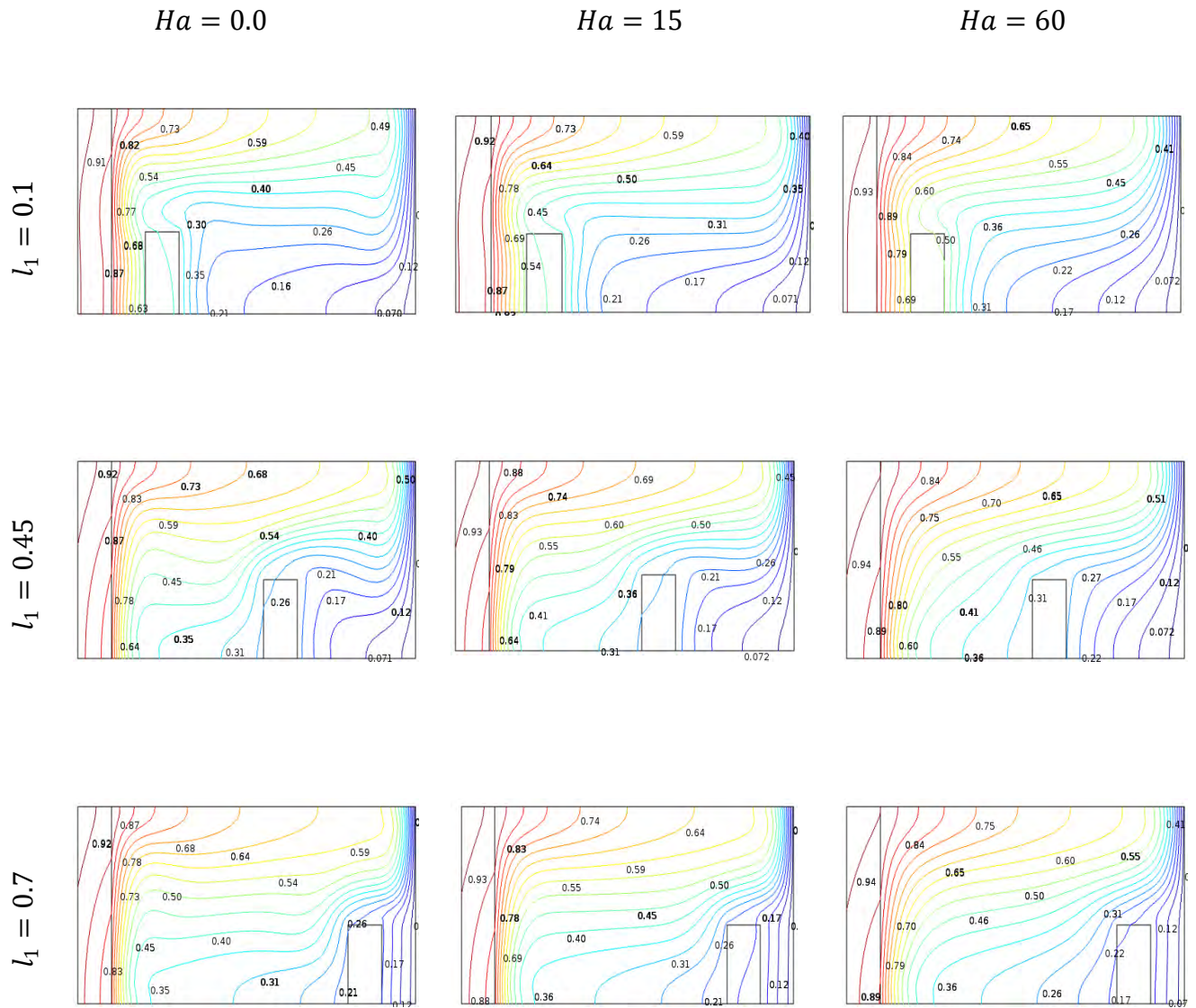
Figure 4.7: (b) Effect of Hartmann number ($Ha = 0.0, 15, 60$) on Isotherms at various Divider Position for $Ra = 10^6, Pr = 6.2,\ h_\infty = 100 W/m^2 \text{K}$, $K_r = 10$ and $w_1 = 0.1$.

Finally, from Figure 4.7 (c) it is found that the average Nusselt number (Nu) decreases mildly with increasing values of Hartmann number (Ha) at various position of divider (l_1).We see that in absence of Hartmann number($Ha = 0$), the heat transfer rate increases as the increase of distance between the solid wall and the divider but it reduces as the value of the Hartmann number (Ha) increase.

Figure 4. 7(c): Average Nusselt number at various l_1 (for $Ha = 0, 15,\ 30,\ 60$, $Ra = 10^6, Pr = 6.2,\ w_1 = 0.1, K_r = 10$ and $h_\infty = 100\ W/m^2\text{K}$)

4.5.5 Effect of Hartmann number on Solid fluid Thermal Conductivity Ratio

The influences of Hartmann number on the streamlines and isotherms for different values of solid fluid thermal conductivity ratio (K_r) with $Ra = 10^6, w_1 = 0.1, l_1 = 0.40, Pr = 6.2$ and $h_\infty = 100\text{W}/m^2\text{K}$ with $\phi = 0.05$ are depicted in Figures 4.8 (a, b). We know at very low thermal wall conductivity ratio $(K_r = 0.5)$, the solid wall acts as a thermal resistance wall, hence a steeper temperature gradient of isotherm is observed here in the solid wall, which indicates less amount of heat transfer to the enclosure. With the increase of wall thermal conductivity ratio the flow strength becomes higher and buoyancy dominates the flow. It is also noticeable in Figure 4.8 (b) that the isotherm becomes horizontal with the increase of thermal conductivity of the solid wall. The effect of Hartmann number (Ha) is more visible here. As we observe with the increase of Hartmann number (Ha) the magnetic field retards the buoyancy flow, and reduces the flow strength. So we see weaker flow pattern on the flow and the temperature field.

Figure 4.8: (a) Effect of Hartmann number ($Ha = 0.0, 15, 60$) on Streamlines at various Solid Fluid thermal conductivity ratio for $Ra = 10^6, Pr = 6.2, h_\infty = 100 W/m^2 \text{K}$, and $w_1 = 0.1$.
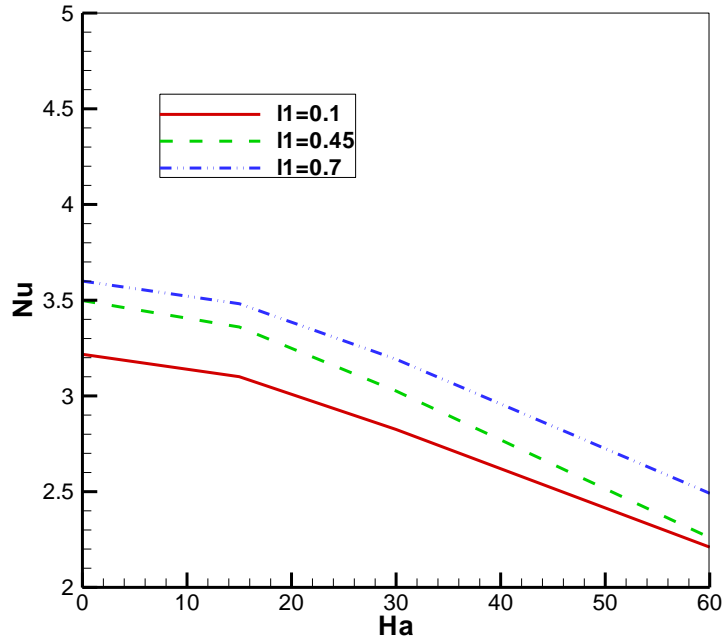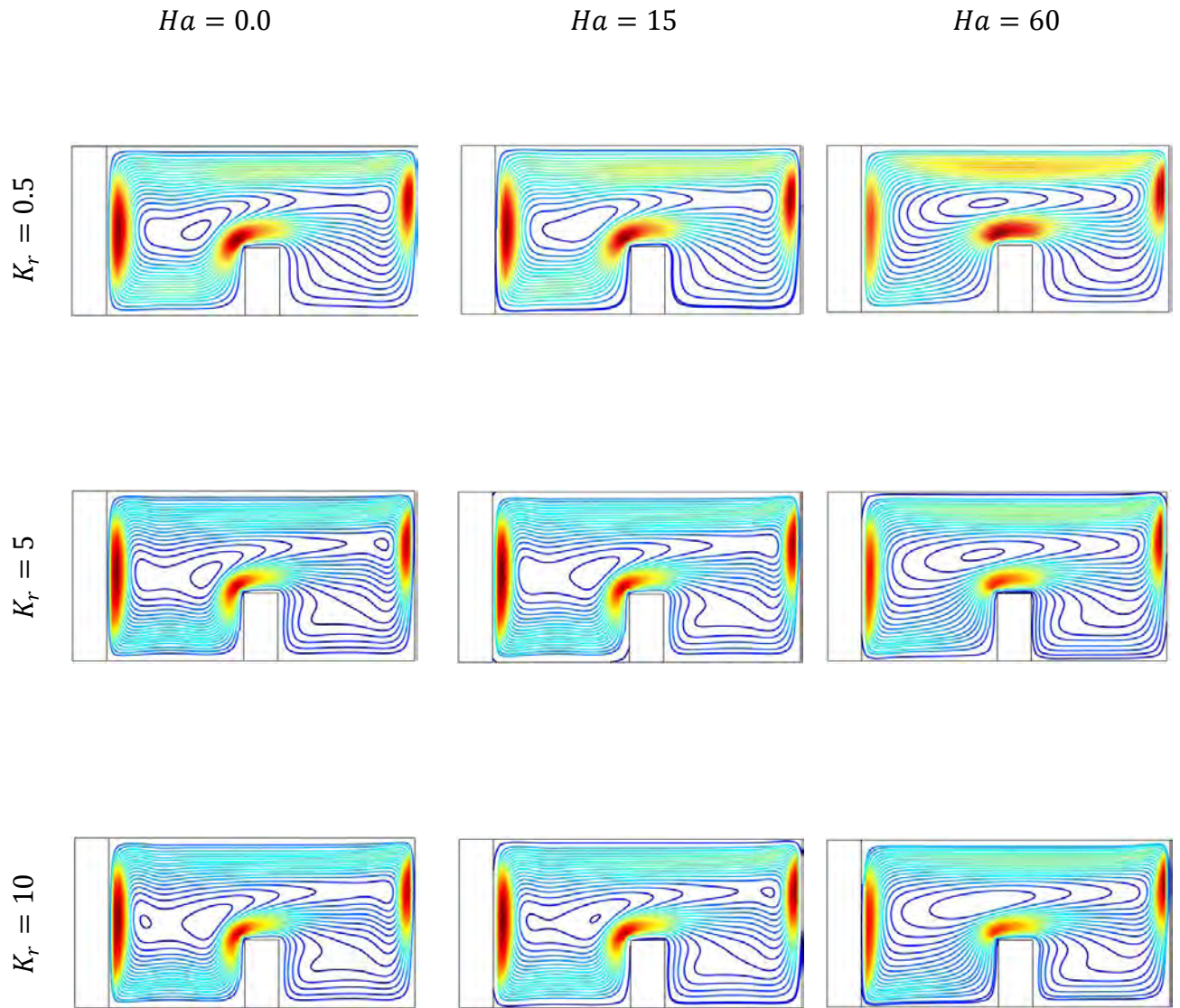
Figure 4.8: (b) Effect of Hartmann number ($Ha = 0.0, 15, 60$) on Isothermss at various Solid Fluid thermal conductivity ratio for $Ra = 10^6, Pr = 6.2,\ h_\infty = 100W/m^2\mathrm{K}$, and $w_1 = 0.1$.

The variation of average Nusselt number (Nu) with the Hartmann number (Ha) is displayed on Figure 4.8 (c) with the different values of solid fluid thermal conductivity ratio (K_r).We see that heat transfer increases with the increase of wall thermal conductivity ratio(K_r), wher the increase of Hartmann number (Ha) results in the reduction of heat transfer performance of the enclosure. This is due to the greater effect of the magnetic field and the stronger suppression of the buoyancy flow in the nanofluid.

Figure 4.8 (c): Average Nusselt number at various K_r (for $Ha = 0, 15, \ 30, \ 60$) $Ra = 10^6, Pr = 6.2, l_1 = 0.40, \ w_1 = 0.1$ and $h_\infty = 100\text{W}/m^2\text{K}$).

4.5.6 Effect of Hartmann number on Solid Wall Thickness

Figures 4.9 (a, b) examines the effect of Hartmann number (Ha) at various values of Solid wall thickness $(w_1 = 0.1, 0.2, 0.3)$ on the fluid flow and temperature field for $Ra = 10^6, l_1 = 0.40, \ Pr = 6.2$ and $h_\infty = 100\text{W}/m^2\text{K}$ with $\phi = 0.05$. Here we notice that the strength of the circulating cell is much higher for a thin solid wall. When the thickness of the solid wall increases it acts as a resistance wall, so less heat is transferred from the solid wall to the enclosure for higher value of solid wall thickness(w_1). We also observe that two core are created in the enclosure for lower wall thickness and it becomes turn as elliptic shape as solid wall thickness increase, which is an indication of weaker convection flow. As in the case of isotherms we see with the increase of solid wall thickness from $w_1 = 0.1$ to $w_1 = 0.3$ the temperature gradient within the wall decreases, which make the less convection amount within the enclosure. When the Hartmann number (Ha) applies to the fluid, the strength of the flow circulations decrease with increase of the Hartmann number (Ha) . As discussed earlier the magnetic field results in the decrease of convective circulating flows within the enclosures filled with electrically conducting fluid, this turn the reduction of heat transfer, which is also noticeable in the isotherms curves.

$Ha = 0.0$ $Ha = 15$ $Ha = 60$
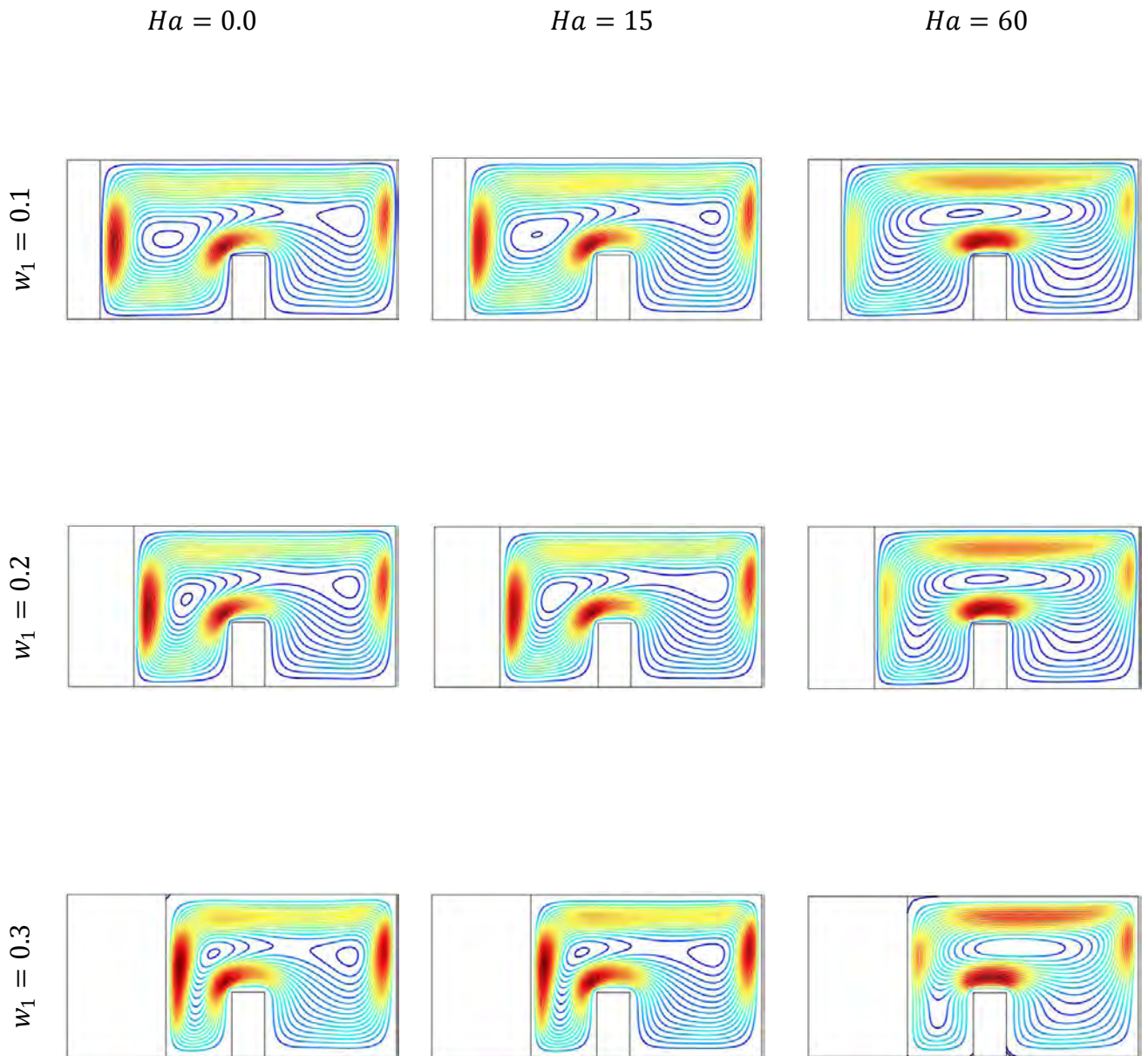
Figure 4.9: (a) Effect of Hartmann number ($Ha = 0.0, 15, 60$) on Streamlines at various Solid wall thickness for $Ra = 10^6, Pr = 6.2, \; h_\infty = 100 W/m^2 \mathrm{K}, K_r = 10$ and $l_1 = 0.4$.
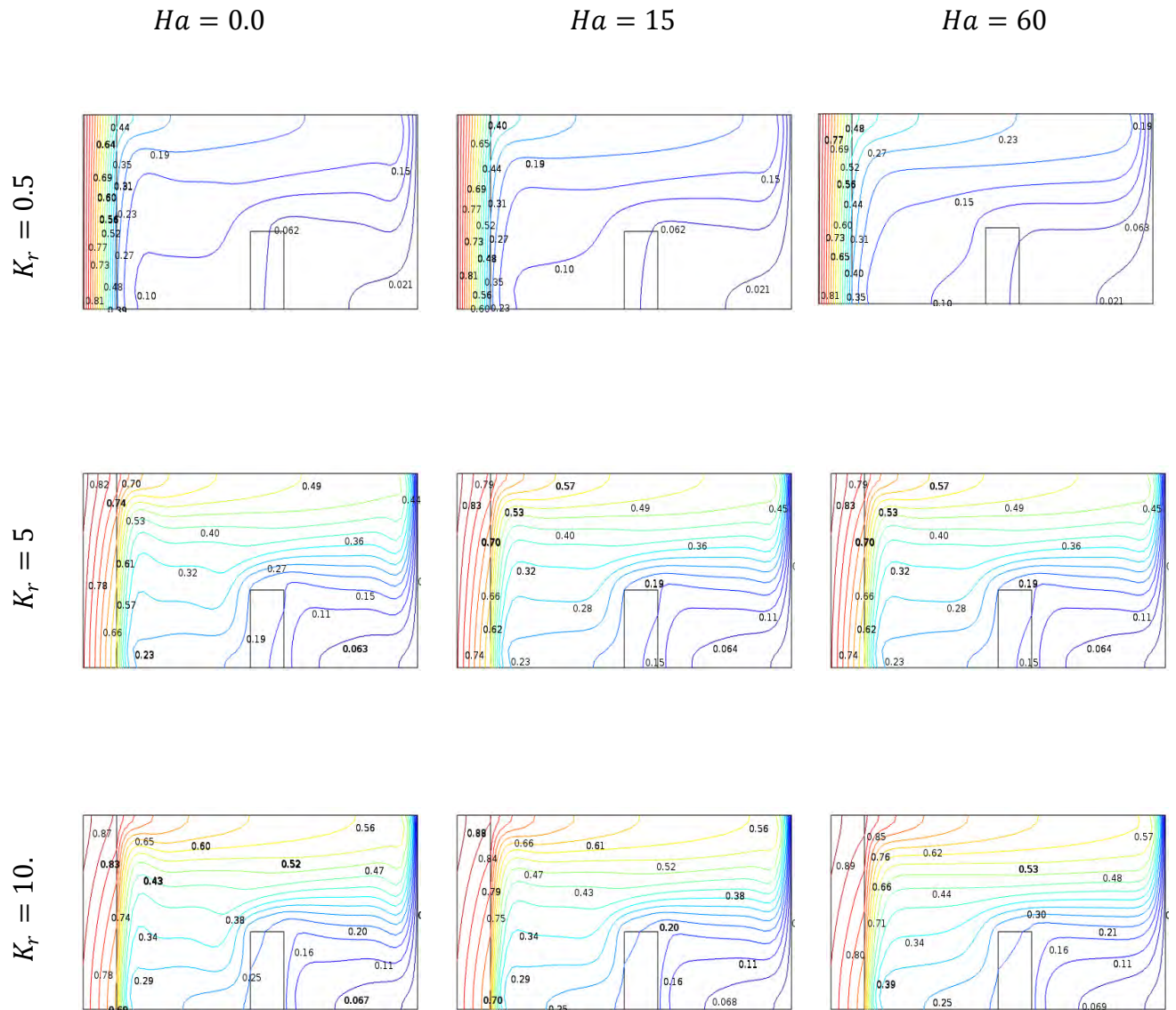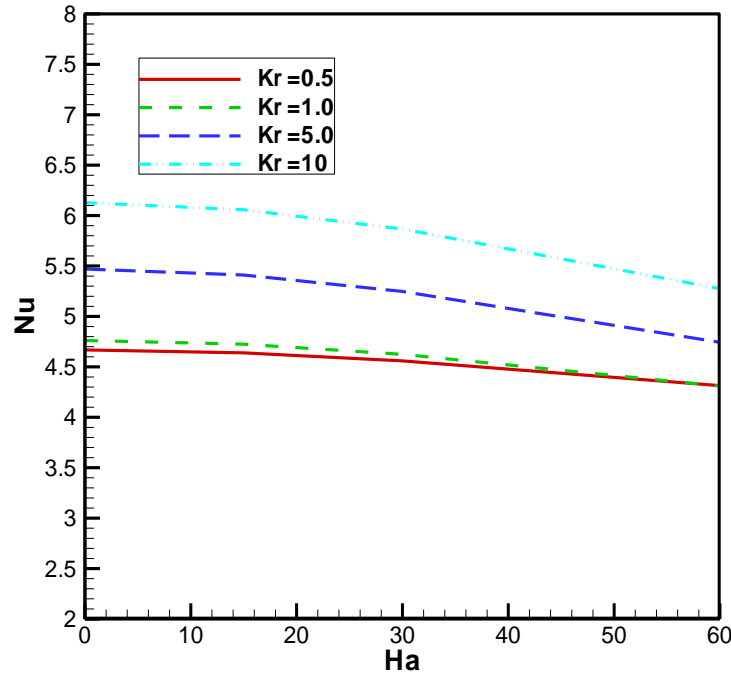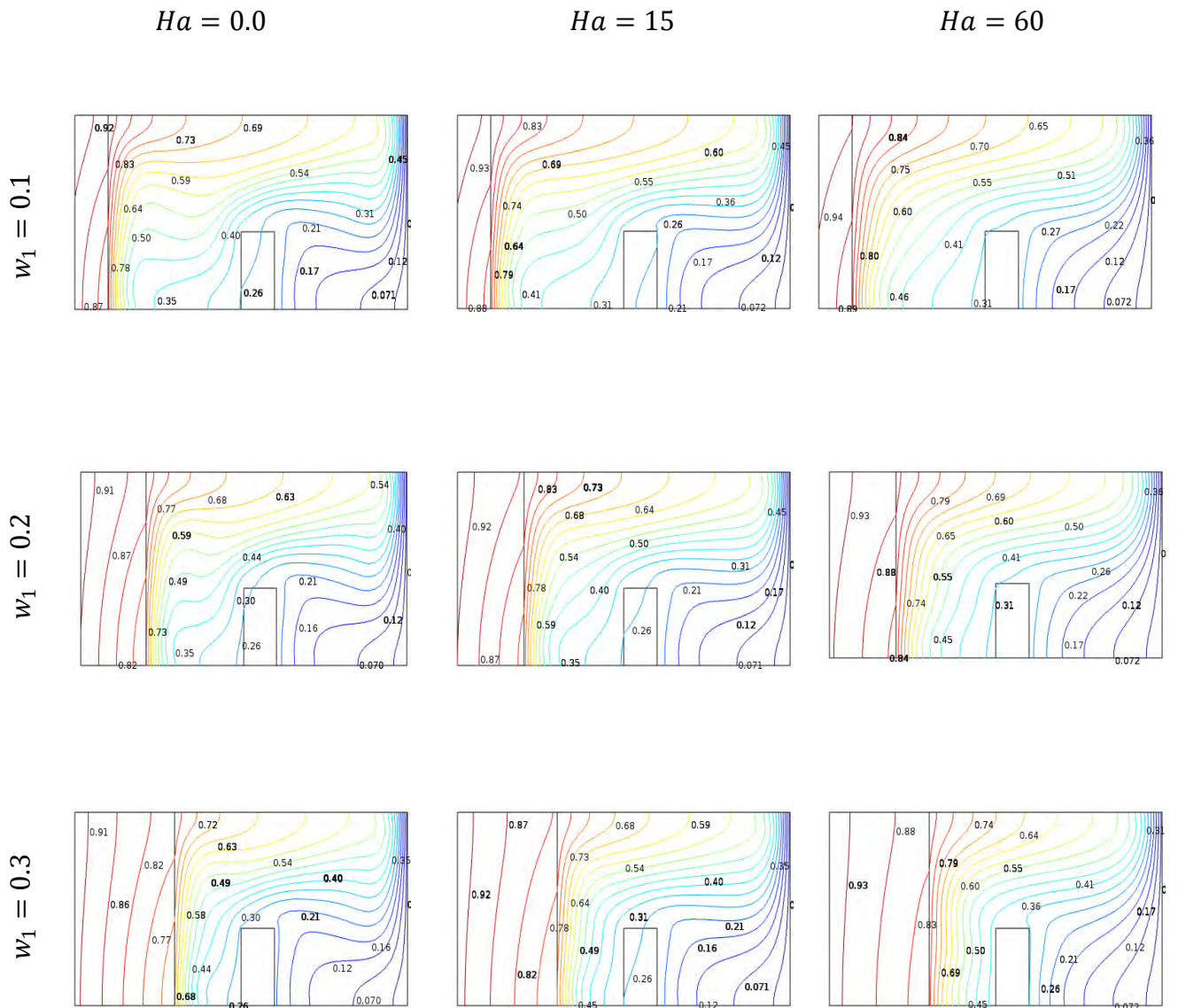
Figure 4.9: (b) Effect of Hartmann number ($Ha = 0.0, 15, 60$) on Isotherms at various Solid wall thickness for $Ra = 10^6, Pr = 6.2,\ h_\infty = 100W/m^2\text{K}$, $K_r = 10$ and $l_1 = 0.4$.

An examination of average Nusselt number (Nu) with respect to the Hartmann number (Ha) are seen for three values of Solid wall thickness (w_1) on taking $Ra = 10^6, l_1 = 0.40$, $Pr = 6.2$ and $h_\infty = 100\text{W}/m^2\text{K}$ with $\phi = 0.05$. We observe that the average Nusselt number (Nu) decreases with the increase of Solid wall thickness (w_1) and Hartmann number (Ha) due to the effect of wall thermal resistance and magnetic field.

Figure 4. 9 (c): Average Nusselt number at various w_1 (for $Ha = 0, 15, \ 30, \ 60$, $Ra = 10^6, Pr = 6.2 \ l_1 = 0.4$, $K_r = 10$ and $h_\infty = 100 \text{W}/m^2\text{K}$)

4.6 Conclusion of Chapter Four

Considering the results and discussion the following conclusions are made.

1) Stronger flow circulations within the enclosure and intensified isotherms near the vertical walls are evident at higher Rayleigh number and at lower Rayleigh number for a fixed solid volume fraction. The magnetic field reduces the circu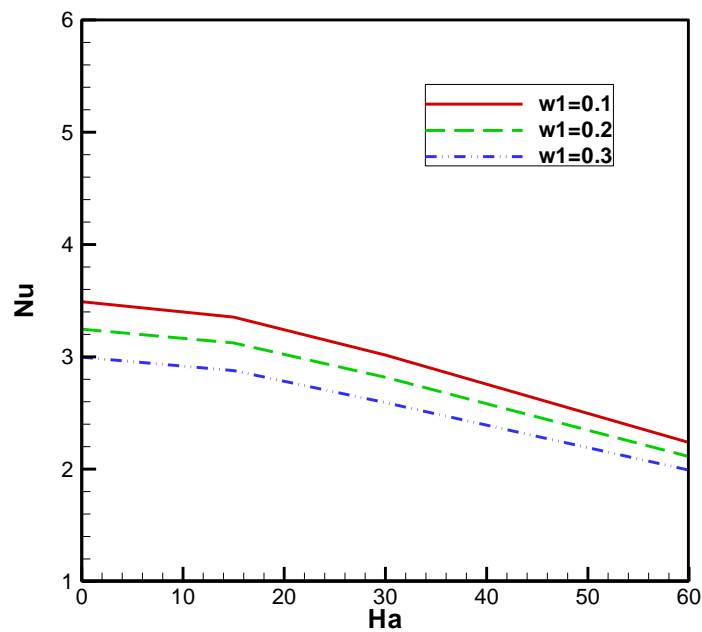lation in the cavity. When the magnetic field becomes stronger, it causes the convective heat transfer to reduce and, subsequently, conduction heat transfer becomes dominate.

2) The increase in the convective heat transfer coefficient leads to the decrease in the heat transfer. The average Nusselt number along the solid wall verifies that when the Hartmann number increase, the heat transfer rate decreases. The rate of this decrease is a function of Rayleigh number.

3) Adding nanoparticles to the fluid, the average Nusselt number increases and by increasing the value of Hartmann number it decrease.

4) The strength of the magnetic field affects significantly the flow, temperature and heat transfer inside the enclosure. When the position of the divider gets closure to the cold wall, the heat transfer is enhanced but it reduces with the increase of Hartmann number.

5) Natural convection inside the fluid part is driven by the temperature difference between the interface and the cold wall. This difference is lower for walls with poor thermal conductivity, but it becomes more important with the increase of K_r, and leads to increase the average Nusselt number. Here it is found that heat transfer decreases with an increase of the magnetic field. So, convective heat transfer can be controlled by the magnetic field.

6) The natural convection inside the nanofluid filled cavity decrease with increasing of its wall thickness and by the influence of applied magnetic field due to thermal resistance of solid wall and the suppression of convective circulating flow. As a result average Nusselt number also reduced.

Chapter 5: Conclusions and Recommendations

Numerical investigation on the effect of conjugate heat transfer in a thick walled cavity filled with copper-water nanofluid has been performed for heat transfer and fluid flow by solving steady state two dimensional Naviers-Stokes equations, energy equation and continuity equation. The work reported in this thesis is dependent of conjugate effect on convective heat transfer phenomena in a rectangular cavity configuration. Based on the outcome of the numerical investigation, specific conclusions and recommendations for future work have been presented in this section.

5.1 Summary of Major Outcomes

In view of the results the following conclusions may be summarized.

- Increasing the Rayleigh number resulted in stronger flow pattern and streamlines within the cavity. The nanofluid associates with stronger circulation cell compared with pure water at high Rayleigh numbers.

- The nanoparticles when immersed in a fluid are capable of increasing the heat transfer capacity of base fluid. As solid volume fraction increases, the effect is more pronounced.

- When the divider gets closer to the cold wall, the heat transfer is enhanced.

- The increase of Rayleigh number and conductivity ratio increase heat transfer between the wall and fluid on the solid-fluid interface.

- The natural convection inside the cavity filled with nanofluid decrease with increasing its wall thickness. So it can be said that, the strength of the circulation cell can be controlled by the thickness of the solid wall.

- Magnetic force has considerable effect on the flow and temperature field. Stronger magnetic field slows down the heat transfer rate as well as the average velocity of the fluid because of resistive effect of Lorentz force.

- Increasing Hartmann number reduces the fluid motion causing the core of the primary vortex smaller. Owing to this effect, lower heat transfer rate and lower average velocity is observed.

- At the zero magnetic force, the flow as well as heat transfer performance is found to be most effective. Increasing Ha causes higher fluid temperature whereas the fluid motion is weaker for the greater values of magnetic parameter Ha.

In general, the present study reveals that the fluid flow and temperature is significantly affected by the conjugate heat transfer and MHD effect. It is also observed that the MHD effect decreases the rate of heat transfer remarkably in the cavity.

Indeed, the aim of the present study is to investigate the effect of present parameters and also the effect of nanofluid on the natural convection flow and temperature fields in the rectangular enclosure. This geometry is mainly formulated for the cooling of electronic devices.

5.2 Recommendations

In consideration of the present investigation on the effect of conjugate heat transfer on flow of nanofluid in an enclosure with heat conducting vertical wall and uniform heat flux, the following recommendation for future works have been provided.

1) In future, the study can be extended by choosing different shape of enclosures.

2) The study can be extended by incorporating different physics like radiation effects, internal heat generation / absorption, viscous dissipations, Joule heating, entropy generation etc.

3) This study can be extended by changing the boundary conditions of the enclosure.

4) This numerical analysis can be extended for mass transfer problem.

5) Investigation can be performed by using the porous medium and changing the boundary conditions of the cavity's walls.

6) The study can be extended for turbulent flow using different fluids, different thermal boundary conditions.

7) This simulation can be extended by considering the moving surface.

8) This investigation can be performed by talking wavy bottom surface.

9) Only two-dimensional fluid flow and heat transfer have been analyzed in this thesis. So this deliberation may be extended to three-dimensional analyses to investigate the effects of parameters on flow fields and heat in cavities.

10) Single phase flow is considered here. The problem can be extended for double diffusive natural convection as well as for multiphase flow also.

11) The problems can be analyzed by including the temperature dependent properties of thermal conductivity, viscosity or density.

References

Abdullatif, Ben-Nakhi, Ali, J., Chamkha,–Conjugate natural convection in a square enclosure with inclined thin fin of arbitrary length", International Journal of Thermal Sciences, Vol. 46, pp. 467-478, 2007.

Acharya, S., Tsang, C.H., –Influence of wall conduction on natural convection in an inclined square enclosure", Warn and stoffubertragunug, Vol. 21, pp. 19-30, 1987.

Alchaar, S., Vasseur, P. E., Bilgen, –Natural convection heat transfer in a rectangular enclosure with a transverse magnetic field", Journal of Heat Transfer, Vol. 117, No. 3, pp. 668-573, 1995.

Aminossadati, S. M., Ghasemi, B., –Natural Convection Cooling of a localized heat source at the bottom of a nanofluid filled enclosure", European Journal of Mechanics B| Fluids., Vol. 28, pp. 630-640, 2009.

Aminossadati, S.M., Ghasemi, B., –Conjugate natural convection in an inclined nanofluid-filled enclosure", International Journal of Numerical Methods for Heat and Fluid Flow, Vol. 22, No. 4, pp. 403-423, 2012.

Bednarz, T.P., Lei, Ch, Patterson, J.C., –A numerical study of unsteady natural convection induced by iso-flux surface cooling in a reservoir model", International Journal of Heat and Mass Transfer, Vol. 52, pp. 56-66, 2009.

Belazizia, A., Belazizia, S., Abboudi, S., –Effect of Wall Conductivity on Conjugate Natural Convection in a Square Enclosure with Finite vertical wall thickness, Advanced Theory of Applied Mechanics, Vol. 15, No. 4, pp. 179-190, 2012.

Ben Yedder, R., Bilgen, E., –Laminar and natural convection in inclined enclosures bounded by a solid wall", Heat and Mass Transfer, Vol. 32, No. 6, pp. 455-462, 1997.

Brinkman, H.C, –The viscosity of concentrated suspensions and solution", Journal of Chem. Phys. Vol. 20, pp. 571–581, 1952.

Ching, C.Y., Wu, W., –Laminar natural convection in an air-filled square cavity with partitions on the top wall", International Journal of Heat and Mass Transfer, Vol. 53, pp. 17591772, 2010.

Choi, S.U.S.,–Enhancing thermal conductivity of fluids with nanoparticles", ASME Fluids Engineering Division, Vol. 231, pp. 99-105, 1995.

Chung, T. J., –Computational fluid dynamics", First Ed., Cambridge University Press, 2002.

Das, M.K., Reddy, K.S.K., ―Conjugate natural convection heat transfer in an inclined square cavity containing a conducting block", International Journal of Heat and Mass Transfer, Vol. 49, pp. 4987-5000, 2006.

Dechaumphai, P., ―Finite Element Method in Engineering", second Ed., Chulalongkorn University Press, Bangkok, 1999.

Du, Z.G., Bilgen, E., ―Coupled of wall conduction with natural convection in a rectangular enclosure", International Journal of Heat and Mass Transfer, Vol. 335, pp. 1969-1975, 1992.

Dulikravich, G.S., Colaco, M.J., ―Convective heat transfer control using magnetic and electric fields", Journal of Enhanced Heat transfer, Vol. 13, No. 2, pp. 139-155, 2006.

Ece, M.C., Byuk, E., ―Natural convection flow under a magnetic field in an inclined rectangular enclosure heated and cooled on adjacent walls", Fluid Dynamics Research, Vol. 38, No. 8, pp. 564-590, 2006.

Eiyad Abu-Nada, Chamkha, Ali J., ―Mixed convection flow in a lid-driven inclined square enclosure filled with a nanofluid", European Journal of Mechanics-B/Fluids (in press), Corrected proof, doi:10.1016/j. euromechflu, 2010,06,008.

Ferziger, J. H. and Perić, M.,―Computational methods for fluid dynamics", Second Ed., Springer Verlag, Berlin Hedelberg, 1997.

Garandet, J. P., Alboussiere, T., and Moreau, R., ―Buoyancy driven convection in a rectangular enclosure with a transverse magnetic field", International Journal of Heat and Mass Transfer, Vol. 35, No. 4, pp. 741-748, 1992.

Ghasemi, B., Aminossadati, S.M., Raisi, A., ―Magnetic field effect on natural convection in a nanofluid–filled square enclosure", International Journal of Thermal Sciences, Vol. 50, pp. 1748-1756, 2011.

Ho, C.J., Chen, M.W., Li, Z.W., ―Numerical simulation of natural convection of nanofluid in a square enclosure: effects due to uncertainties of viscosity and thermal conductivity", International Journal of Heat and Mass Transfer, Vol. 51, pp. 4506-4516, 2008.

Jeng., D.Z., Yang, C.S., Gau, C., ―Experimental and numerical study of transient natural convection due to mass transfer in inclined enclosures", International Journal of Heat and Mass Transfer, Vol. 52, pp. 181-192, 2009.

Jou, R.Y. and Tzeng, S.C., ―Numerical research of natural convection heat transfer enhancement filled with nanofluids in rectangular enclosure",International Communications in Heat and Mass Transfer, Vol. 33, pp.727-736, 2006.

Kahveci, K and Oztuna, S., ―MHD natural convection flow and heat transfers I a laterally heated partitioned enclosure", European Journal of Mechanics-B: Fluids, Vol. 28, No. 6, pp. 744-752, 2009.

Kaminski, D.A and Prakash, C., ―Conjugate natural convection in a square enclosure: effect of conduction in one of the vertical walls", , International Journal of Heat and Mass Transfer, Vol. 12, pp. 1979-1954, 1986.

Kim, D. M., Viskanta, R., ―Effect of wall heat conduction on natural convection heat transfer in a square enclosure", Journal of Heat Transfer, Vol. 107, pp. 139-146, 1985.

Kim, D.M., Viskanta, R. ―Study of effects of wall conductance on natural convection in differently oriented square cavities", Journal of Fluid Mechanics, Vol. 144, pp. 153-176, 1984.

Kimura, S., Kiwata, T., Okajimi, A., Pop, I., ―Conjugate natural convection in porous media", Advanced in Water Resources, Vol. 20, pp. 111-26, 1997.

Kuiken, H.K., ―Magnetohydrodynamic free convection in strong cross flow field". Journal of Fluid Mechanics, Vol. 40, pp. 21-38, 1970.

Lei, Ch., Armfield, S.W., Patterson, J.C. ―Unsteady convection in a water-filled isosceles triangular enclosure heated from below" International Communications in Heat and Mass Transfer, Vol. 37, pp. 201-2`13, 2010.

Liaqat, A. and Baytas, A.C, ―Conjugate natural convection in a square enclosure containing volumetric sources", International Journal of Heat and Mass Transfer, Vol. 44, pp. 3273-3280, 2001.

Mamum, A. A., Chowdhury, Z.R., Azim, M.A., Molla, M.M., ―MHD-Conjugate heat transfer analysis for a vertical flat plate in presence of viscous dissipation and heat generation", International Communications in Heat and Mass Transfer, Vol. 32, pp. 1275-1280, 2008.

Mansour, M.A. , Chamkha, A.J., Mohamed, R.A., Abd El-Aziz, M.M. and Ahmed, S.E., ―MHD natural convection in an inclined cavity filled with a fluid saturated porous medium with heat source in the solid phase", Nonlinear Analysis: Modeling and Control, Vol. 15, No. 1, pp. 55-70, 2010.

Martins, R.C., Lopes, V., Vicente, A.A. and Teixeira, J.A., ―Numerical Solutions", Optimization in Food Engineering, CRC Press, 2008.

Maxwell-Garnett, J.C, ―Colors in metal glasses and in metallic films", Philos. Trans. Roy. Soc. A, Vol. 203, pp. 385–420, 1904

Mbaye, M., Bilgen, M., Vasseur, P., ―Natural convection heat transfer in an inclined porous layer bounded by a finite thickness wall", International Journal of Heat and Fluid Flow, Vol. 14, pp. 284-91, 1993.

Misra, D., Sarkar, D.A.,―Finite element analysis of conjugate natural convection in a square enclosure with a conducting vertical wall, Computational Methods of Applied Mechanical Engineering ",Vol. 141, pp. 205-219, 1997.

Mobedi, M., ―Conjugate natural convection in a square cavity with finite thickness horizontal walls", International Communications in Heat and Mass Transfer, Vol. 35, pp. 503-513, 2008.

Moens, D. and Vandepitte, D., ―A survey of non-probabilistic uncertainty treatment in finite element analysis", Computer Methods in Applied Mechanics and Engineering, Vol. 194, No.12-16, pp. 1527-1555, 2005.

Mohamed, I.O, ―Development of a Simple and Robust Inverse Method for Determination of Thermal Diffusivity of Solid Foods" Journal of Food Engineering, Vol. 101, No.1, pp.1-7, 2010.

Nawaf, H,and Saeid, ―Conjugate natural convection in a porous enclosure: effect of conduction in one of the vertical walls", International Journal of Thermal Sciences, Vol. 46, pp. 531-539, 2007.

Nemati, H., Farhadi, M., Sedighi, K., Ashorynejad, H.R., Fattahi, E., ―Magnetic field effects on natural convection flow of nanofluid in a rectangular enclosure cavity using the Lattice Boltzmann model", Scientia Iranica B, Vol. 19, No. 2, pp. 303-310, 2012.

Nouanegue, H., Muftuoglu, A., Bilgen, E., ―Heat transfer by natural convection, conduction and radiation in an inclined square enclosure bounded with a solid wall", International Journal of Thermal Sciences, Vol. 48, pp. 871-880, 2009.

Oreper, G.M. and Szekely, J., ―The effect of an externally imposed magnetic field on buoyancy driven flow in a rectangular cavity", Journal of Crystal Growth, Vol. 64, No. 3, pp. 505-515, 1983.

Ostrach, S., ―Natural convection in an enclosures", Journal of Heat Transfer, Vol. 110, pp. 175-1190, 1988.

Ozoe, H. and Maruo, M., ―Magnetic and gravitational natural convection of melted silicon-two dimensional numerical computations for the rate of heat transfer", JSME International Journal, Vol. 30, pp. 774-784, 1987.

Ozoe, H. and Okada, K., ―The effect of the direction of the external magnetic field on the three –dimensional natural convection in a cubical enclosure ‖, International Journal of Heat and Mass Transfer, Vol. 32, No. 10, pp. 1939-1954, 1989.

Öztop, H.F. and AL-Salem, K., ―Effects of joule heating on MHD natural convection in non-isothermally heated enclosure‖, Journal of Thermal Science and Technology, Vol. 32, No. 1, pp. 81-90, 2012.

Patankar, S. V., ―Numerical heat transfer and fluid flow‖, Second Ed., Washington, D. C. Homisphere, 1980.

Pesso, T., Iiva, S., ―Laminar natural convection in a square cavity: low Prandtl numbers and large density differences‖, International Journal of Heat and Mass Transfer, Vol. 52, pp. 1036-1043, 2009.

Puri, V.M. and Anantheswaran R.C., ―The finite-element method in food processing: A Review‖ Journal of Food Engineering, Vol. 19, No. 3, pp. 247-274, 1993.

Rahman, M. M and Alim, M. A., ―MHD Mixed Convection flow in a vertical lid-driven square enclosure including a heat Conducting horizontal circular cylinder with Joule Heating‖, Nonlinear Analysis: Modeling and Control, Vol. 15, No. 2, pp. 199-211, 2010.

Rahman, M. M., Saidur, R.and Rahim, N.A., ―Conjugated effect of joule heating and magneto-hydrodynamic on double-diffusive mixed convection in a horizontal channel with an open cavity‖, International Journal of Heat and Mass Transfer, Vol. 54, No. 15–16, pp 3201–3213, 2011.

Reddy, J.N., An Introduction to Finite Element Method, McGraw-Hill, New York, 1993.

Riley, N., ―Magnetohydrodynamic free convection‖, Journal of Fluid Mechanics, Vol. 18, pp. 577-586, 1964.

Rudraiah, N., Barron, R.M., Venkatachalappa, M. and Subbaraya, C.K., ―Effect of magnetic field on free convection in a rectangular enclosure‖, International Journal of Engineering Sciences, Vol. 33, No. 8, pp. 1075-1084, 1995a.

Rudraiah, N., Venkatachalappa, M., and Subbaraya, C.K., ―Combined surface tension and buoyancy-driven convection in a rectangular open cavity in the presence of magnetic field‖, International Journal of Non-linear Mechanics, Vol. 30, No. 5, pp. 759-770, 1995b.

Saleh, H. and Hashmi, I., ―Conjugate Heat Transfer in Rayleigh- Bénard Convection in a square Enclosure‖, The Scientific World Journal, 2014, 786102.

Sandeep, K., Soojin J., and Joseph, I., ―Introduction to Modeling and Numerical Simulation‖, Food Processing Operations Modeling, CRC Press, pp. 1-11, 2008.

Sankar, M. and Younghae, Do.," Numerical simulation of free convection heat transfer in a vertical annular cavity with discrete heating", International Communications in Heat and Mass Transfer, Vol. 37, pp. 600-606, 2010.

Sarris, I.E., Kakarantzas, S.C., Grecos, A.P. and Vlachos, N.S., ―MHD natural convection in a laterally and volumetrically heated square cavity", International Journal of Heat and Mass Transfer, Vol. 48, No. 16, pp. 3443-3453, 2005.

Sathiyamoorthy, M., Chamkha, A., ―Effect of magnetic field on natural convection flow in a liquid gallium filled square cavity for linearly heated side wall (s)", International Journal of Thermal Sciences, Vol. 49, No. 9, pp. 1856-1865, 2010.

Shao-Feng Dong, Yin-Tang Li, ―Conjugate of natural convection and conduction in complicated enclosure", International Journal of Heat and Mass Transfer, Vol. 47, pp. 2233-2239, 2004.

Sing, K.R. and Cowling, T.G., ―Thermal conduction in magnetohydrodynamics", Journal of Mechanical and Applied Mathematics, Vol. 16, pp. 1-5, 1963.

Sivasankaran, S. and Ho, C.J., ―Effect of temperature dependent properties on MHD convection of water near its density maximum in a square cavity", International Journal of Thermal Sciences, Vol. 47, No. 9, pp. 1184-1194, 2008.

Sparrow, E. M. and Cess, R.D., ―Effect of magnetic field on free convection heat transfer", International Journal of Heat and Mass Transfer, Vol. 3, pp. 267-274, 1961.

Taylor, C. and Hood, P., ―A numerical solution of the Navier-Stokes equations using finite element technique", Computer and Fluids, Vol. 1, pp. 73–89, 1973.

Teamah, M. A., ―Numerical simulation of double diffusive natural convection in rectangular enclosure in the presences of magnetic field and heat source", International Journal of Thermal Sciences, Vol. 47, No. 3, pp. 237-248, 2008.

Varol, Y., Oztop, H.F., Pop , I., ―Conjugate Heat Transfer in Porous triangular enclosures with thick bottom wall", International Journal of Numerical Methods for Heat & Fluid Flow,Vol. 19, No. 5, pp. 650-664, 2009.

Venkatachalappa, M., Subbaraya, C.K., ―Natural convection in a rectangular enclosure in the presence of a magnetic field with uniform heat flux from the side walls", Acta Mechanica , Vol. 9, No. 1-4, pp. 13-26, 1993

Vorol, Y., Hakan, F. Oztop, Ahmed, K., ―Effects of inclination angel on conduction – natural convection in divided enclosures filled with different fluids", International Journal of Heat and Mass Transfer, Vol. 37, pp. 182-191, 2010.

Wang, L. and Sun, D., ―Recent developments in numerical modeling of heating and cooling processes in the food industry—a Review", Trends in Food Science & Technology, Vol. 14, No.10, pp. 408-423, 2003.

Zhang, W., Zang, C, Xi, G. ―Conjugate conduction- natural convection in an enclosure with time-periodic sidewall temperature and inclination,", International Journal of Heat and Mass Fluid Flow, Vol. 32, No. 1 pp. 52-64, 2011.

Zienkiewicz, O.C. and Taylor, R.L., The finite element method, Fourth ed., McGraw-Hill, 1991.